

# Nested Graph Pseudo-Label Refinement for Noisy Label Domain Adaptation Learning

Yingxu Wang<sup>1</sup>, Mengzhu Wang<sup>2</sup>, Zhichao Huang<sup>3</sup>, Suyu Liu<sup>4</sup>, Nan Yin<sup>5</sup>

<sup>1</sup>Mohamed bin Zayed University of Artificial Intelligence <sup>2</sup>Hebei University of Technology

<sup>3</sup>JD Industrial <sup>4</sup>Nanyang Technological University

<sup>5</sup>Hong Kong University of Science and Technology

yingxu.wang@gmail.com, dreamkily@gmail.com, iceshzc@gmail.com,

suyu.liu@ntu.edu.sg, yinnan8911@gmail.com

## Abstract

Graph Domain Adaptation (GDA) facilitates knowledge transfer from labeled source graphs to unlabeled target graphs by learning domain-invariant representations, which is essential in applications such as molecular property prediction and social network analysis. However, most existing GDA methods rely on the assumption of clean source labels, which rarely holds in real-world scenarios where annotation noise is pervasive. This label noise severely impairs feature alignment and degrades adaptation performance under domain shifts. To address this challenge, we propose **Nested Graph Pseudo-Label Refinement (NeGPR)**, a novel framework tailored for graph-level domain adaptation with noisy labels. NeGPR first pretrains dual branches, i.e., semantic and topology branches, by enforcing neighborhood consistency in the feature space, thereby reducing the influence of noisy supervision. To bridge domain gaps, NeGPR employs a nested refinement mechanism in which one branch selects high-confidence target samples to guide the adaptation of the other, enabling progressive cross-domain learning. Furthermore, since pseudo-labels may still contain noise and the pre-trained branches are already overfitted to the noisy labels in the source domain, NeGPR incorporates a noise-aware regularization strategy. This regularization is theoretically proven to mitigate the adverse effects of pseudo-label noise, even under the presence of source overfitting, thus enhancing the robustness of the adaptation process. Extensive experiments on benchmark datasets demonstrate that NeGPR consistently outperforms state-of-the-art methods under severe label noise, achieving gains of up to 12.7% in accuracy.

## Introduction

Graph Domain Adaptation (GDA) (You et al. 2022; Cai et al. 2024) has emerged as a prominent technique for leveraging labeled graph data from a source domain to enhance learning on an unlabeled target graph domain. Its efficacy has been demonstrated across diverse applications, including temporally-evolved social network analysis (Wang et al. 2021, 2024c; Yao et al. 2023), molecular property prediction (Zhu et al. 2023; Yin et al. 2024c), and protein-protein interaction modeling (Cho, Berger, and Peng 2016; Wang et al. 2024a). The core paradigm typically involves learning domain-invariant node/graph representations that bridge the distributional shift between source and target domains, thus enabling effective inference on the target data.

However, the success of standard GDA methods crucially relies on the accurately labeled source data. In practice, source domain labels are often corrupted by noise arising from annotation errors (Dai, Aggarwal, and Wang 2021; Yuan et al. 2023b), subjective judgments (Platanios, Dubey, and Mitchell 2016; Yin et al. 2024d), or inherent ambiguities in data collection (Chen, Shah, and Kyrillidis 2020; Wang et al. 2024b). This prevalent issue of label noise can severely misguide the learning of domain-invariant representations (Li, Socher, and Hoi 2020; Yin et al. 2024b), leading to suboptimal or even detrimental adaptation performance on the target domain (Yin et al. 2025; Wang et al. 2025). Existing noise label learning methods typically rely on loss function design to mitigate the impact of noisy labels (Han et al. 2018; Natarajan et al. 2013), which selects clean instances for joint training, and robust loss functions (Wei et al. 2020; Li, Socher, and Hoi 2020), which leverage small-loss selection or instance mixture models. While effective in controlled settings, these approaches fall short in the presence of domain shifts. The coexistence of distribution shift and label noise leads to misaligned feature spaces, causing noise-robust losses to erroneously align clean features with noisy targets, thereby amplifying negative transfer (Yu et al. 2020; Yin et al. 2022a). While recent efforts have been made to address GDA under noisy labels (Yuan et al. 2023a; Wang and Yang 2022), they primarily target node classification tasks, leaving a critical gap in addressing graph-level scenarios. Many real-world applications, such as molecular property prediction (Stokes et al. 2020) and social network analysis (Hamilton, Ying, and Leskovec 2017), inherently depend on graph-level classification, where label noise can severely compromise the identification of functional groups and the modeling of community behaviors. The lack of attention to graph-level adaptation under noisy labels significantly limits the practical applicability of existing methods in high-impact domains.

In this paper, we investigate the development of an efficient GDA framework for scenarios involving label noise. However, designing such a framework poses several fundamental challenges: (1) *Distribution shift undermines loss-based denoising*. Conventional noise-robust loss functions are primarily designed for specific domains and often struggle under distribution shifts. In the presence of noisy labels in the source domain, aligning target features with cor-

rupted source representations can lead to noise-aligned embeddings, degrading generalization due to feature misalignment and increased risk of negative transfer. Recent studies in GDA have highlighted that noisy supervision severely hinders feature alignment across domains, especially when relying on pseudo labels or unreliable source signals (Yuan et al. 2023a). These findings underscore the need for noise-aware mechanisms that explicitly account for both label noise and domain discrepancy. (2) *Imperfect pseudo labels compromise domain adaptation*. Probability-based pseudo-labeling has shown promise in bridging distribution shift and mitigating supervision noise (Yuan et al. 2023a; Yin et al. 2023a). However, the reliability of selected pseudo labels is often compromised by erroneous source annotations, leading to residual noise being transferred into the target domain. In Graph Neural Networks (GNNs), such corrupted pseudo labels can propagate through message passing, triggering self-reinforcing error cascades. As each GNN layer aggregates information from potentially mislabeled neighbors, the accumulated noise progressively deteriorates local neighborhood structures and distorts global representations over successive adaptation rounds (Wang et al. 2024d). (3) *Label noise impairs distribution alignment in GDA*. Existing methods typically adopt explicit (Long et al. 2015) or implicit (Long et al. 2018) strategies to align feature distributions across domains. However, significant label noise corrupts supervision signals, causing samples to drift toward incorrect class regions and disrupting the formation of domain-invariant features. This misalignment undermines the effectiveness of domain discriminators and hampers reliable adaptation. These challenges call for a unified framework that combines noise-robust representation learning, trustworthy pseudo-label refinement, and alignment strategies that preserve class-level semantics across domains.

To tackle these challenges, we propose **Nested Graph Pseudo-Label Refinement (NeGPR)**, a novel framework designed for GDA under noisy labels. To effectively disentangle the impact of label noise from domain distribution shift, NeGPR first pre-trains noise-resilient models from implicit and explicit perspectives by enforcing semantic consistency among neighboring samples in the feature space. The implicit branch promotes feature-level consistency based on learned representations, while the explicit branch captures structural patterns by leveraging graph topology. This dual-perspective design improves robustness to noisy supervision and provides a reliable foundation for domain adaptation. Then, to align the domain distribution, NeGPR iteratively leverages cross-branch knowledge, where one branch filters highly reliable target domain samples, and the other branch is fine-tuned accordingly, enabling mutual enhancement and progressive adaptation. However, the filtered pseudo-labels may still contain erroneous category information, and the pre-trained branches have already overfitted to the label noise in the source domain. The interplay of these two factors exacerbates performance degradation during domain adaptation. To tackle this, NeGPR employs a regularization along with a theoretical analysis demonstrating its effectiveness in suppressing the influence of noisy pseudo-labels. Extensive experiments demonstrate that NeGPR sig-

nificantly outperforms state-of-the-art methods under severe label noise. Our main contributions are summarized as:

- We investigate a novel problem setting, graph domain adaptation learning under label noise, where label noise and domain shift coexist and jointly pose significant challenges for graph representation learning.
- We propose NeGPR, a dual-branch framework that integrates noise-resilient pre-training, nested pseudo-label refinement, and theoretically grounded regularization to tackle graph domain adaptation under label noise.
- We evaluate NeGPR on extensive datasets, showing that NeGPR significantly outperforms existing approaches under various noise levels and domain shift scenarios.

## Related work

**Graph Domain Adaptation.** Graph Domain Adaptation (GDA) has emerged as a critical research topic, aiming to leverage labeled source domain graphs to enable robust representation learning on unlabeled or sparsely labeled target graphs (Lin et al. 2023; Luo et al. 2023; Liu et al. 2024a). To achieve this, most existing approaches first employ Graph Neural Networks (GNNs) (Kipf and Welling 2017a; Chen et al. 2023) to generate representations for each graph (Wu, Pan, and Zhu 2022; Zhu et al. 2021; Yin et al. 2022b). They then commonly use adversarial learning to implicitly align feature distributions and reduce domain discrepancies, apply pseudo-labeling to iteratively refine predictions in the target domain, or incorporate structure-aware strategies to explicitly align graph-level semantics and topological structures, thereby improving generalization across diverse graph domains (Yin et al. 2023b; Wang et al. 2024b; Liu et al. 2024b). However, these methods often overlook the impact of noisy labels, which can distort learned representations and lead to misaligned distributions and unreliable predictions in the target domain. Although a few label-denoising GDA methods have been proposed, they primarily focus on node-level tasks (Yuan et al. 2023a). To address these limitations, we propose a novel label-denoising domain adaptation method designed for graph-level classification tasks.

**Learning with Noise Labels.** Learning with noisy labels has garnered significant attention for its crucial role in developing robust models under imperfect supervision, which has been widely used in machine learning and computer vision (Zhu et al. 2024). Existing methods typically address label noise by employing robust loss functions, identifying and filtering out noisy samples, or refining labels through correction mechanisms (Feng et al. 2021; Xu et al. 2025). However, existing methods still insufficiently investigate the interplay between label noise and domain adaptation (Yin et al. 2024a; Zhu et al. 2024). In particular, applying a model trained on the source domain to the target domain can be regarded as a noisy inference process due to distributional shifts inherent in domain adaptation (Yu et al. 2020; Dan et al. 2024). Furthermore, label noise in the source domain can also degrade model performance (Yuan et al. 2023a; Yu et al. 2024). Critically, conventional methods cannot disentangle whether the observed performance degradation is primarily attributable to domain shift or label noise, thereby

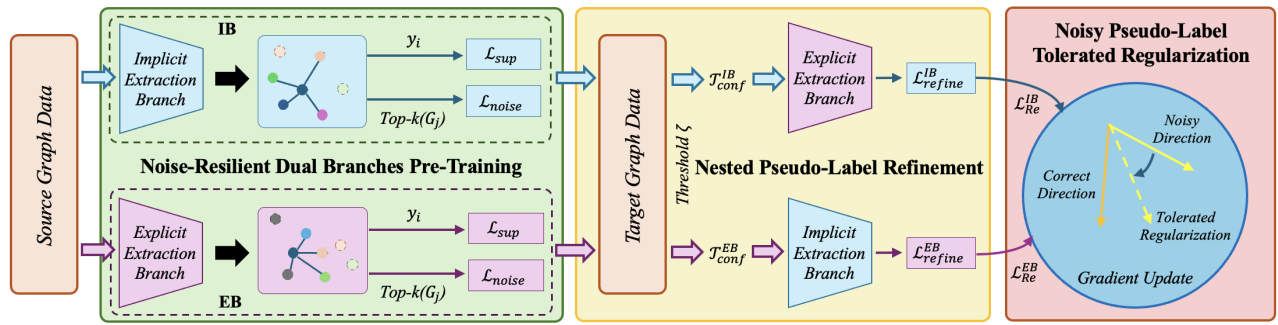


Figure 1: Overview of the proposed NeGPR. NeGPR consists of a dual-branch pretraining module that captures complementary semantic and structural features under label noise. Then, a nested pseudo-label refinement module alternately selects high-confidence target samples from one branch to guide the other, enabling progressive cross-domain adaptation. The noisy pseudo-label tolerated regularization penalizes overconfident predictions to suppress the effect of noisy pseudo labels.

limiting their ability to address the underlying causes of adaptation failure effectively. To address this challenge, we propose a novel learning framework designed to mitigate the effects of domain shift and label noise.

## Methodology

### Overview of Framework

This work studies the problem of unsupervised graph domain adaptation in the presence of noisy labels and proposes a novel framework, NeGPR, as illustrated in Fig. 1. NeGPR comprises three key components: (1) **Noise-Resilient Dual Branches Pre-Training**. To effectively suppress the impact of label noise, we first pre-train noise-resilient models from implicit and explicit perspectives by enforcing semantic consistency among neighboring samples in the feature space; (2) **Nested Pseudo-Label Refinement**. To align category-level distributions, each branch selects high-confidence pseudo-labeled target samples based on prediction confidence and uses them to fine-tune the other branch. This cross-branch refinement mitigates error accumulation from noisy pseudo labels and enables progressive domain adaptation through mutual supervision; (3) **Noisy Pseudo-Label Tolerated Regularization**. To alleviate the negative impact of noisy pseudo labels, we introduce a noise-aware regularization term with theoretical guarantees. This regularization effectively suppresses error propagation induced by noisy pseudo labels during the adaptation process.

### Problem Formulation

Given a graph  $G = (\mathcal{V}, \mathcal{E}, \mathbf{X})$  with the set of nodes  $\mathcal{V}$  and edges  $\mathcal{E} \subseteq \mathcal{V} \times \mathcal{V}$ . The  $\mathbf{X} \in \mathbb{R}^{|\mathcal{V}| \times d}$  is the node feature matrix, where each row  $\mathbf{x}_v \in \mathbb{R}^d$  denotes the feature of node  $v \in \mathcal{V}$ ,  $|\mathcal{V}|$  is the number of nodes, and  $d$  denotes the dimension of node features. In our setting, we have access to a labeled source domain  $\mathcal{D}^s = \{(G_i^s, y_i^s)\}_{i=1}^{n_s}$  with  $n_s$  samples, where the labels  $y_i^s$  may be corrupted by noise, and an unlabeled target domain  $\mathcal{D}^t = \{G_j^t\}_{j=1}^{n_t}$  with  $n_t$  samples. Both domains share the label space  $\mathcal{Y} = \{1, 2, \dots, C\}$  but follow different data distributions. The goal is to train

the graph classification model using both  $\mathcal{D}^s$  and  $\mathcal{D}^t$  and achieve high accuracy on the target domain.

### Noise-Resilient Dual Branches Pre-Training

To mitigate the adverse impact of noisy labels in the source domain, we adopt a dual-branch architecture that captures semantic consistency from implicit and explicit perspectives. Noisy supervision can distort the feature space by pulling semantically similar graphs toward incorrect class boundaries. In contrast, the local relationships among neighboring samples often remain reliable despite label corruption. Motivated by this, we construct two parallel branches that exploit neighborhood consistency to learn robust representations. One branch captures semantic similarity through learned features, while the other incorporates structural information derived from graph topology. This design enhances the model’s resilience to noise and provides a stable foundation for subsequent domain adaptation.

**Implicit Extraction Branch.** The implicit branch follows the MPNNs mechanism (Gilmer et al. 2017), which extracts graph semantics by aggregating neighborhood representations to update the central node embeddings. Specifically, we update the embedding of node  $u$  at layer  $l$  and then summarize the node embeddings into graph-level:

$$\mathbf{h}_u^l = \text{COM} \left( \mathbf{h}_u^{l-1}, \text{AGG} \left( \mathbf{h}_{v \in \mathcal{N}(u)}^{l-1} \right) \right),$$

$$\mathbf{z}_G^{lB} = \text{READOUT} \left( \left\{ \mathbf{h}_u^L \right\}_{u \in \mathcal{V}} \right),$$

where  $\mathcal{N}(u)$  is the neighbours of node  $u$ . COM and AGG denote the combination and aggregation operations, READOUT is the graph pooling function. This formulation allows the implicit branch to capture structural information indirectly through supervised learning with noisy labels.

**Explicit Extraction Branch.** While the implicit branch captures structural semantics indirectly, its performance may deteriorate under domain shifts due to limited sensitivity to distributional changes. To enhance structural awareness, we introduce a complementary branch that explicitly encodes topological information by extracting high-order subgraph patterns (Shervashidze et al. 2011; Nikolentzos, Siglidis, and

Vazirgiannis 2021). This design enables the model to generate graph-level representations that are more robust to structural discrepancies across domains. Specifically, we formulate the explicit extraction branch as:

$$\begin{aligned} \mathbf{h}_v &= \phi(\mathcal{S}_v(G)), \quad \forall v \in \mathcal{V}, \\ \mathbf{z}_G^{EB} &= \text{READOUT}(\{\mathbf{h}_v\}_{v \in \mathcal{V}}), \end{aligned}$$

where  $\mathcal{S}_v(G)$  denotes a set of high-order substructures extracted from  $G$  (e.g., shortest paths (Borgwardt and Kriegel 2005) or subtree patterns (Shervashidze et al. 2011)),  $\phi(\cdot)$  encodes each substructure into a latent representation, and  $\text{READOUT}(\cdot)$  aggregates these representations into a graph-level embedding. The resulting  $\mathbf{z}_G^{EB}$  serves as the explicit topological representation of the graph.

**Noise-Resilient Pre-Training.** To mitigate the impact of label noise in the source domain, we exploit local semantic consistency among graphs in the feature space. Empirically, semantically similar graphs tend to exhibit stable feature distributions, even under corrupted labels (Wang and Isola 2020; Iscen et al. 2022). Based on this insight, we construct a semantic neighbor graph by identifying the top- $k$  nearest neighbors for each source sample using similarity  $\alpha_{ij} = \mathbf{z}_{G_i}^B \top \mathbf{z}_{G_j}^B / (\|\mathbf{z}_{G_i}^B\| \cdot \|\mathbf{z}_{G_j}^B\|)$  over graph-level embeddings obtained from each branch, where  $B \in \{\text{IB}, \text{EB}\}$ . To enforce prediction consistency within local neighborhoods, we encourage the predicted distribution to align with a weighted average of its semantic neighbors’ predictions:

$$\mathcal{L}_{\text{noise}}^B = \frac{1}{n_s} \sum_{i=1}^{n_s} \text{KL} \left( \mathbf{z}_{G_i}^B \parallel \sum_{j \in \text{top-}k(G_i)} \alpha_{ij} \cdot \mathbf{z}_{G_j}^B \right),$$

where KL is the Kullback-Leibler divergence,  $\text{top-}k(G_i)$  is the top- $k$  nearest neighbors samples of  $G_i$ . This regularization guides the model to learn noise-resilient representations by aligning each prediction with its semantic context, rather than relying solely on potentially corrupted labels. In formulation, we pre-train the dual branches with:

$$\mathcal{L}_{\text{pre}}^B = \mathcal{L}_{\text{sup}}^B + \beta \mathcal{L}_{\text{noise}}^B, \quad (1)$$

where  $\mathcal{L}_{\text{sup}}^B = \frac{1}{n_s} \sum_{i=1}^{n_s} l(\sigma(\mathbf{z}_{G_i}^B), y_i)$  is the supervised classification loss,  $l$  is the cross-entropy loss and  $\sigma$  is the softmax function.  $B \in \{\text{IB}, \text{EB}\}$  indicates the implicit and explicit branches pre-training.

### Nested Pseudo-Label Refinement

While various domain adaptation techniques such as distribution alignment (Long et al. 2015; Ganin et al. 2016) and adversarial training (Tzeng et al. 2017; Pei et al. 2018) have been widely explored, they often rely on strong assumptions regarding the existence of domain-invariant representations, which may not hold in the presence of label noise. In contrast, pseudo-labeling provides a flexible and data-driven alternative by leveraging model predictions on unlabeled target samples to guide adaptation (Lee et al. 2013; Xie et al. 2020). In our setting, the dual-branch encoder offers two complementary perspectives for estimating target semantics, enabling more reliable pseudo-label selection through

confidence-based filtering. This design facilitates progressive adaptation by gradually incorporating trustworthy target samples into training, while retaining the robustness of the noise-resilient pre-trained branches.

Specifically, at each iteration of cross-branch pseudo-label refinement, we select one branch to generate predictions for all target domain samples. For each sample  $G_j^t \in \mathcal{D}^t$ , we compute the predicted class probability vector  $\hat{\mathbf{y}}_j = \text{Softmax}(\mathbf{z}_{G_j^t}^B)$ , where  $B \in \{\text{IB}, \text{EB}\}$ . We then select a set of high-confidence samples  $\mathcal{T}_{\text{conf}}$  defined as:

$$\mathcal{T}_{\text{conf}}^B = \{G_j^t \in \mathcal{D}^t \mid \max(\hat{\mathbf{y}}_j) \geq \zeta\}, \quad (2)$$

where  $\zeta$  is a pre-defined threshold. The corresponding pseudo-labels are assigned as:  $\tilde{y}_j = \arg \max(\hat{\mathbf{y}}_j), \forall G_j^t \in \mathcal{T}_{\text{conf}}^B$ . The selected pseudo-labeled samples  $\{(G_j^t, \tilde{y}_j)\}_j$  are then used to fine-tune the other branch with:

$$\mathcal{L}_{\text{refine}}^{B'} = \mathcal{L}_{\text{pre}}^{B'} - \frac{1}{|\mathcal{T}_{\text{conf}}^B|} \sum_{G_j^t \in \mathcal{T}_{\text{conf}}^B} \tilde{y}_j \log \sigma(\mathbf{z}_{G_j^t}^{B'}), \quad (3)$$

where  $\sigma(\mathbf{z}_{G_j^t}^{B'})$  denotes the predicted probability from the other branch  $B'$  and  $\sigma$  is the Softmax operation. The two branches are alternated in subsequent iterations, allowing the model to progressively adapt through mutual supervision.

### Noisy Pseudo-Label Tolerated Regularization

Pseudo-labeling facilitates adaptation to the target domain by providing surrogate supervision, yet it inevitably introduces label noise that may compromise model performance (Rizve et al. 2021). To address this issue, we propose a noise-aware regularization term that penalizes overconfident or unstable predictions during refinement. This regularization serves as a soft constraint to suppress the influence of unreliable pseudo-labels, guiding the model toward more consistent and robust predictions. Moreover, we provide a theoretical analysis, which guarantees its ability to mitigate the negative impact of noisy supervision and enhance generalization in the target domain. Specifically, we define the refinement loss with the noisy tolerated regularization as:

$$\mathcal{L}_{\text{Re}}^{B'} = \mathcal{L}_{\text{refine}}^{B'} - \frac{\lambda}{|\mathcal{T}_{\text{conf}}^B|} \sum_{G_j^t \in \mathcal{T}_{\text{conf}}^B} \log \left( \langle \sigma(\mathbf{z}_{G_j^t}^{B'}), \sigma(\mathbf{z}_{G_j^t}^B) \rangle \right), \quad (4)$$

where  $\langle \sigma(\mathbf{z}_{G_j^t}^{B'}), \sigma(\mathbf{z}_{G_j^t}^B) \rangle$  denotes the inner product between the softmax predictions of the two branches. Here,  $\sigma$  represents the Softmax function, and  $\mathbf{z}_{G_j^t}^{B'}$ ,  $\mathbf{z}_{G_j^t}^B$  are the graph-level embeddings of  $G_j^t$  produced by branches  $B'$  and  $B$ , respectively.  $B, B' \in \{\text{IB}, \text{EB}\}$  with  $B \neq B'$ . For future analysis of the effectiveness of noisy-tolerant regularization, we derive the gradient of Eq. (4) and introduce Lemma 1.

**Lemma 1** *Let  $\Theta$  denote the parameters of branch  $B'$ . The gradient of Eq. 4 with respect to  $\Theta$  is given by:*

$$\nabla_{\Theta} \mathcal{L}_{\text{Re}}^{B'} = \frac{1}{|\mathcal{T}_{\text{conf}}^B|} \sum_{G_j^t \in \mathcal{T}_{\text{conf}}^B} \nabla_{\Theta} \mathbf{z}_{G_j^t}^{B'} \cdot (\mathbf{p}_j - \tilde{y}_j + \lambda \cdot \mathbf{g}_j),$$

where  $\mathbf{p}_j = \sigma(\mathbf{z}_{G_j^t}^{B'})$ ,  $\mathbf{q}_j = \sigma(\mathbf{z}_{G_j^t}^B)$ , and the regularization gradient  $\mathbf{g}_j \in \mathbb{R}^C$  is defined as:

$$\mathbf{g}_j := \frac{1}{\langle \mathbf{p}_j, \mathbf{q}_j \rangle} \cdot \mathbf{J}_{\mathbf{p}_j}^\top \mathbf{q}_j,$$

with  $[\mathbf{J}_{\mathbf{p}_j}]_{ck} = \frac{\partial p_{j,c}}{\partial z_{j,k}^{B'}} = p_{j,c}(\delta_{ck} - p_{j,k})$ .

Here,  $\delta_{ck}$  denotes the Kronecker delta, which equals 1 if  $c = k$  and 0 otherwise.

---

Algorithm 1: Nested Pseudo-Label Refinement (NeGPR)

---

**Input:** Source domain data  $\mathcal{D}_s = \{(G_i^s, y_i^s)\}$ , target domain data  $\mathcal{D}_t = \{G_j^t\}$ , number of iterations  $T$   
**Output:** Trained model parameters  $\Theta$  for implicit branch (IB) and  $\Theta'$  for explicit branch (EB)

/Stage 1: Dual Branches Pre-Training/  
1: **for**  $B, B' \in \{\text{IB}, \text{EB}\}, B \neq B'$  **do**  
2:   Update  $\Theta$  with Eq. (1)  
3:   Update  $\Theta'$  with Eq. (1)  
4: **end for**

/Stage 2: Nested Refinement with Regularization/  
5: **for**  $i = 1$  to  $T$  **do**  
6:   Filter high-confidence samples  $\mathcal{T}_{\text{conf}}^B$  from branch  $B$  with Eq.(2)  
7:   Update  $\Theta'$  of EB branch by Eq. (4)  
8:   Filter high-confidence samples  $\mathcal{T}_{\text{conf}}^{B'}$  from branch  $B'$  with Eq.(2)  
9:   Update  $\Theta$  of IB branch by Eq. (4)  
10: **end for**  
11: **return** Dual branches parameters  $\Theta$  and  $\Theta'$

---

From Lemma 1, we observe that when the pseudo label  $\tilde{y}_j$  is correct, the prediction  $\mathbf{p}_j$  increasingly aligns with it during training, causing the cross-entropy gradient to diminish. This reduction weakens the learning signal from clean samples and allows noisy examples to dominate the optimization. The regularization term  $\mathbf{g}_j$  alleviates this issue by maintaining substantial gradient contributions for clean instances, thus preserving their supervisory effect even as the loss converges. When  $\tilde{y}_j$  is incorrect, the cross-entropy term  $\mathbf{p}_j - \tilde{y}_j$  becomes positive, leading to updates that push the model away from the true class. The regularization term  $\mathbf{g}_j$ , which is typically negative at the true class index, counteracts this effect by reducing the gradient magnitude on mislabeled examples. This dampening mechanism limits the influence of noisy labels during optimization.

## Learning Framework

The overall learning framework is outlined in Algorithm 1, which adopts an alternating dual-branch strategy to progressively refine pseudo labels and suppress the influence of label noise. The process begins with noise-resilient pre-training on the source domain to initialize both the implicit and explicit branches (lines 1–3). At each iteration, one branch generates pseudo labels for the target domain, and

high-confidence samples are selected based on prediction probability (lines 6 and 8). These samples are then used to update the other branch via a regularized training objective (lines 7 and 9). The two branches alternate roles throughout training (lines 5–10), enabling mutual correction and promoting robust adaptation under noisy supervision.

## Experiments

### Experimental Settings

**Datasets.** To assess the effectiveness of the proposed NeGPR, we conduct extensive experiments on multiple benchmark datasets from TUDataset, covering diverse types of domain shifts. For structure-based domain shifts, we utilize MUTAGENICITY (Kazius, McGuire, and Bursi 2005), NCI1 (Wale, Watson, and Karypis 2008), FRANKENSTEIN (Orsini, Frasconi, and De Raedt 2015), and PROTEINS (Dobson and Doig 2003), where each dataset is partitioned into source and target domains based on variations in edge, node and graph flux density to simulate structural distribution shifts (Yin et al. 2023b). For feature-based domain shifts, we evaluate NeGPR on PROTEINS, DD, BZR, BZR\_MD, COX2, and COX2\_MD (Sutherland, O’Brien, and Weaver 2003), where domain discrepancies primarily arise from differences in semantic feature distributions. Detailed dataset statistics are provided in Appendix C.

**Baselines.** We compare the proposed NeGPR with a comprehensive set of competitive baselines on the datasets above. These baselines include two graph kernel methods: WL (Shervashidze et al. 2011) and PathNN (Michel et al. 2023); four general graph neural networks: GCN (Kipf and Welling 2017b), GIN (Xu et al. 2018), GAT (Veličković et al. 2018), and GMT (Baek, Kang, and Hwang 2021); five label denoising methods: Co-teaching (Han et al. 2018), RTGNN (Qian et al. 2023), Taylor-CE (Feng et al. 2021), OMG (Yin et al. 2023c), and SPORT (Yin et al. 2024a); six graph domain adaptation methods: DEAL (Yin et al. 2022b), CoCo (Yin et al. 2023b), SGDA (Qiao et al. 2023), A2GNN (Liu et al. 2024a), StruRW (Liu et al. 2023), and PA-BOTH (Liu et al. 2024b); and two methods that address both label noise and domain adaptation: ALEX (Yuan et al. 2023a) and ROAD (Feng et al. 2023). More detailed descriptions of the baseline settings are provided in Appendix D.

**Implementation Details.** We implement NeGPR and all baseline models using PyTorch and conduct all experiments on NVIDIA A100 GPUs to ensure a fair comparison. For NeGPR, the implicit branch (IB) is instantiated with the GMT (Baek, Kang, and Hwang 2021) architecture to capture semantic consistency via message passing, while the explicit branch (EB) employs the PathNN model (Michel et al. 2023) to extract high-order topological structures explicitly. Both branches use 4 GNN layers, with a hidden dimension of 256 and a weight decay of  $10^{-12}$ . The models are trained using the Adam optimizer with a learning rate of  $10^{-4}$ . All the models are trained on noisy labeled source graphs and evaluated on unlabeled target graphs. We set the noise ratio  $\alpha = 0.3$  and the pseudo-label threshold  $\zeta = 0.9$  by default. All reported results are averaged over five independent runs.

Table 1: The graph classification results (in %) on the PROTEINS dataset under graph flux density domain shift (source  $\rightarrow$  target). P0, P1, P2 and P3 denote the sub-datasets partitioned with graph flux density. **Bold** results indicate the best performance.

Methods	P0 $\rightarrow$ P1	P1 $\rightarrow$ P0	P0 $\rightarrow$ P2	P2 $\rightarrow$ P0	P0 $\rightarrow$ P3	P3 $\rightarrow$ P0	P1 $\rightarrow$ P2	P2 $\rightarrow$ P1	P1 $\rightarrow$ P3	P3 $\rightarrow$ P1	P2 $\rightarrow$ P3	P3 $\rightarrow$ P2
WL	67.5 $\pm$ 1.4	31.9 $\pm$ 1.9	54.7 $\pm$ 0.8	67.0 $\pm$ 1.5	24.2 $\pm$ 2.4	21.6 $\pm$ 1.8	49.8 $\pm$ 1.0	43.3 $\pm$ 1.7	33.4 $\pm$ 1.9	61.2 $\pm$ 1.3	32.9 $\pm$ 0.8	43.6 $\pm$ 2.1
PathNN	68.0 $\pm$ 1.4	72.6 $\pm$ 2.6	55.1 $\pm$ 2.3	38.2 $\pm$ 2.8	25.4 $\pm$ 2.5	22.6 $\pm$ 4.6	39.9 $\pm$ 3.1	63.6 $\pm$ 1.7	34.4 $\pm$ 2.5	27.6 $\pm$ 2.2	67.0 $\pm$ 1.9	46.7 $\pm$ 2.0
GCN	67.3 $\pm$ 3.5	73.3 $\pm$ 4.3	55.9 $\pm$ 1.7	72.1 $\pm$ 2.6	23.8 $\pm$ 1.7	22.5 $\pm$ 1.4	52.3 $\pm$ 3.9	63.9 $\pm$ 2.4	27.3 $\pm$ 1.0	45.6 $\pm$ 1.7	30.3 $\pm$ 2.1	47.7 $\pm$ 1.4
GIN	62.3 $\pm$ 2.3	59.5 $\pm$ 2.5	50.6 $\pm$ 2.1	49.4 $\pm$ 2.4	24.8 $\pm$ 1.3	60.0 $\pm$ 0.9	45.2 $\pm$ 0.3	56.4 $\pm$ 3.1	66.0 $\pm$ 1.2	34.3 $\pm$ 1.7	33.4 $\pm$ 1.4	48.5 $\pm$ 1.9
GAT	62.8 $\pm$ 0.8	68.1 $\pm$ 1.2	50.1 $\pm$ 1.7	66.2 $\pm$ 1.4	64.6 $\pm$ 2.3	18.0 $\pm$ 1.4	48.9 $\pm$ 1.0	62.8 $\pm$ 1.8	46.5 $\pm$ 1.4	25.5 $\pm$ 1.1	33.1 $\pm$ 0.9	49.0 $\pm$ 2.7
GMT	49.6 $\pm$ 1.0	51.3 $\pm$ 1.3	54.1 $\pm$ 1.6	50.6 $\pm$ 1.3	53.8 $\pm$ 1.1	51.4 $\pm$ 1.7	52.9 $\pm$ 1.9	53.0 $\pm$ 1.1	53.5 $\pm$ 1.0	50.4 $\pm$ 1.1	52.5 $\pm$ 1.2	50.2 $\pm$ 1.0
Co-teaching	67.4 $\pm$ 0.5	69.2 $\pm$ 1.2	54.2 $\pm$ 1.7	69.4 $\pm$ 0.4	24.7 $\pm$ 1.9	25.5 $\pm$ 1.3	49.4 $\pm$ 0.8	61.4 $\pm$ 2.6	38.9 $\pm$ 2.1	47.4 $\pm$ 2.5	43.0 $\pm$ 1.8	46.4 $\pm$ 3.3
Taylor-CE	65.7 $\pm$ 3.6	66.4 $\pm$ 4.3	49.3 $\pm$ 3.5	53.6 $\pm$ 2.9	27.9 $\pm$ 1.5	57.4 $\pm$ 2.4	50.6 $\pm$ 2.2	42.7 $\pm$ 1.8	69.7 $\pm$ 1.9	39.6 $\pm$ 1.7	40.4 $\pm$ 1.3	42.0 $\pm$ 2.7
RTGNN	63.0 $\pm$ 1.8	70.3 $\pm$ 1.2	61.1 $\pm$ 1.8	67.7 $\pm$ 2.5	26.0 $\pm$ 0.7	20.0 $\pm$ 0.9	55.1 $\pm$ 1.4	67.3 $\pm$ 1.7	24.4 $\pm$ 1.3	48.9 $\pm$ 1.5	34.8 $\pm$ 1.2	44.0 $\pm$ 1.5
OMG	64.9 $\pm$ 1.4	72.2 $\pm$ 1.7	47.1 $\pm$ 1.1	63.3 $\pm$ 1.9	68.1 $\pm$ 1.3	22.3 $\pm$ 0.8	46.3 $\pm$ 2.3	59.3 $\pm$ 2.2	52.5 $\pm$ 1.8	21.8 $\pm$ 1.9	35.1 $\pm$ 1.5	43.6 $\pm$ 1.3
SPORT	60.7 $\pm$ 1.4	65.4 $\pm$ 1.8	49.0 $\pm$ 1.2	69.1 $\pm$ 0.5	54.7 $\pm$ 1.1	51.8 $\pm$ 1.5	55.3 $\pm$ 2.1	64.3 $\pm$ 2.4	51.6 $\pm$ 1.3	25.8 $\pm$ 1.2	34.1 $\pm$ 1.7	42.3 $\pm$ 1.9
CoCo	66.9 $\pm$ 1.3	50.9 $\pm$ 1.9	55.2 $\pm$ 1.5	64.4 $\pm$ 1.4	71.4 $\pm$ 1.7	25.9 $\pm$ 1.2	51.6 $\pm$ 2.6	55.1 $\pm$ 2.4	36.7 $\pm$ 1.8	56.3 $\pm$ 1.2	38.3 $\pm$ 1.9	44.5 $\pm$ 3.0
DEAL	66.7 $\pm$ 2.3	71.6 $\pm$ 2.1	55.2 $\pm$ 1.9	70.4 $\pm$ 3.0	34.7 $\pm$ 1.0	58.6 $\pm$ 1.7	51.0 $\pm$ 2.0	65.3 $\pm$ 1.6	43.7 $\pm$ 1.8	66.5 $\pm$ 1.9	63.4 $\pm$ 3.1	46.4 $\pm$ 2.3
SGDA	67.8 $\pm$ 2.1	59.4 $\pm$ 1.3	57.7 $\pm$ 1.6	73.1 $\pm$ 1.8	38.3 $\pm$ 2.4	31.9 $\pm$ 2.7	48.2 $\pm$ 2.0	48.8 $\pm$ 2.2	39.2 $\pm$ 2.0	58.6 $\pm$ 1.6	40.2 $\pm$ 1.8	46.8 $\pm$ 2.3
A2GNN	60.7 $\pm$ 2.2	65.5 $\pm$ 1.8	54.3 $\pm$ 2.0	67.5 $\pm$ 2.0	60.2 $\pm$ 1.9	60.2 $\pm$ 1.9	53.3 $\pm$ 1.7	44.2 $\pm$ 1.5	63.1 $\pm$ 1.8	42.9 $\pm$ 2.3	35.7 $\pm$ 2.5	46.5 $\pm$ 2.1
StruRW	62.5 $\pm$ 2.1	72.9 $\pm$ 1.4	59.2 $\pm$ 1.8	71.0 $\pm$ 2.0	39.8 $\pm$ 1.9	34.9 $\pm$ 2.1	49.6 $\pm$ 1.6	66.6 $\pm$ 2.1	37.4 $\pm$ 2.3	61.1 $\pm$ 1.7	40.5 $\pm$ 1.5	45.9 $\pm$ 2.2
PA-BOTH	64.9 $\pm$ 1.7	73.6 $\pm$ 2.1	58.0 $\pm$ 2.2	69.1 $\pm$ 1.9	36.5 $\pm$ 2.3	54.3 $\pm$ 1.5	53.9 $\pm$ 1.8	67.2 $\pm$ 1.4	42.2 $\pm$ 1.6	67.6 $\pm$ 2.0	63.1 $\pm$ 1.9	45.3 $\pm$ 2.1
ROAD	52.2 $\pm$ 2.6	53.8 $\pm$ 3.2	60.9 $\pm$ 2.7	55.9 $\pm$ 2.1	63.1 $\pm$ 2.0	57.2 $\pm$ 2.7	58.6 $\pm$ 2.4	58.2 $\pm$ 1.7	62.5 $\pm$ 2.0	58.2 $\pm$ 1.8	61.1 $\pm$ 2.5	57.2 $\pm$ 1.7
ALEX	68.7 $\pm$ 2.7	<b>74.9<math>\pm</math>3.0</b>	62.5 $\pm$ 2.8	68.6 $\pm$ 2.6	73.7 $\pm$ 2.8	61.3 $\pm$ 3.4	62.8 $\pm$ 2.6	64.9 $\pm$ 2.1	68.2 $\pm$ 2.0	61.7 $\pm$ 2.2	64.1 $\pm$ 3.0	58.0 $\pm$ 2.2
NeGPR	<b>71.7<math>\pm</math>2.4</b>	74.7 $\pm$ 2.6	<b>64.5<math>\pm</math>2.1</b>	<b>73.3<math>\pm</math>2.1</b>	<b>77.1<math>\pm</math>2.4</b>	<b>63.2<math>\pm</math>1.7</b>	<b>63.8<math>\pm</math>2.5</b>	<b>68.1<math>\pm</math>2.2</b>	<b>70.5<math>\pm</math>2.1</b>	<b>68.4<math>\pm</math>2.4</b>	<b>67.2<math>\pm</math>2.3</b>	<b>61.0<math>\pm</math>1.6</b>

Table 2: The graph classification results (in %) under semantic information shift (source $\rightarrow$ target). P, D, C, CM, B, and BM denote PROTEINS, DD, COX2, COX2\_MD, BZR, and BZR\_MD, respectively. **Bold** indicates the best performance. OOM means out of memory.

Methods	P $\rightarrow$ D	D $\rightarrow$ P	C $\rightarrow$ CM	CM $\rightarrow$ C	B $\rightarrow$ BM	BM $\rightarrow$ B
WL	42.5 $\pm$ 2.0	43.6 $\pm$ 2.4	50.7 $\pm$ 1.5	54.8 $\pm$ 2.0	50.6 $\pm$ 2.2	25.3 $\pm$ 2.3
PathNN	47.5 $\pm$ 1.5	41.1 $\pm$ 2.0	49.8 $\pm$ 1.6	66.9 $\pm$ 2.6	50.3 $\pm$ 1.6	37.2 $\pm$ 2.4
GCN	53.7 $\pm$ 2.3	51.8 $\pm$ 2.0	49.8 $\pm$ 1.6	32.7 $\pm$ 2.9	49.7 $\pm$ 2.1	55.5 $\pm$ 2.7
GIN	48.3 $\pm$ 1.9	49.9 $\pm$ 1.7	51.2 $\pm$ 2.0	52.6 $\pm$ 2.5	48.7 $\pm$ 2.0	55.8 $\pm$ 1.9
GAT	59.2 $\pm$ 1.7	57.4 $\pm$ 2.0	49.3 $\pm$ 2.1	36.4 $\pm$ 2.5	51.3 $\pm$ 1.9	32.7 $\pm$ 2.0
GMT	55.7 $\pm$ 2.5	53.9 $\pm$ 2.6	50.7 $\pm$ 2.1	44.4 $\pm$ 1.9	49.2 $\pm$ 1.7	32.7 $\pm$ 2.2
Co-teaching	55.9 $\pm$ 2.2	60.1 $\pm$ 1.8	47.7 $\pm$ 2.3	48.8 $\pm$ 2.0	50.8 $\pm$ 2.4	44.2 $\pm$ 1.9
Taylor-CE	55.2 $\pm$ 2.0	55.7 $\pm$ 2.2	51.2 $\pm$ 1.8	55.6 $\pm$ 2.5	48.7 $\pm$ 2.0	44.2 $\pm$ 1.9
RTGNN	53.7 $\pm$ 2.0	52.6 $\pm$ 1.9	51.2 $\pm$ 2.0	54.3 $\pm$ 1.6	49.2 $\pm$ 2.8	55.5 $\pm$ 2.3
OMG	56.7 $\pm$ 1.7	53.4 $\pm$ 2.2	54.5 $\pm$ 1.8	57.3 $\pm$ 2.7	50.8 $\pm$ 2.0	59.3 $\pm$ 2.3
SPORT	OOM	OOM	53.7 $\pm$ 2.1	63.9 $\pm$ 3.3	51.4 $\pm$ 2.6	65.8 $\pm$ 3.0
CoCo	62.6 $\pm$ 2.5	67.1 $\pm$ 2.0	56.8 $\pm$ 2.5	67.0 $\pm$ 2.8	50.5 $\pm$ 2.0	79.3 $\pm$ 2.2
DEAL	69.7 $\pm$ 1.9	60.0 $\pm$ 2.5	52.7 $\pm$ 2.1	60.4 $\pm$ 2.2	52.4 $\pm$ 2.9	68.6 $\pm$ 2.8
SGDA	53.3 $\pm$ 1.9	55.2 $\pm$ 3.3	54.1 $\pm$ 2.8	52.6 $\pm$ 2.7	49.6 $\pm$ 2.4	48.3 $\pm$ 2.1
A2GNN	61.6 $\pm$ 2.9	68.8 $\pm$ 2.7	51.2 $\pm$ 2.0	65.4 $\pm$ 2.5	52.1 $\pm$ 2.7	61.1 $\pm$ 2.7
StruRW	52.8 $\pm$ 1.9	56.4 $\pm$ 3.3	52.8 $\pm$ 2.8	51.3 $\pm$ 2.7	48.7 $\pm$ 2.4	49.7 $\pm$ 3.1
PA-BOTH	56.5 $\pm$ 2.9	54.2 $\pm$ 2.6	51.2 $\pm$ 2.9	58.9 $\pm$ 2.3	48.7 $\pm$ 2.7	47.7 $\pm$ 2.5
ROAD	55.2 $\pm$ 2.0	59.5 $\pm$ 3.0	55.2 $\pm$ 2.6	70.2 $\pm$ 2.7	52.7 $\pm$ 2.1	79.0 $\pm$ 2.3
ALEX	68.8 $\pm$ 2.1	68.1 $\pm$ 2.2	56.2 $\pm$ 2.0	69.2 $\pm$ 2.9	54.3 $\pm$ 2.1	78.8 $\pm$ 3.0
NeGPR	<b>72.3<math>\pm</math>2.6</b>	<b>69.9<math>\pm</math>2.8</b>	<b>57.3<math>\pm</math>2.6</b>	<b>73.0<math>\pm</math>2.3</b>	<b>55.9<math>\pm</math>3.0</b>	<b>80.0<math>\pm</math>2.7</b>

## Performance Comparison

We present the results of the proposed NeGPR with all baseline models under the setting of graph domain adaptation on different datasets in Tables 1, 2, and 8-18. From these tables, we observe that: (1) Label denoising methods consistently outperform general graph-based approaches, as the presence of noisy labels significantly impairs the performance of standard graph models lacking dedicated noise-handling mechanisms. (2) Graph domain adaptation methods generally outperform graph-based and label-denoising

approaches by effectively mitigating domain distribution shifts. However, their performance may still degrade when source labels are corrupted, highlighting the need for methods that jointly address domain shift and label noise specific for graphs. (3) Label denoising domain adaptation methods demonstrate superior performance over graph domain adaptation methods, which highlights the importance of explicitly addressing label noise alongside domain alignment to enhance model generalization in noisy cross-domain settings. (4) The proposed NeGPR consistently achieves the highest performance across datasets in most cases, demonstrating its superiority. The outstanding performance is attributed primarily to two factors: (i) the integration of implicit branch and explicit branch enables comprehensive extraction of both structural and semantic features, substantially enhancing representation quality and classification accuracy; and (ii) the nested refinement and noisy tolerated regularization modules jointly promote robust cross-domain adaptation by progressively selecting reliable supervision and suppressing noisy signals. Additional results on other datasets are provided in Appendix E.

## Ablation Study

We conduct ablation studies to examine the contributions of each component in the proposed NeGPR: (1) NeGPR w/o IB: It removes the implicit extraction branch; (2) NeGPR w/o EB: It removes the explicit extraction branch; (3) NeGPR w/o NRL: It removes the noise resilient loss in the pretraining stage; (4) NeGPR w/o NTR: It remove the noisy pseudo-label tolerated regularization loss during fine-tuning.

Experimental results are reported in Table 3, 5-7. From the results, we find that: (1) NeGPR outperforms NeGPR w/o IB and NeGPR w/o EB, underscoring the importance of integrating implicit and explicit branches that capture semantic and structural information. Their joint modeling

Table 3: The results of ablation studies on the PROTEINS dataset (source  $\rightarrow$  target). **Bold** results indicate the best performance.

Methods	P0 $\rightarrow$ P1	P1 $\rightarrow$ P0	P0 $\rightarrow$ P2	P2 $\rightarrow$ P0	P0 $\rightarrow$ P3	P3 $\rightarrow$ P0	P1 $\rightarrow$ P2	P2 $\rightarrow$ P1	P1 $\rightarrow$ P3	P3 $\rightarrow$ P1	P2 $\rightarrow$ P3	P3 $\rightarrow$ P2
NeGPR w/o IB	50.8	50.6	50.7	52.2	50.0	48.6	52.0	52.2	47.7	50.8	52.5	50.3
NeGPR w/o EB	50.4	52.1	49.0	52.1	49.0	51.6	46.5	50.4	51.6	50.4	53.3	49.9
NeGPR w/o NRL	68.5	71.4	62.5	70.0	73.6	60.9	61.2	65.2	68.4	64.6	63.8	58.4
NeGPR w/o NTR	69.7	71.0	63.8	70.3	74.8	62.4	62.4	66.2	69.0	65.5	65.8	58.9
NeGPR	<b>71.7</b>	<b>74.7</b>	<b>64.5</b>	<b>73.3</b>	<b>77.1</b>	<b>63.2</b>	<b>63.8</b>	<b>68.1</b>	<b>70.5</b>	<b>68.4</b>	<b>67.2</b>	<b>61.0</b>

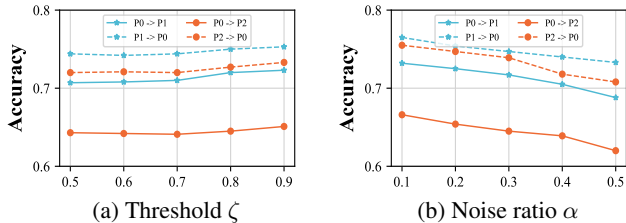


Figure 2: Hyperparameter sensitivity analysis of threshold  $\zeta$  and noise ratio  $\alpha$  on the PROTEINS datasets.

enforces multi-view prediction consistency, providing a robust foundation for effective domain adaptation. (2) NeGPR w/o NRL demonstrates inferior performance compared to NeGPR. The NRL effectively reduces the negative impact of noisy labels in the source domain by promoting local consistency among neighboring nodes. This constraint enables NeGPR to learn noise-resistant representations suitable for domain adaptation. (3) NeGPR outperforms NeGPR w/o NTR, demonstrating that the noise tolerant regularization effectively mitigates the impact of noisy pseudo-labels by preserving reliable supervision from clean samples. This constraint prevents overfitting and enhances the model’s robustness and generalization across domains. Additional results on other datasets are provided in Appendix E.

### Sensitivity Analysis

We perform a sensitivity analysis to examine how the key hyperparameters of NeGPR, namely the pseudo-label confidence threshold  $\zeta$  and the noise ratio  $\alpha$ , affect its performance. Specifically,  $\zeta$  governs the selection of high-confidence pseudo-labeled target samples, while  $\alpha$  determines the proportion of corrupted labels in the source domain. Both parameters play a critical role in balancing supervision quality and model robustness.

Figure 2 illustrates how  $\zeta$  and  $\alpha$  affect the performance of NeGPR on the PROTEINS dataset. We vary  $\zeta$  within the range of  $\{0.5, 0.6, 0.7, 0.8, 0.9\}$  and  $\alpha$  in  $\{0.1, 0.2, 0.3, 0.4, 0.5\}$ . From the results, we observe that: (1) The performance of NeGPR in Figure 2(a) steadily increases as threshold  $\zeta$  rises. A higher threshold can effectively filter out pseudo-labels with lower confidence, which reduces the risk of propagating incorrect information during model training, enabling the model to learn from more reliable supervision signals. Thus, we set the threshold  $\zeta$  to 0.9 as default to ensure optimal pseudo-label reliability. (2) Figure 2(b) illustrates a decreasing accuracy trend with an in-

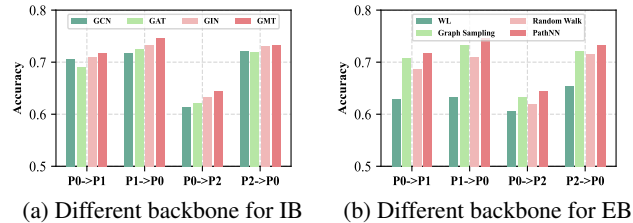


Figure 3: The performance with different backbones for IB and EB on the PROTEINS dataset.

creasing noise ratio  $\alpha$ . A higher noise ratio introduces more incorrectly labeled samples into the source domain, thereby degrading the reliability of supervisory signals during training. Consequently, this prevents the model from accurately learning discriminative representations. To maintain a balance between realistic data conditions and robust performance, we set the noise ratio  $\alpha$  to 0.3 by default. More results on other datasets are shown in Appendix E.

### Flexible Architecture

To assess the impact of different backbone choices for the IB and EB branches, we evaluate various message passing methods in IB, including GCN (Kipf and Welling 2017a), GAT (Veličković et al. 2018), GIN (Xu et al. 2019), and GMT (Baek, Kang, and Hwang 2021), and adopt several graph kernel-based methods in EB, such as Graph Sampling (Leskovec and Faloutsos 2006), Random Walk (Kalofolias, Welke, and Vreeken 2021), WL (Shervashidze et al. 2011), and PathNN (Michel et al. 2023). As shown in Figure 3, and consistently observed across other datasets, GMT and PathNN yield the best performance in most cases. This can be attributed to their superior representation capacity, which provides a solid foundation for capturing both semantic and topological features of graphs. These results further validate our choice of GMT in IB and PathNN in EB, as they offer complementary strengths that enhance the effectiveness of dual-branch modeling. Their strong performance also highlights the importance of backbone selection in ensuring stable adaptation under noisy supervision.

### Conclusion

This paper introduces NeGPR, a noise-aware dual-branch framework for robust GDA under label noise. To tackle noisy supervision and distributional shifts, NeGPR employs a dual-branch pretraining strategy: one branch captures semantic consistency via local message passing, while

the other encodes structural features using a graph kernel method, enabling the extraction of complementary graph representations. A nested pseudo-label refinement mechanism progressively aligns source and target domains by alternately using high-confidence predictions from one branch to supervise the other, enhancing cross-branch consistency and mitigating domain gaps. Additionally, a noise-aware regularization term penalizes overconfident or inconsistent predictions, reducing the impact of noisy labels. Extensive experiments across diverse datasets and noise settings validate the superior robustness and generalization of NeGPR, underscoring its promise for reliable graph transfer learning.

## References

- Baek, J.; Kang, M.; and Hwang, S. J. 2021. Accurate learning of graph representations with graph multiset pooling. *arXiv preprint arXiv:2102.11533*.
- Borgwardt, K. M.; and Kriegel, H.-P. 2005. Shortest-path kernels on graphs. In *Fifth IEEE international conference on data mining (ICDM'05)*, 8–pp. IEEE.
- Cai, R.; Wu, F.; Li, Z.; Wei, P.; Yi, L.; and Zhang, K. 2024. Graph domain adaptation: A generative view. *ACM Transactions on Knowledge Discovery from Data*, 18(3): 1–24.
- Chen, J.; Shah, V.; and Kyriillidis, A. 2020. Negative sampling in semi-supervised learning. In *International Conference on Machine Learning*, 1704–1714. PMLR.
- Chen, X.; Wang, Y.; Fang, J.; Meng, Z.; and Liang, S. 2023. Heterogeneous graph contrastive learning with metapath-based augmentations. *IEEE Transactions on Emerging Topics in Computational Intelligence*, 8(1): 1003–1014.
- Cho, H.; Berger, B.; and Peng, J. 2016. Compact integration of multi-network topology for functional analysis of genes. *Cell systems*, 3(6): 540–548.
- Dai, E.; Aggarwal, C.; and Wang, S. 2021. Nrgnn: Learning a label noise resistant graph neural network on sparsely and noisily labeled graphs. In *Proceedings of the 27th ACM SIGKDD conference on knowledge discovery & data mining*, 227–236.
- Dan, J.; Liu, W.; Xie, X.; Yu, H.; Dong, S.; and Tan, Y. 2024. TFGDA: Exploring topology and feature alignment in semi-supervised graph domain adaptation through robust clustering. *Proceedings of the Conference on Neural Information Processing Systems*, 37: 50230–50255.
- Dobson, P. D.; and Doig, A. J. 2003. Distinguishing enzyme structures from non-enzymes without alignments. *Journal of molecular biology*, 330(4): 771–783.
- Feng, L.; Shu, S.; Lin, Z.; Lv, F.; Li, L.; and An, B. 2021. Can cross entropy loss be robust to label noise? In *Proceedings of the International Joint Conference on Artificial Intelligence*, 2206–2212.
- Feng, Y.; Zhu, H.; Peng, D.; Peng, X.; and Hu, P. 2023. Road: Robust unsupervised domain adaptation with noisy labels. In *Proceedings of the ACM International Conference on Multimedia*, 7264–7273.
- Ganin, Y.; Ustinova, E.; Ajakan, H.; Germain, P.; Larochelle, H.; Laviolette, F.; March, M.; and Lempitsky, V. 2016. Domain-adversarial training of neural networks. *Journal of machine learning research*, 17(59): 1–35.
- Gilmer, J.; Schoenholz, S. S.; Riley, P. F.; Vinyals, O.; and Dahl, G. E. 2017. Neural message passing for quantum chemistry. In *International conference on machine learning*, 1263–1272. Pmlr.
- Hamilton, W. L.; Ying, R.; and Leskovec, J. 2017. Inductive representation learning on large graphs. In *Proceedings of the Conference on Neural Information Processing Systems*.
- Han, B.; Yao, Q.; Yu, X.; Niu, G.; Xu, M.; Hu, W.; Tsang, I.; and Sugiyama, M. 2018. Co-teaching: Robust training of deep neural networks with extremely noisy labels. *Advances in neural information processing systems*, 31.
- Isken, A.; Valmadre, J.; Arnab, A.; and Schmid, C. 2022. Learning with neighbor consistency for noisy labels. 2022 IEEE. In *CVF Conference on Computer Vision and Pattern Recognition (CVPR)*, 4662–4671.
- Kalofolias, J.; Welke, P.; and Vreeken, J. 2021. SUSAN: The Structural Similarity Random Walk Kernel. In *Proceedings of the SIAM International Conference on Data Mining*, 298–306.
- Kazius, J.; McGuire, R.; and Bursi, R. 2005. Derivation and validation of toxicophores for mutagenicity prediction. *Journal of medicinal chemistry*, 48(1): 312–320.
- Kipf, T. N.; and Welling, M. 2017a. Semi-supervised classification with graph convolutional networks. In *Proceedings of the International Conference on Learning Representations*.
- Kipf, T. N.; and Welling, M. 2017b. Semi-Supervised Classification with Graph Convolutional Networks. In *Proceedings of the International Conference on Machine Learning*.
- Lee, D.-H.; et al. 2013. Pseudo-label: The simple and efficient semi-supervised learning method for deep neural networks. In *Workshop on challenges in representation learning, ICML*, volume 3, 896. Atlanta.
- Leskovec, J.; and Faloutsos, C. 2006. Sampling from large graphs. In *Proceedings of the International ACM SIGKDD Conference on Knowledge Discovery & Data Mining*, 631–636.
- Li, J.; Socher, R.; and Hoi, S. C. 2020. Dividemix: Learning with noisy labels as semi-supervised learning. *arXiv preprint arXiv:2002.07394*.
- Lin, M.; Li, W.; Li, D.; Chen, Y.; Li, G.; and Lu, S. 2023. Multi-domain generalized graph meta learning. In *Proceedings of the AAAI Conference on Artificial Intelligence*, 4479–4487.
- Liu, M.; Fang, Z.; Zhang, Z.; Gu, M.; Zhou, S.; Wang, X.; and Bu, J. 2024a. Rethinking propagation for unsupervised graph domain adaptation. In *Proceedings of the AAAI Conference on Artificial Intelligence*, 13963–13971.
- Liu, S.; Li, T.; Feng, Y.; Tran, N.; Zhao, H.; Qiu, Q.; and Li, P. 2023. Structural re-weighting improves graph domain adaptation. In *Proceedings of the International Conference on Machine Learning*, 21778–21793. PMLR.

- Liu, S.; Zou, D.; Zhao, H.; and Li, P. 2024b. Pairwise Alignment Improves Graph Domain Adaptation. In *Proceedings of the International Conference on Machine Learning*, 32552–32575. PMLR.
- Long, M.; Cao, Y.; Wang, J.; and Jordan, M. 2015. Learning transferable features with deep adaptation networks. In *International conference on machine learning*, 97–105. PMLR.
- Long, M.; Cao, Z.; Wang, J.; and Jordan, M. I. 2018. Conditional adversarial domain adaptation. In *Proceedings of the Conference on Neural Information Processing Systems*.
- Luo, Y.; Wang, Z.; Chen, Z.; Huang, Z.; and Baktashmotlagh, M. 2023. Source-free progressive graph learning for open-set domain adaptation. *IEEE Transactions on Pattern Analysis and Machine Intelligence*, 45(9): 11240–11255.
- Michel, G.; Nikolentzos, G.; Lutzeyer, J. F.; and Vazirgiannis, M. 2023. Path neural networks: Expressive and accurate graph neural networks. In *Proceedings of the International Conference on Machine Learning*, 24737–24755. PMLR.
- Natarajan, N.; Dhillon, I. S.; Ravikumar, P. K.; and Tewari, A. 2013. Learning with noisy labels. *Advances in neural information processing systems*, 26.
- Nikolentzos, G.; Siglidis, G.; and Vazirgiannis, M. 2021. Graph kernels: A survey. *Journal of Artificial Intelligence Research*, 72: 943–1027.
- Orsini, F.; Frasconi, P.; and De Raedt, L. 2015. Graph invariant kernels. In *Proceedings of the International Joint Conference on Artificial Intelligence*.
- Pei, Z.; Cao, Z.; Long, M.; and Wang, J. 2018. Multi-adversarial domain adaptation. In *Proceedings of the AAAI conference on artificial intelligence*, volume 32.
- Platanios, E. A.; Dubey, A.; and Mitchell, T. 2016. Estimating accuracy from unlabeled data: A bayesian approach. In *International Conference on Machine Learning*, 1416–1425. PMLR.
- Qian, S.; Ying, H.; Hu, R.; Zhou, J.; Chen, J.; Chen, D. Z.; and Wu, J. 2023. Robust training of graph neural networks via noise governance. In *Proceedings of the International ACM Conference on Web Search & Data Mining*, 607–615.
- Qiao, Z.; Luo, X.; Xiao, M.; Dong, H.; Zhou, Y.; and Xiong, H. 2023. Semi-supervised domain adaptation in graph transfer learning. In *Proceedings of the International Joint Conference on Artificial Intelligence*, 2279–2287.
- Rizve, M. N.; Duarte, K.; Rawat, Y. S.; and Shah, M. 2021. In Defense of Pseudo-Labeling: An Uncertainty-Aware Pseudo-label Selection Framework for Semi-Supervised Learning. In *International Conference on Learning Representations*.
- Shervashidze, N.; Schweitzer, P.; Van Leeuwen, E. J.; Mehlhorn, K.; and Borgwardt, K. M. 2011. Weisfeiler-lehman graph kernels. *Journal of Machine Learning Research*, 12(9).
- Stokes, J. M.; Yang, K.; Swanson, K.; Jin, W.; Cubillos-Ruiz, A.; Donghia, N. M.; MacNair, C. R.; French, S.; Carfrae, L. A.; Bloom-Ackermann, Z.; et al. 2020. A deep learning approach to antibiotic discovery. *Cell*, 180(4): 688–702.
- Sutherland, J. J.; O’Brien, L. A.; and Weaver, D. F. 2003. Spline-fitting with a genetic algorithm: A method for developing classification structure- activity relationships. *Journal of chemical information and computer sciences*, 43(6): 1906–1915.
- Tzeng, E.; Hoffman, J.; Saenko, K.; and Darrell, T. 2017. Adversarial discriminative domain adaptation. In *Proceedings of the IEEE conference on computer vision and pattern recognition*, 7167–7176.
- Veličković, P.; Cucurull, G.; Casanova, A.; Romero, A.; Liò, P.; and Bengio, Y. 2018. Graph Attention Networks. In *Proceedings of the International Conference on Learning Representations*.
- Veličković, P.; Cucurull, G.; Casanova, A.; Romero, A.; Liò, P.; and Bengio, Y. 2018. Graph Attention Networks. *Proceedings of the International Conference on Learning Representations*.
- Wale, N.; Watson, I. A.; and Karypis, G. 2008. Comparison of descriptor spaces for chemical compound retrieval and classification. *Knowledge and Information Systems*, 14: 347–375.
- Wang, M.; Su, H.; Wang, S.; Wang, S.; Yin, N.; Shen, L.; Lan, L.; Yang, L.; and Cao, X. 2025. Graph Convolutional Mixture-of-Experts Learner Network for Long-Tailed Domain Generalization. *IEEE Transactions on Circuits and Systems for Video Technology*.
- Wang, T.; and Isola, P. 2020. Understanding contrastive representation learning through alignment and uniformity on the hypersphere. In *Proceedings of the International Conference on Machine Learning*, 9929–9939. PMLR.
- Wang, Y.; Chang, Y.-Y.; Liu, Y.; Leskovec, J.; and Li, P. 2021. Inductive representation learning in temporal networks via causal anonymous walks. *arXiv*.
- Wang, Y.; Liang, V.; Yin, N.; Liu, S.; and Segal, E. 2024a. SGAC: A Graph Neural Network Framework for Imbalanced and Structure-Aware AMP Classification. *arXiv preprint arXiv:2412.16276*.
- Wang, Y.; Liu, S.; Wang, M.; Liang, S.; and Yin, N. 2024b. Degree distribution based spiking graph networks for domain adaptation. *arXiv e-prints*, arXiv–2410.
- Wang, Y.; and Yang, Y. 2022. Bayesian robust graph contrastive learning. *arXiv preprint arXiv:2205.14109*.
- Wang, Y.; Yin, N.; Xiao, M.; Yi, X.; Liu, S.; and Liang, S. 2024c. Dusego: Dual second-order equivariant graph ordinary differential equation. *arXiv preprint arXiv:2411.10000*.
- Wang, Z.; Sun, D.; Zhou, S.; Wang, H.; Fan, J.; Huang, L.; and Bu, J. 2024d. NoisyGL: A Comprehensive Benchmark for Graph Neural Networks under Label Noise. *arXiv preprint arXiv:2406.04299*.
- Wei, H.; Feng, L.; Chen, X.; and An, B. 2020. Combating noisy labels by agreement: A joint training method with co-regularization. In *Proceedings of the IEEE/CVF conference on computer vision and pattern recognition*, 13726–13735.
- Wu, M.; Pan, S.; and Zhu, X. 2022. Attraction and repulsion: Unsupervised domain adaptive graph contrastive learning network. *IEEE Transactions on Emerging Topics in Computational Intelligence*, 6(5): 1079–1091.

- Xie, Q.; Luong, M.-T.; Hovy, E.; and Le, Q. V. 2020. Self-training with noisy student improves imagenet classification. In *Proceedings of the IEEE/CVF conference on computer vision and pattern recognition*, 10687–10698.
- Xu, G.; Yi, L.; Xu, P.; Li, J.; Pu, R.; Shui, C.; Ling, C.; McLeod, A. I.; and Wang, B. 2025. Unraveling the Mysteries of Label Noise in Source-Free Domain Adaptation: Theory and Practice. *IEEE Transactions on Pattern Analysis and Machine Intelligence*.
- Xu, K.; Hu, W.; Leskovec, J.; and Jegelka, S. 2018. How Powerful are Graph Neural Networks? In *Proceedings of the International Conference on Machine Learning*.
- Xu, K.; Hu, W.; Leskovec, J.; and Jegelka, S. 2019. How Powerful are Graph Neural Networks? In *Proceedings of the International Conference on Learning Representations*.
- Yao, T.; Wang, Y.; Zhang, K.; and Liang, S. 2023. Improving the expressiveness of k-hop message-passing gnns by injecting contextualized substructure information. In *Proceedings of the International ACM SIGKDD Conference on Knowledge Discovery & Data Mining*, 3070–3081.
- Yin, N.; Feng, F.; Luo, Z.; Zhang, X.; Wang, W.; Luo, X.; Chen, C.; and Hua, X.-S. 2022a. Dynamic hypergraph convolutional network. In *2022 IEEE 38th International Conference on Data Engineering (ICDE)*, 1621–1634. IEEE.
- Yin, N.; Shen, L.; Chen, C.; Hua, X.-S.; and Luo, X. 2024a. Sport: A subgraph perspective on graph classification with label noise. *ACM Transactions on Knowledge Discovery from Data*, 18(9): 1–20.
- Yin, N.; Shen, L.; Li, B.; Wang, M.; Luo, X.; Chen, C.; Luo, Z.; and Hua, X.-S. 2022b. Deal: An unsupervised domain adaptive framework for graph-level classification. In *Proceedings of the ACM International Conference on Multimedia*, 3470–3479.
- Yin, N.; Shen, L.; Wang, M.; Lan, L.; Ma, Z.; Chen, C.; Hua, X.-S.; and Luo, X. 2023a. CoCo: A Coupled Contrastive Framework for Unsupervised Domain Adaptive Graph Classification. In *Proceedings of the International Conference on Machine Learning*, 40040–40053.
- Yin, N.; Shen, L.; Wang, M.; Lan, L.; Ma, Z.; Chen, C.; Hua, X.-S.; and Luo, X. 2023b. Coco: A coupled contrastive framework for unsupervised domain adaptive graph classification. In *Proceedings of the International Conference on Machine Learning*, 40040–40053. PMLR.
- Yin, N.; Shen, L.; Wang, M.; Luo, X.; Luo, Z.; and Tao, D. 2023c. Omg: Towards effective graph classification against label noise. *IEEE Transactions on Knowledge and Data Engineering*, 35(12): 12873–12886.
- Yin, N.; Wan, M.; Shen, L.; Patel, H. L.; Li, B.; Gu, B.; and Xiong, H. 2024b. Continuous spiking graph neural networks. *arXiv preprint arXiv:2404.01897*.
- Yin, N.; Wang, M.; Chen, Z.; De Masi, G.; Xiong, H.; and Gu, B. 2024c. Dynamic spiking graph neural networks. In *Proceedings of the AAAI Conference on Artificial Intelligence*, volume 38, 16495–16503.
- Yin, N.; Wang, M.; Chen, Z.; Shen, L.; Xiong, H.; Gu, B.; and Luo, X. 2024d. DREAM: Dual structured exploration with mixup for open-set graph domain adaptation. In *Proceedings of the International Conference on Learning Representations*.
- Yin, Z.; Feng, Y.; Yan, M.; Song, X.; Peng, D.; and Wang, X. 2025. RoDA: Robust Domain Alignment for Cross-Domain Retrieval Against Label Noise. In *Proceedings of the AAAI Conference on Artificial Intelligence*, volume 39, 9535–9543.
- You, Y.; Chen, T.; Wang, Z.; and Shen, Y. 2022. Bringing your own view: Graph contrastive learning without pre-fabricated data augmentations. In *Proceedings of the International ACM Conference on Web Search & Data Mining*, 1300–1309.
- Yu, X.; Liu, T.; Gong, M.; Zhang, K.; Batmanghelich, K.; and Tao, D. 2020. Label-noise robust domain adaptation. In *Proceedings of the International Conference on Machine Learning*, 10913–10924. PMLR.
- Yu, Y.; Ko, M.; Shin, S.; Kim, K.; and Lee, K. 2024. Curriculum Fine-tuning of Vision Foundation Model for Medical Image Classification Under Label Noise. *Proceedings of the Conference on Neural Information Processing Systems*, 37: 18205–18224.
- Yuan, J.; Luo, X.; Qin, Y.; Mao, Z.; Ju, W.; and Zhang, M. 2023a. Alex: Towards effective graph transfer learning with noisy labels. In *Proceedings of the ACM International Conference on Multimedia*, 3647–3656.
- Yuan, J.; Luo, X.; Qin, Y.; Zhao, Y.; Ju, W.; and Zhang, M. 2023b. Learning on graphs under label noise. In *ICASSP 2023-2023 IEEE International Conference on Acoustics, Speech and Signal Processing (ICASSP)*, 1–5. IEEE.
- Zhu, Q.; Jiao, Y.; Ponomareva, N.; Han, J.; and Perozzi, B. 2023. Explaining and Adapting Graph Conditional Shift. *arxiv*.
- Zhu, Q.; Yang, C.; Xu, Y.; Wang, H.; Zhang, C.; and Han, J. 2021. Transfer learning of graph neural networks with ego-graph information maximization. *Proceedings of the Conference on Neural Information Processing Systems*, 34: 1766–1779.
- Zhu, Y.; Feng, L.; Deng, Z.; Chen, Y.; Amor, R.; and Witbrock, M. 2024. Robust node classification on graph data with graph and label noise. In *Proceedings of the AAAI Conference on Artificial Intelligence*, volume 38, 17220–17227.

## A. Proof of Lemma 1

**Lemma 1** Let  $\Theta$  denote the parameters of branch  $B'$ . The gradient of the loss function in Eq. 4 with respect to  $\Theta$  is given by

$$\nabla_{\Theta} \mathcal{L}_{Re}^{B'} = \frac{1}{|\mathcal{T}_{conf}^B|} \sum_{G_j^t \in \mathcal{T}_{conf}^B} \nabla_{\Theta} \mathbf{z}_{G_j^t}^{B'} \cdot (\mathbf{p}_j - \tilde{\mathbf{y}}_j + \lambda \cdot \mathbf{g}_j),$$

where the regularization gradient  $\mathbf{g}_j \in \mathbb{R}^C$  is defined as

$$\mathbf{g}_j := \frac{1}{\langle \mathbf{p}_j, \mathbf{q}_j \rangle} \cdot \mathbf{J}_{\mathbf{p}_j}^{\top} \mathbf{q}_j, \quad \text{with} \quad [\mathbf{J}_{\mathbf{p}_j}]_{ck} = \frac{\partial p_{j,c}}{\partial z_{j,k}^{B'}} = p_{j,c}(\delta_{ck} - p_{j,k}).$$

Here,  $\delta_{ck}$  denotes the Kronecker delta, which equals 1 if  $c = k$  and 0 otherwise.

*Proof:*

$$\begin{aligned} \mathcal{L}_{Re}^{B'} &= \mathcal{L}_{refine}^{B'} - \frac{\lambda}{|\mathcal{T}_{conf}^B|} \sum_{G_j^t \in \mathcal{T}_{conf}^B} \log \left( \langle \sigma(\mathbf{z}_{G_j^t}^{B'}), \sigma(\mathbf{z}_{G_j^t}^B) \rangle \right) \\ &= \mathcal{L}_{pre}^{B'} - \frac{1}{|\mathcal{T}_{conf}^B|} \sum_{G_j^t \in \mathcal{T}_{conf}^B} \tilde{\mathbf{y}}_j \log \sigma(\mathbf{z}_{G_j^t}^{B'}) - \frac{\lambda}{|\mathcal{T}_{conf}^B|} \sum_{G_j^t \in \mathcal{T}_{conf}^B} \log \left( \langle \sigma(\mathbf{z}_{G_j^t}^{B'}), \sigma(\mathbf{z}_{G_j^t}^B) \rangle \right) \\ &= \mathcal{L}_{pre}^{B'} + \mathcal{L}_{rest}^{B'}. \end{aligned} \quad (5)$$

Due to the pre-training process of dual branches, models are overfitted to the loss  $\mathcal{L}_{pre}^{B'}$ , therefore, we simply focus on the remaining term  $\mathcal{L}_{rest}^{B'}$ . Denote  $\mathbf{p}_j = \sigma(\mathbf{z}_{G_j^t}^{B'})$ ,  $\mathbf{q}_j = \sigma(\mathbf{z}_{G_j^t}^B)$ , we have:

$$\nabla_{\Theta} \mathcal{L}_{rest}^{B'} = \frac{1}{|\mathcal{T}_{conf}^B|} \sum_{G_j^t \in \mathcal{T}_{conf}^B} \nabla_{\Theta} \mathbf{z}_{G_j^t}^{B'} \cdot \frac{\partial l_{G_j^t}^{B'}}{\partial \mathbf{z}_{G_j^t}^{B'}}, \quad (6)$$

where  $l_{G_j^t}^{B'}$  is the loss on the sample  $G_j^t$  of branch  $B'$ . Then, we compute the partial derivative of the loss with respect to  $\mathbf{z}_{G_j^t}^{B'}$ :

$$\begin{aligned} \frac{\partial l_{G_j^t}^{B'}}{\partial \mathbf{z}_{G_j^t}^{B'}} &= \frac{\partial}{\partial \mathbf{z}_{G_j^t}^{B'}} \left( -\tilde{\mathbf{y}}_j^{\top} \log \mathbf{p}_j - \lambda \log \langle \mathbf{p}_j, \mathbf{q}_j \rangle \right) \\ &= \mathbf{p}_j - \tilde{\mathbf{y}}_j + \lambda \cdot \frac{1}{\langle \mathbf{p}_j, \mathbf{q}_j \rangle} \cdot \mathbf{J}_{\mathbf{p}_j}^{\top} \mathbf{q}_j, \end{aligned} \quad (7)$$

where  $\mathbf{J}_{\mathbf{p}_j}$  is the Jacobian of the softmax function:

$$[\mathbf{J}_{\mathbf{p}_j}]_{ck} = \frac{\partial p_{j,c}}{\partial z_{j,k}^{B'}} = p_{j,c}(\delta_{ck} - p_{j,k}), \quad (8)$$

where  $\delta_{ck}$  is the Kronecker delta, equal to 1 if  $c = k$ , and 0 otherwise. Define the regularizer gradient vector  $\mathbf{g}_j \in \mathbb{R}^C$  as:

$$\mathbf{g}_j := \frac{1}{\langle \mathbf{p}_j, \mathbf{q}_j \rangle} \cdot \mathbf{J}_{\mathbf{p}_j}^{\top} \mathbf{q}_j. \quad (9)$$

The  $c$ -th entry of  $\mathbf{g}_j$  can be explicitly expanded as:

$$g_{j,c} = \frac{p_{j,c}}{\langle \mathbf{p}_j, \mathbf{q}_j \rangle} \sum_{k=1}^C (q_{j,k} - q_{j,c}) p_{j,k}. \quad (10)$$

where  $c \in \{1, \dots, C\}$  denotes the class index;  $p_{j,c}$  and  $q_{j,k}$  are softmax probabilities from branches  $B'$  and  $B$ , respectively. Substituting Eq. (7) into Eq. (6), we obtain the final expression:

$$\nabla_{\Theta} \mathcal{L}_{rest}^{B'} = \frac{1}{|\mathcal{T}_{conf}^B|} \sum_{G_j^t \in \mathcal{T}_{conf}^B} \nabla_{\Theta} \mathbf{z}_{G_j^t}^{B'} \cdot (\mathbf{p}_j - \tilde{\mathbf{y}}_j + \lambda \cdot \mathbf{g}_j), \quad (11)$$

where  $\mathbf{g}_j$  is defined as in Eq. (10).

## B. Complexity Analysis

The overall time complexity of the proposed NeGPR framework is determined by two main stages: noise-resilient pre-training and nested pseudo-label refinement. In the pre-training phase, the Implicit Branch (IB) incurs a complexity of  $\mathcal{O}(L \cdot (|\mathcal{V}| + |\mathcal{E}|) \cdot d_g)$ , while the Explicit Branch (EB) has a complexity of  $\mathcal{O}(|\mathcal{V}| \cdot (|\mathcal{V}| + |\mathcal{E}|))$  for shortest-path computation, along with an additional  $\mathcal{O}(n_s^2 \cdot d_g)$  for semantic neighbor search, where  $d_g$  is the embedding dimension and  $L$  represents the number of GNN layers. During the refinement stage, the forward pass over  $n_t$  target graphs incurs a cost of  $\mathcal{O}(n_t \cdot L \cdot (|\mathcal{V}| + |\mathcal{E}|) \cdot d_g \cdot T)$ . The total time complexity of NeGPR is:  $\mathcal{O}(n_s \cdot (L \cdot (|\mathcal{V}| + |\mathcal{E}|) \cdot d_g + |\mathcal{V}| \cdot (|\mathcal{V}| + |\mathcal{E}|)) + n_s^2 \cdot d_g) + \mathcal{O}(n_t \cdot L \cdot (|\mathcal{V}| + |\mathcal{E}|) \cdot d_g \cdot T)$ .

## C. Dataset

Table 4: Statistics of the experimental datasets.

Datasets	Graphs	Avg. Nodes	Avg. Edges	Classes
NCI1	4,110	29.87	32.30	2
MUTAGENICITY	4,337	30.32	30.77	2
FRANKENSTEIN	4,337	16.9	17.88	2
PROTEINS	1,113	39.1	72.8	2
DD	1,178	284.32	715.66	2
COX2	467	41.22	43.45	2
COX2_MD	303	26.28	335.12	2
BZR	405	35.75	38.36	2
BZR_MD	306	21.30	225.06	2

### Dataset Description

We conduct extensive experiments on four public benchmark graph datasets from TUDataset. The dataset statistics can be found in Table 4, and their details are shown as follows:

- For structure-based domain shifts:
  - **PROTEINS.** The PROTEINS dataset (Dobson and Doig 2003) contains 1,113 protein graphs. Each graph is labeled to indicate whether the corresponding protein is an enzyme. Nodes represent amino acids, and edges are constructed between amino acids within 6 Å along the sequence. We divide the PROTEINS dataset into four subsets, P0, P1, P2, and P3, based on edge density, node density, and graph flux, which exhibit significant domain shifts.
  - **NCI1.** The NCI1 (Wale, Watson, and Karypis 2008) dataset consists of 4,100 molecular graphs, with atoms as nodes and chemical bonds as edges. Each graph is labeled based on its ability to inhibit cancer cell growth. Following the PROTEINS dataset, we divide the NCI1 dataset into four subsets, N0, N1, N2, and N3, based on edge density, node density, and graph flux.
  - **FRANKENSTEIN.** The FRANKENSTEIN (Orsini, Frasconi, and De Raedt 2015) dataset comprises 4,337 molecular graphs, with atoms as nodes and chemical bonds as edges. Each graph is labeled according to the molecule’s biological activity. Following the PROTEINS dataset, we divide the FRANKENSTEIN dataset into four subsets, F0, F1, F2, and F3, based on edge density, node density, and graph flux.
  - **MUTAGENICITY.** The MUTAGENICITY (Kazius, McGuire, and Bursi 2005) dataset includes 4,337 molecular graphs, where atoms serve as nodes and chemical bonds as edges. Labels indicate whether a compound is mutagenic, contributing to research in toxicology and chemical risk assessment. Following the PROTEINS dataset, we divide the MUTAGENICITY dataset into four subsets, M0, M1, M2, and M3, based on edge density, node density, and graph flux.
- For feature-based domain shifts:
  - **DD.** The DD dataset (Dobson and Doig 2003) contains 1,178 graphs representing protein structures, where nodes represent amino acids and edges capture spatial or chemical proximity. DD graphs are larger and denser than PROTEINS graphs, introducing structural variations while maintaining similar label semantics.
  - **COX2.** The COX2 dataset (Sutherland, O’Brien, and Weaver 2003) contains 467 molecular graphs, while COX2\_MD includes 303 modified molecular graphs. In both datasets, nodes represent atoms and edges correspond to chemical bonds. COX2\_MD introduces structural variations to COX2 while maintaining semantic consistency, making them suitable for evaluating model robustness under domain shifts.
  - **BZR.** The BZR dataset (Sutherland, O’Brien, and Weaver 2003) consists of 405 molecular graphs. The BZR\_MD dataset contains 306 graphs with modified structures derived from BZR. Nodes correspond to atoms, and edges represent chemical bonds. BZR\_MD introduces structural variations to simulate domain shifts while maintaining consistent label semantics.

## Data processing

In our implementation, we first process the raw graph-structured data, where each instance comprises an adjacency matrix, node features, and a graph-level label. Then, node representations are generated using available information, such as labels, attributes, or structural statistics, to ensure consistency across graphs. Furthermore, we incorporate path-based features and subgraph samples obtained through topology-aware and random sampling strategies to enhance structural representation. These components are integrated into a unified representation that captures global topology and local substructure information.

## D. Baselines

In this part, we introduce the details of the compared baselines as follows:

- **Graph kernel method.** We compare our NeGPR with two graph kernel methods:
  - **WL:** The Weisfeiler-Lehman (WL) subtree method (Shervashidze et al. 2011) iteratively refines node labels by hashing the concatenation of each node’s current label and the sorted multiset of its neighbors’ labels. This process enables efficient and expressive encoding of hierarchical structural features.
  - **PathNN:** Path Neural Networks (PathNN) (Michel et al. 2023) enhance expressiveness by explicitly modeling paths between nodes. They aggregate path-based features through attention mechanisms, capturing higher-order structural dependencies beyond immediate neighbors while preserving permutation invariance and computational efficiency.
- **Graph neural networks.** We compare our NeGPR with four general graph neural networks:
  - **GCN:** Graph Convolutional Networks (GCN) (Kipf and Welling 2017b) update node representations by aggregating and transforming features from immediate neighbors. They employ a normalized adjacency matrix to ensure numerical stability and preserve local graph structure during message passing.
  - **GIN:** Graph Isomorphism Networks (GIN) (Xu et al. 2018) aggregate features from neighboring nodes using a sum operation, followed by a multi-layer perceptron. This design enables maximally expressive representations while mitigating over-smoothing through injective aggregation functions.
  - **GAT:** Graph Attention Networks (GAT) (Veličković et al. 2018) compute node representations by assigning learnable attention weights to neighboring nodes through self-attention mechanisms. This allows for adaptive, weighted feature aggregation without relying on predefined graph structures or normalization constraints.
  - **GMT:** Graph Multiset Transformer (GMT) (Baek, Kang, and Hwang 2021) employs attention-based pooling with learnable queries to aggregate node features into graph-level representations. It decouples feature selection from structural bias, enabling flexible and expressive global information extraction.
- **Label denoising methods.** We compare our NeGPR with five label denoising methods:
  - **Co-teaching:** Co-teaching (Han et al. 2018) trains two networks simultaneously, where each selects small-loss samples to teach the other, effectively filtering out noisy labels. This mutual-update strategy dynamically adjusts sample selection, enhancing robustness against severe label noise.
  - **RTGNN:** RTGNN (Qian et al. 2023) introduces a noise governance framework for graph neural networks by identifying and mitigating noisy nodes through confidence estimation and adaptive neighbor selection. It further incorporates consistency regularization to ensure stable representation learning under noisy supervision.
  - **Taylor-CE:** Taylor-CE (Feng et al. 2021) enhances the robustness of cross-entropy loss to label noise by approximating it with a Taylor series expansion, which attenuates the influence of mislabeled samples through bounded gradients and smoother optimization dynamics.
  - **OMG:** OMG (Yin et al. 2023c) mitigates label noise in graph classification by jointly optimizing graph embeddings and label reliability. It employs an online sample reweighting mechanism that dynamically adjusts the training focus based on prediction confidence and noise estimation.
  - **SPORT:** SPORT (Yin et al. 2024a) addresses label noise by modeling graph classification from a subgraph perspective, identifying reliable substructures through contrastive learning and sample selection. These substructures are then integrated using a noise-tolerant voting mechanism to enhance representation fidelity.
- **Graph domain adaptation methods.** We compare our NeGPR with six graph domain adaptation methods:
  - **DEAL:** DEAL (Yin et al. 2022b) is an unsupervised domain adaptation framework that aligns source and target domains at both the feature and prediction levels using adversarial learning. It further enhances cross-domain generalization by iteratively refining pseudo-labels through entropy minimization and consistency regularization.
  - **CoCo:** CoCo (Yin et al. 2023b) introduces a coupled contrastive framework that simultaneously aligns instance-level and class-level representations across domains to capture both fine-grained and semantic-level consistency. It leverages contrastive objectives to enhance feature discrimination and cross-domain coherence.

- **SGDA:** SGDA (Qiao et al. 2023) integrates semi-supervised learning with domain adaptation by leveraging limited labeled target data to guide feature alignment between domains. It employs consistency regularization and entropy minimization to enhance representation transfer and reduce domain shift.
  - **A2GNN:** A2GNN (Liu et al. 2024a) reexamines feature propagation in graph domain adaptation by introducing a structure-aware propagation strategy that mitigates noise amplification. It further incorporates domain-specific normalization to enhance stability and alignment during unsupervised adaptation.
  - **StruRW:** StruRW (Liu et al. 2023) introduces a structural re-weighting mechanism that dynamically adjusts the importance of nodes and edges based on their domain relevance. It enhances feature alignment by emphasizing transferable structures while suppressing domain-specific noise.
  - **PA-BOTH:** PA-BOTH (Liu et al. 2024b) leverages pairwise alignment to explicitly match semantically similar node pairs across domains, enhancing structural and feature-level consistency. It further refines domain adaptation by integrating alignment signals into the representation learning process.
- **Label denoising domain adaptation methods.** We compare our NeGPR with two label denoising domain adaptation methods:
    - **ALEX:** ALEX (Yuan et al. 2023a) proposes a noise-robust graph transfer learning framework that addresses label noise in the source domain through adaptive label correction and structure-aware contrastive learning. It jointly refines pseudo-labels and aligns domain-invariant representations to improve cross-domain generalization under noisy supervision.
    - **ROAD:** ROAD (Feng et al. 2023) introduces a robust Unsupervised Domain Adaptation (UDA) framework that combats source label noise and domain shift by combining source sample weighting, confident target regularization, and adversarial alignment. It enhances model generalization by jointly filtering noisy labels and promoting cross-domain consistency.

For GCN, GIN, GAT, and GMT, we implement the models using PyTorch Geometric<sup>1</sup>. For the other baseline methods, we utilize the official source code released by the respective authors. All models are trained using the Adam optimizer with a learning rate of  $10^{-4}$ , a hidden embedding dimension of 256, a weight decay of  $10^{-12}$ , and GNN layers of 4.

## E. More experimental results

### More Performance Comparison

In this part, we provide additional results for our proposed method NeGPR compared with all baseline models across various datasets, as illustrated in Table 8-18. These results consistently show that NeGPR outperforms the baselines in most cases, validating the superiority of our proposed method.

### More Ablation study

To validate the effectiveness of the different components in NeGPR, we conduct more experiments with four variants on the NCI1, FRANKENSTEIN and MUTAGENICITY datasets, i.e., NeGPR w/o IB, NeGPR w/o EB, NeGPR w/o NRL, and NeGPR w/o NTR. The results are shown in Table 5, 6 and 7. From the results, we have similar observations as summarized in Section 4.3.

### More Sensitivity Analysis

In this part, we provide additional results about the flexible architecturesensitivity analysis of the proposed NeGPR with respect to the impact of its hyperparameters: threshold  $\zeta$  and noise ratio  $\alpha$  on the NCI1, FRANKENSTEIN, and MUTAGENICITY datasets. The results are illustrated in Figure 4 and 5, where we observe trends similar to those discussed in Section 4.4.

### More Flexible Architecture

In this part, we provide additional results about the flexible architecture of the proposed NeGPR on the NCI1, FRANKENSTEIN, and MUTAGENICITY datasets. The results are illustrated in Figure 6 and 7, where we observe trends similar to those discussed in Section 4.5.

---

<sup>1</sup><https://www.pyg.org/>

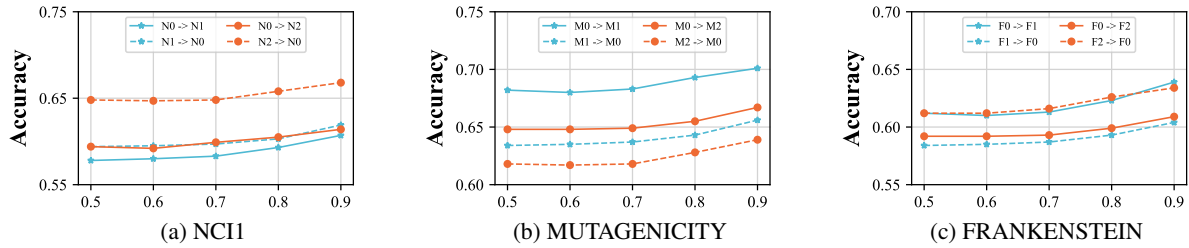


Figure 4: Hyperparameter sensitivity analysis of threshold  $\zeta$  on the NCI1, MUTAGENICITY, and FRANKENSTEIN datasets.

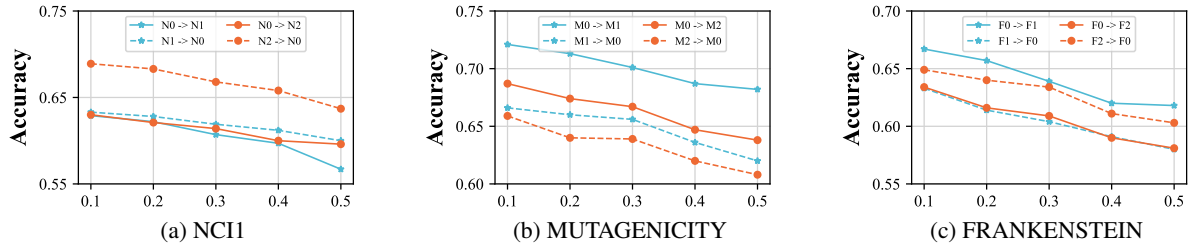


Figure 5: Hyperparameter sensitivity analysis of noise ratio  $\alpha$  on the NCI1, MUTAGENICITY, and FRANKENSTEIN datasets.

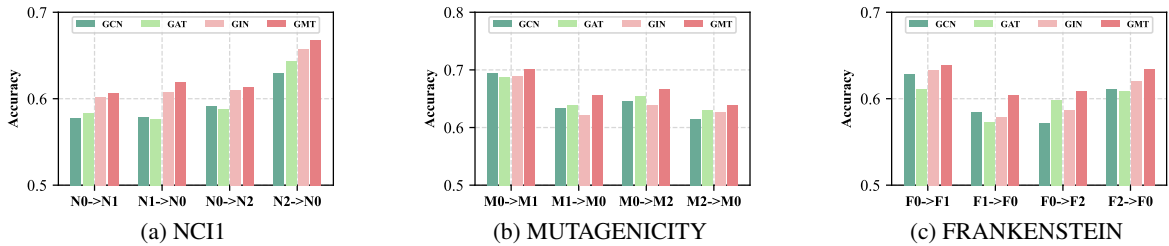


Figure 6: The performance with different backbones for IB on the NCI1, MUTAGENICITY, and FRANKENSTEIN datasets.

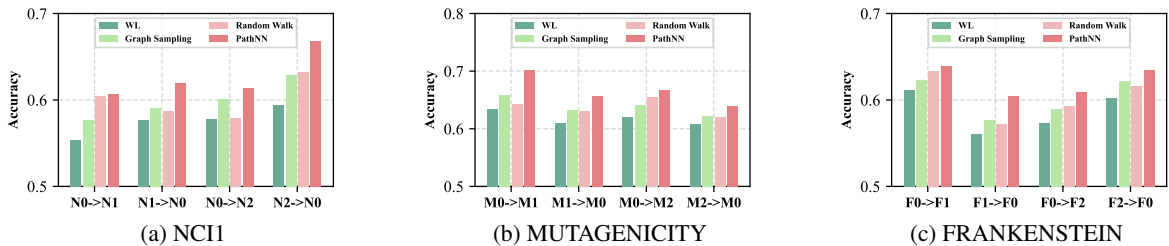


Figure 7: The performance with different backbones for EB on the NCI1, MUTAGENICITY, and FRANKENSTEIN datasets.

Table 5: The results of ablation studies on the NCI1 dataset (source  $\rightarrow$  target). **Bold** results indicate the best performance per column.

Methods	N0 $\rightarrow$ N1	N1 $\rightarrow$ N0	N0 $\rightarrow$ N2	N2 $\rightarrow$ N0	N0 $\rightarrow$ N3	N3 $\rightarrow$ N0	N1 $\rightarrow$ N2	N2 $\rightarrow$ N1	N1 $\rightarrow$ N3	N3 $\rightarrow$ N1	N2 $\rightarrow$ N3	N3 $\rightarrow$ N2
NeGPR w/o IB	51.2	51.3	49.2	49.9	49.7	49.5	49.3	50.2	52.1	50.0	53.5	50.3
NeGPR w/o EB	50.1	50.8	50.6	50.8	51.5	50.7	49.5	50.1	50.1	49.9	51.6	50.7
NeGPR w/o NRL	58.0	58.8	60.1	60.0	59.0	51.8	59.2	60.0	59.1	58.2	57.5	59.1
NeGPR w/o NTR	58.5	60.8	61.1	62.9	58.3	51.2	59.6	57.5	59.8	59.2	58.8	58.7
NeGPR	<b>60.7</b>	<b>61.9</b>	<b>61.4</b>	<b>66.8</b>	<b>60.5</b>	<b>52.3</b>	<b>60.2</b>	<b>62.8</b>	<b>61.5</b>	<b>60.6</b>	<b>63.4</b>	<b>59.6</b>

Table 6: The results of ablation studies on the FRANKENSTEIN dataset (source  $\rightarrow$  target). **Bold** results indicate the best performance.

Methods	F0 $\rightarrow$ F1	F1 $\rightarrow$ F0	F0 $\rightarrow$ F2	F2 $\rightarrow$ F0	F0 $\rightarrow$ F3	F3 $\rightarrow$ F0	F1 $\rightarrow$ F2	F2 $\rightarrow$ F1	F1 $\rightarrow$ F3	F3 $\rightarrow$ F1	F2 $\rightarrow$ F3	F3 $\rightarrow$ F2
NeGPR w/o IB	51.4	49.3	49.5	50.3	49.5	49.7	49.7	50.7	50.4	50.5	50.4	50.7
NeGPR w/o EB	51.4	50.2	48.6	49.9	45.9	48.8	50.6	49.3	49.4	50.2	48.9	50.8
NeGPR w/o NRL	60.4	58.3	58.7	58.2	67.3	58.0	58.8	56.3	68.9	56.0	72.7	58.6
NeGPR w/o NTR	60.3	59.1	59.3	59.3	66.9	58.8	60.1	57.8	67.9	58.9	73.3	57.7
NeGPR	<b>63.9</b>	<b>60.4</b>	<b>60.9</b>	<b>63.4</b>	<b>68.2</b>	<b>59.9</b>	<b>60.6</b>	<b>59.7</b>	<b>72.1</b>	<b>59.6</b>	<b>74.7</b>	<b>59.4</b>

Table 7: The results of ablation studies on the MUTAGENICITY dataset (source  $\rightarrow$  target). **Bold** results indicate the best performance.

Methods	M0 $\rightarrow$ M1	M1 $\rightarrow$ M0	M0 $\rightarrow$ M2	M2 $\rightarrow$ M0	M0 $\rightarrow$ M3	M3 $\rightarrow$ M0	M1 $\rightarrow$ M2	M2 $\rightarrow$ M1	M1 $\rightarrow$ M3	M3 $\rightarrow$ M1	M2 $\rightarrow$ M3	M3 $\rightarrow$ M2
NeGPR w/o IB	52.7	50.3	50.8	48.5	50.5	50.9	51.2	50.7	50.5	49.5	48.8	49.4
NeGPR w/o EB	52.7	51.0	51.5	50.8	44.3	49.0	52.6	50.1	51.8	48.7	46.0	49.8
NeGPR w/o NRL	67.5	64.9	62.5	62.9	57.7	64.2	62.6	69.1	62.2	61.4	57.1	63.3
NeGPR w/o NTR	66.4	64.8	60.6	62.2	58.2	65.1	63.5	70.8	63.9	61.7	58.5	61.4
NeGPR	<b>70.1</b>	<b>65.6</b>	<b>66.7</b>	<b>63.9</b>	<b>59.7</b>	<b>65.9</b>	<b>65.8</b>	<b>72.3</b>	<b>64.2</b>	<b>63.6</b>	<b>59.1</b>	<b>65.6</b>

Table 8: The classification results (in %) on the PROTEINS dataset under edge density domain shift (source  $\rightarrow$  target). P0, P1, P2, and P3 denote the sub-datasets partitioned with node density. **Bold** results indicate the best performance.

Methods	P0 $\rightarrow$ P1	P1 $\rightarrow$ P0	P0 $\rightarrow$ P2	P2 $\rightarrow$ P0	P0 $\rightarrow$ P3	P3 $\rightarrow$ P0	P1 $\rightarrow$ P2	P2 $\rightarrow$ P1	P1 $\rightarrow$ P3	P3 $\rightarrow$ P1	P2 $\rightarrow$ P3	P3 $\rightarrow$ P2
WL	68.1 $\pm$ 1.7	31.2 $\pm$ 0.9	54.3 $\pm$ 1.5	66.7 $\pm$ 2.3	24.8 $\pm$ 1.2	21.9 $\pm$ 1.1	50.2 $\pm$ 2.0	42.8 $\pm$ 1.5	34.0 $\pm$ 1.1	61.0 $\pm$ 0.8	33.6 $\pm$ 0.9	44.1 $\pm$ 2.2
PathNN	68.3 $\pm$ 1.1	73.0 $\pm$ 1.2	55.4 $\pm$ 0.8	38.5 $\pm$ 1.0	25.7 $\pm$ 0.9	22.9 $\pm$ 1.1	40.1 $\pm$ 0.7	64.0 $\pm$ 1.4	34.7 $\pm$ 1.2	27.9 $\pm$ 1.3	67.3 $\pm$ 0.9	46.9 $\pm$ 1.0
GCN	67.6 $\pm$ 1.2	73.7 $\pm$ 1.1	56.2 $\pm$ 0.8	71.8 $\pm$ 2.0	24.1 $\pm$ 1.1	22.8 $\pm$ 0.7	52.7 $\pm$ 1.3	64.3 $\pm$ 1.5	27.7 $\pm$ 1.2	46.0 $\pm$ 0.9	30.7 $\pm$ 1.0	47.3 $\pm$ 1.4
GIN	62.7 $\pm$ 1.3	49.1 $\pm$ 0.8	50.9 $\pm$ 1.2	49.7 $\pm$ 0.9	25.1 $\pm$ 1.1	60.3 $\pm$ 0.7	45.6 $\pm$ 1.0	46.1 $\pm$ 1.2	66.4 $\pm$ 1.0	44.6 $\pm$ 1.4	43.1 $\pm$ 0.6	48.8 $\pm$ 0.9
GAT	63.0 $\pm$ 1.2	68.5 $\pm$ 1.0	50.5 $\pm$ 0.9	65.9 $\pm$ 2.1	64.8 $\pm$ 1.3	17.7 $\pm$ 0.8	49.3 $\pm$ 1.0	63.1 $\pm$ 1.5	46.2 $\pm$ 1.2	25.8 $\pm$ 1.1	33.4 $\pm$ 0.7	49.3 $\pm$ 1.4
GMT	54.9 $\pm$ 1.5	51.4 $\pm$ 1.4	53.5 $\pm$ 1.2	51.9 $\pm$ 1.4	43.1 $\pm$ 1.2	46.1 $\pm$ 1.0	51.4 $\pm$ 1.4	46.5 $\pm$ 0.6	47.8 $\pm$ 1.9	47.8 $\pm$ 0.7	54.3 $\pm$ 2.4	49.0 $\pm$ 1.4
Co-teaching	67.7 $\pm$ 1.3	69.5 $\pm$ 0.9	54.6 $\pm$ 1.0	69.1 $\pm$ 2.1	24.9 $\pm$ 0.8	25.9 $\pm$ 0.7	49.6 $\pm$ 1.1	61.7 $\pm$ 1.5	39.2 $\pm$ 1.0	47.8 $\pm$ 1.2	43.3 $\pm$ 0.9	46.7 $\pm$ 1.0
Taylor-CE	66.1 $\pm$ 1.2	66.0 $\pm$ 0.9	49.6 $\pm$ 1.1	54.1 $\pm$ 0.8	28.2 $\pm$ 1.3	57.7 $\pm$ 1.0	50.9 $\pm$ 0.7	42.3 $\pm$ 1.2	70.0 $\pm$ 0.6	40.2 $\pm$ 0.8	40.1 $\pm$ 1.0	42.3 $\pm$ 0.9
RTGNN	63.3 $\pm$ 1.2	76.0 $\pm$ 1.1	61.5 $\pm$ 0.8	67.4 $\pm$ 1.3	26.3 $\pm$ 0.9	20.3 $\pm$ 0.7	55.5 $\pm$ 1.0	67.7 $\pm$ 1.4	24.7 $\pm$ 1.0	49.1 $\pm$ 1.2	34.5 $\pm$ 1.1	44.3 $\pm$ 0.8
OMG	65.2 $\pm$ 1.0	72.5 $\pm$ 1.1	47.4 $\pm$ 0.9	63.5 $\pm$ 1.2	68.3 $\pm$ 1.0	22.7 $\pm$ 0.7	46.6 $\pm$ 1.3	59.6 $\pm$ 1.5	52.8 $\pm$ 1.2	21.5 $\pm$ 0.8	35.3 $\pm$ 0.9	43.9 $\pm$ 1.1
SPORT	61.0 $\pm$ 1.1	65.0 $\pm$ 1.2	48.8 $\pm$ 0.9	68.8 $\pm$ 1.0	54.9 $\pm$ 1.3	52.1 $\pm$ 1.0	55.6 $\pm$ 0.8	64.6 $\pm$ 1.4	51.9 $\pm$ 1.1	26.0 $\pm$ 1.2	34.5 $\pm$ 1.0	42.6 $\pm$ 1.1
CoCo	67.3 $\pm$ 1.2	51.1 $\pm$ 0.9	55.5 $\pm$ 1.0	64.7 $\pm$ 1.3	71.7 $\pm$ 1.1	26.1 $\pm$ 0.7	51.9 $\pm$ 1.0	55.4 $\pm$ 1.1	37.0 $\pm$ 1.2	56.6 $\pm$ 0.8	38.5 $\pm$ 1.0	44.8 $\pm$ 1.3
DEAL	66.2 $\pm$ 1.1	72.3 $\pm$ 1.0	54.2 $\pm$ 0.9	71.9 $\pm$ 1.3	35.2 $\pm$ 1.0	58.5 $\pm$ 0.8	50.6 $\pm$ 1.2	65.5 $\pm$ 0.7	44.5 $\pm$ 1.0	67.4 $\pm$ 1.2	64.5 $\pm$ 0.9	47.4 $\pm$ 1.1
SGDA	67.4 $\pm$ 1.2	58.7 $\pm$ 1.1	58.3 $\pm$ 0.9	73.0 $\pm$ 1.4	38.8 $\pm$ 0.8	32.4 $\pm$ 1.0	48.1 $\pm$ 1.2	49.4 $\pm$ 0.9	39.9 $\pm$ 1.0	59.2 $\pm$ 1.1	40.8 $\pm$ 0.7	46.7 $\pm$ 1.0
A2GNN	60.6 $\pm$ 1.0	66.3 $\pm$ 1.2	54.0 $\pm$ 0.9	68.6 $\pm$ 1.3	59.9 $\pm$ 1.1	53.9 $\pm$ 0.8	44.0 $\pm$ 1.0	62.9 $\pm$ 1.2	43.5 $\pm$ 0.7	36.6 $\pm$ 1.0	46.4 $\pm$ 1.1	54.3 $\pm$ 0.9
StruRW	62.4 $\pm$ 1.1	73.0 $\pm$ 1.2	60.2 $\pm$ 0.9	71.6 $\pm$ 1.3	40.5 $\pm$ 0.8	34.8 $\pm$ 1.0	49.5 $\pm$ 1.2	66.5 $\pm$ 1.4	37.1 $\pm$ 1.0	61.7 $\pm$ 1.1	41.2 $\pm$ 0.7	46.8 $\pm$ 1.0
PA-BOTH	64.9 $\pm$ 1.1	73.0 $\pm$ 1.2	57.7 $\pm$ 0.9	68.9 $\pm$ 1.3	36.3 $\pm$ 1.0	55.0 $\pm$ 1.0	53.9 $\pm$ 0.8	67.1 $\pm$ 1.1	42.9 $\pm$ 1.0	68.3 $\pm$ 0.9	62.8 $\pm$ 1.0	45.3 $\pm$ 1.2
ROAD	64.4 $\pm$ 3.4	83.5 $\pm$ 2.0	57.7 $\pm$ 1.8	70.2 $\pm$ 2.1	44.0 $\pm$ 3.0	43.4 $\pm$ 2.2	56.9 $\pm$ 2.6	62.4 $\pm$ 3.1	59.0 $\pm$ 2.3	62.1 $\pm$ 1.7	60.6 $\pm$ 2.0	57.6 $\pm$ 1.7
ALEX	<b>70.7<math>\pm</math>3.3</b>	73.8 $\pm$ 2.1	60.5 $\pm$ 2.4	73.8 $\pm$ 2.8	69.0 $\pm$ 3.3	62.4 $\pm$ 3.0	58.0 $\pm$ 2.5	64.3 $\pm$ 3.2	69.0 $\pm$ 2.8	67.1 $\pm$ 2.6	68.7 $\pm$ 2.2	60.2 $\pm$ 2.7
NeGPR	70.3 $\pm$ 1.9	<b>77.2<math>\pm</math>2.1</b>	<b>61.6<math>\pm</math>1.5</b>	<b>76.9<math>\pm</math>1.0</b>	<b>76.6<math>\pm</math>2.2</b>	<b>66.7<math>\pm</math>2.0</b>	<b>60.1<math>\pm</math>1.2</b>	<b>70.5<math>\pm</math>2.3</b>	<b>72.3<math>\pm</math>1.4</b>	<b>69.3<math>\pm</math>2.7</b>	<b>70.5<math>\pm</math>1.4</b>	<b>62.3<math>\pm</math>2.8</b>

Table 9: The classification results on the PROTEINS dataset under node density domain shift (source  $\rightarrow$  target). P0, P1, P2 and P3 denote the sub-datasets partitioned with graph flux density. **Bold** results indicate the best performance.

Methods	P0 $\rightarrow$ P1	P1 $\rightarrow$ P0	P0 $\rightarrow$ P2	P2 $\rightarrow$ P0	P0 $\rightarrow$ P3	P3 $\rightarrow$ P0	P1 $\rightarrow$ P2	P2 $\rightarrow$ P1	P1 $\rightarrow$ P3	P3 $\rightarrow$ P1	P2 $\rightarrow$ P3	P3 $\rightarrow$ P2
WL	67.2 $\pm$ 2.0	33.2 $\pm$ 3.1	56.5 $\pm$ 2.3	69.4 $\pm$ 1.9	26.5 $\pm$ 2.4	20.9 $\pm$ 2.0	51.2 $\pm$ 2.5	44.1 $\pm$ 2.3	32.8 $\pm$ 2.0	60.5 $\pm$ 2.1	34.1 $\pm$ 2.0	41.8 $\pm$ 2.4
PathNN	69.2 $\pm$ 2.1	71.2 $\pm$ 2.2	55.9 $\pm$ 2.0	37.7 $\pm$ 2.1	26.0 $\pm$ 2.0	21.8 $\pm$ 2.2	41.1 $\pm$ 2.3	62.8 $\pm$ 2.0	33.2 $\pm$ 2.1	28.2 $\pm$ 2.0	66.5 $\pm$ 2.3	47.0 $\pm$ 2.1
GCN	68.0 $\pm$ 2.1	72.0 $\pm$ 2.0	56.5 $\pm$ 2.2	71.7 $\pm$ 2.3	25.4 $\pm$ 2.1	24.1 $\pm$ 2.0	54.0 $\pm$ 2.3	63.6 $\pm$ 2.2	28.0 $\pm$ 2.1	46.0 $\pm$ 2.0	31.2 $\pm$ 2.0	47.4 $\pm$ 2.1
GIN	61.7 $\pm$ 2.3	50.2 $\pm$ 2.4	52.1 $\pm$ 2.2	49.9 $\pm$ 2.1	43.2 $\pm$ 2.0	56.5 $\pm$ 2.3	44.7 $\pm$ 2.1	47.0 $\pm$ 2.2	58.6 $\pm$ 2.1	43.1 $\pm$ 2.0	42.8 $\pm$ 2.1	49.2 $\pm$ 2.2
GAT	63.2 $\pm$ 2.2	67.4 $\pm$ 2.1	51.0 $\pm$ 2.3	67.1 $\pm$ 2.2	64.0 $\pm$ 2.3	19.1 $\pm$ 2.0	50.3 $\pm$ 2.2	62.3 $\pm$ 2.3	45.9 $\pm$ 2.1	26.2 $\pm$ 2.1	32.5 $\pm$ 2.1	48.6 $\pm$ 2.3
GMT	56.2 $\pm$ 1.7	51.2 $\pm$ 1.6	51.4 $\pm$ 0.7	53.0 $\pm$ 1.3	43.0 $\pm$ 1.0	48.5 $\pm$ 1.1	51.6 $\pm$ 1.9	52.2 $\pm$ 1.6	47.6 $\pm$ 1.4	49.0 $\pm$ 1.2	46.1 $\pm$ 0.9	47.9 $\pm$ 1.8
Co-teaching	66.9 $\pm$ 2.3	69.5 $\pm$ 2.1	54.5 $\pm$ 2.2	68.9 $\pm$ 2.1	25.2 $\pm$ 2.0	26.2 $\pm$ 2.3	50.1 $\pm$ 2.1	62.0 $\pm$ 2.2	39.3 $\pm$ 2.0	47.0 $\pm$ 2.1	43.5 $\pm$ 2.0	46.1 $\pm$ 2.2
Taylor-CE	66.2 $\pm$ 2.1	67.0 $\pm$ 2.0	48.6 $\pm$ 2.2	53.2 $\pm$ 2.3	28.4 $\pm$ 2.1	58.0 $\pm$ 2.0	51.2 $\pm$ 2.1	42.1 $\pm$ 2.3	60.0 $\pm$ 2.0	40.2 $\pm$ 2.1	39.7 $\pm$ 2.0	41.6 $\pm$ 2.2
RTGNN	62.5 $\pm$ 2.2	76.8 $\pm$ 2.3	60.5 $\pm$ 2.1	68.0 $\pm$ 2.2	26.3 $\pm$ 2.0	19.8 $\pm$ 2.1	55.4 $\pm$ 2.3	66.7 $\pm$ 2.0	24.1 $\pm$ 2.0	49.3 $\pm$ 2.2	34.2 $\pm$ 2.1	44.3 $\pm$ 2.0
OMG	65.2 $\pm$ 2.1	72.5 $\pm$ 2.2	47.4 $\pm$ 2.1	63.6 $\pm$ 2.3	68.4 $\pm$ 2.0	22.6 $\pm$ 2.0	46.8 $\pm$ 2.1	59.6 $\pm$ 2.2	52.8 $\pm$ 2.0	21.5 $\pm$ 2.0	35.3 $\pm$ 2.1	43.9 $\pm$ 2.0
SPORT	61.0 $\pm$ 2.1	65.7 $\pm$ 2.0	48.8 $\pm$ 2.2	69.4 $\pm$ 2.3	55.1 $\pm$ 2.1	52.0 $\pm$ 2.1	55.6 $\pm$ 2.1	64.5 $\pm$ 2.0	51.9 $\pm$ 2.2	25.6 $\pm$ 2.1	34.3 $\pm$ 2.0	42.5 $\pm$ 2.2
CoCo	67.2 $\pm$ 2.0	51.2 $\pm$ 2.1	55.5 $\pm$ 2.2	64.7 $\pm$ 2.0	71.7 $\pm$ 2.3	26.1 $\pm$ 2.1	51.9 $\pm$ 2.1	55.3 $\pm$ 2.1	37.0 $\pm$ 2.0	56.5 $\pm$ 2.2	38.5 $\pm$ 2.1	44.7 $\pm$ 2.0
DEAL	65.9 $\pm$ 1.8	72.0 $\pm$ 1.3	53.9 $\pm$ 2.9	71.6 $\pm$ 1.8	35.0 $\pm$ 1.4	58.2 $\pm$ 1.7	50.3 $\pm$ 2.5	65.8 $\pm$ 1.8	44.2 $\pm$ 1.6	67.7 $\pm$ 2.3	64.3 $\pm$ 1.1	47.2 $\pm$ 2.5
SGDA	67.2 $\pm$ 1.3	59.0 $\pm$ 2.5	58.0 $\pm$ 2.2	72.7 $\pm$ 1.7	38.6 $\pm$ 0.9	32.7 $\pm$ 1.3	47.9 $\pm$ 1.9	49.1 $\pm$ 2.7	39.6 $\pm$ 1.5	58.9 $\pm$ 3.1	40.5 $\pm$ 2.4	46.4 $\pm$ 1.2
A2GNN	60.3 $\pm$ 1.3	66.0 $\pm$ 1.9	53.7 $\pm$ 1.2	68.3 $\pm$ 2.4	59.7 $\pm$ 1.8	53.6 $\pm$ 1.7	43.7 $\pm$ 0.6	62.6 $\pm$ 1.9	43.2 $\pm$ 1.4	36.3 $\pm$ 2.3	46.1 $\pm$ 1.5	54.1 $\pm$ 3.4
StruRW	62.1 $\pm$ 0.7	73.3 $\pm$ 1.5	59.9 $\pm$ 1.4	71.3 $\pm$ 0.9	40.2 $\pm$ 1.4	34.5 $\pm$ 2.5	49.2 $\pm$ 1.8	66.2 $\pm$ 1.9	36.8 $\pm$ 3.5	61.4 $\pm$ 1.7	40.9 $\pm$ 1.2	46.5 $\pm$ 1.8
PA-BOTH	64.6 $\pm$ 0.5	73.3 $\pm$ 1.1	57.4 $\pm$ 3.6	68.7 $\pm$ 3.9	36.0 $\pm$ 2.7	54.8 $\pm$ 3.1	53.6 $\pm$ 3.3	66.8 $\pm$ 1.5	42.6 $\pm$ 1.4	68.0 $\pm$ 1.7	62.5 $\pm$ 1.2	45.0 $\pm$ 1.8
ROAD	64.4 $\pm$ 2.4	68.0 $\pm$ 2.2	59.4 $\pm$ 2.6	70.3 $\pm$ 1.7	54.4 $\pm$ 2.0	57.5 $\pm$ 1.8	59.1 $\pm$ 2.3	64.6 $\pm$ 2.7	54.4 $\pm$ 2.0	64.5 $\pm$ 3.1	54.9 $\pm$ 2.9	57.1 $\pm$ 2.3
ALEX	<b>73.6<math>\pm</math>2.2</b>	73.7 $\pm$ 2.3	61.5 $\pm$ 3.2	73.6 $\pm$ 2.8	68.7 $\pm$ 1.4	63.7 $\pm$ 2.9	<b>62.2<math>\pm</math>1.5</b>	68.5 $\pm$ 2.2	61.1 $\pm$ 2.6	66.9 $\pm$ 2.3	67.1 $\pm$ 1.6	60.5 $\pm$ 2.4
NeGPR	72.8 $\pm$ 2.4	<b>77.7<math>\pm</math>1.5</b>	<b>63.3<math>\pm</math>1.7</b>	<b>75.1<math>\pm</math>1.9</b>	<b>77.5<math>\pm</math>2.7</b>	<b>66.1<math>\pm</math>1.6</b>	61.9 $\pm$ 1.8	<b>70.9<math>\pm</math>1.4</b>	<b>63.9<math>\pm</math>1.9</b>	<b>73.1<math>\pm</math>2.7</b>	<b>67.8<math>\pm</math>1.5</b>	<b>61.9<math>\pm</math>2.3</b>

Table 10: The classification results (in %) on the NCI1 dataset under graph flux density domain shift (source  $\rightarrow$  target). N0, N1, N2 and N3 denote the sub-datasets partitioned with graph flux. **Bold** results indicate the best performance.

Methods	N0 $\rightarrow$ N1	N1 $\rightarrow$ N0	N0 $\rightarrow$ N2	N2 $\rightarrow$ N0	N0 $\rightarrow$ N3	N3 $\rightarrow$ N0	N1 $\rightarrow$ N2	N2 $\rightarrow$ N1	N1 $\rightarrow$ N3	N3 $\rightarrow$ N1	N2 $\rightarrow$ N3	N3 $\rightarrow$ N2
WL	45.3 $\pm$ 1.2	55.2 $\pm$ 3.0	44.3 $\pm$ 2.4	35.6 $\pm$ 1.8	33.5 $\pm$ 0.9	30.6 $\pm$ 2.2	49.2 $\pm$ 1.5	53.2 $\pm$ 2.0	63.3 $\pm$ 1.6	51.2 $\pm$ 3.1	47.5 $\pm$ 1.0	47.9 $\pm$ 2.3
PathNN	53.3 $\pm$ 1.5	42.1 $\pm$ 1.3	54.0 $\pm$ 0.8	64.2 $\pm$ 1.9	42.8 $\pm$ 2.2	29.3 $\pm$ 1.1	50.8 $\pm$ 2.0	55.7 $\pm$ 0.9	60.1 $\pm$ 2.1	48.3 $\pm$ 2.3	58.9 $\pm$ 1.0	51.5 $\pm$ 1.7
GCN	45.7 $\pm$ 2.2	63.4 $\pm$ 1.5	44.8 $\pm$ 2.0	28.3 $\pm$ 1.0	34.4 $\pm$ 1.2	30.4 $\pm$ 1.7	50.5 $\pm$ 0.9	46.3 $\pm$ 2.1	42.0 $\pm$ 1.6	45.3 $\pm$ 2.0	55.1 $\pm$ 1.5	45.1 $\pm$ 1.8
GIN	45.7 $\pm$ 2.4	63.0 $\pm$ 2.1	47.2 $\pm$ 1.6	34.2 $\pm$ 2.0	57.0 $\pm$ 1.0	28.3 $\pm$ 1.7	46.2 $\pm$ 0.9	47.6 $\pm$ 2.0	59.3 $\pm$ 1.5	49.1 $\pm$ 2.3	60.8 $\pm$ 1.9	49.7 $\pm$ 0.8
GAT	45.2 $\pm$ 1.9	29.1 $\pm$ 1.3	44.4 $\pm$ 1.7	62.8 $\pm$ 2.1	33.0 $\pm$ 1.0	31.1 $\pm$ 1.5	46.1 $\pm$ 2.2	48.2 $\pm$ 1.0	57.4 $\pm$ 1.8	50.2 $\pm$ 2.4	54.9 $\pm$ 0.9	47.3 $\pm$ 2.3
GMT	48.4 $\pm$ 0.8	49.8 $\pm$ 1.7	49.0 $\pm$ 1.5	49.7 $\pm$ 0.9	50.2 $\pm$ 1.0	48.9 $\pm$ 2.6	49.7 $\pm$ 2.4	50.5 $\pm$ 2.3	48.7 $\pm$ 1.1	50.4 $\pm$ 1.0	48.7 $\pm$ 1.3	49.8 $\pm$ 1.6
Co-teaching	48.9 $\pm$ 2.2	51.1 $\pm$ 1.9	48.3 $\pm$ 1.5	62.4 $\pm$ 1.8	31.8 $\pm$ 1.1	29.3 $\pm$ 1.0	45.5 $\pm$ 2.3	47.2 $\pm$ 0.9	44.8 $\pm$ 1.7	40.9 $\pm$ 1.5	57.0 $\pm$ 2.0	46.5 $\pm$ 1.2
Taylor-CE	56.1 $\pm$ 2.3	56.4 $\pm$ 1.8	45.4 $\pm$ 1.7	51.0 $\pm$ 2.1	50.1 $\pm$ 1.5	28.4 $\pm$ 1.0	45.2 $\pm$ 1.9	55.1 $\pm$ 1.0	60.8 $\pm$ 1.4	46.8 $\pm$ 2.0	56.0 $\pm$ 1.2	53.0 $\pm$ 2.3
RTGNN	40.6 $\pm$ 1.5	60.1 $\pm$ 2.1	47.9 $\pm$ 1.8	31.7 $\pm$ 0.9	38.1 $\pm$ 1.3	27.7 $\pm$ 1.1	51.7 $\pm$ 2.0	53.5 $\pm$ 1.3	44.3 $\pm$ 1.6	51.0 $\pm$ 1.5	59.2 $\pm$ 0.8	42.6 $\pm$ 1.9
OMG	51.6 $\pm$ 2.0	33.8 $\pm$ 1.3	49.2 $\pm$ 1.5	65.5 $\pm$ 2.2	35.5 $\pm$ 1.1	27.7 $\pm$ 1.0	50.4 $\pm$ 2.0	51.8 $\pm$ 1.1	54.1 $\pm$ 1.3	47.2 $\pm$ 1.5	58.7 $\pm$ 0.8	41.3 $\pm$ 1.2
SPORT	52.2 $\pm$ 2.3	44.9 $\pm$ 1.7	50.8 $\pm$ 1.2	57.6 $\pm$ 1.8	52.3 $\pm$ 1.5	28.0 $\pm$ 1.0	50.7 $\pm$ 1.9	51.2 $\pm$ 1.3	50.0 $\pm$ 1.5	53.0 $\pm$ 1.1	53.4 $\pm$ 1.2	47.1 $\pm$ 1.0
CoCo	52.2 $\pm$ 1.7	56.7 $\pm$ 1.8	47.7 $\pm$ 1.5	42.3 $\pm$ 1.0	35.7 $\pm$ 1.2	30.5 $\pm$ 1.0	48.2 $\pm$ 1.4	55.9 $\pm$ 1.1	53.3 $\pm$ 1.2	53.5 $\pm$ 1.5	56.1 $\pm$ 1.0	49.6 $\pm$ 1.2
DEAL	58.0 $\pm$ 1.8	53.8 $\pm$ 1.3	56.8 $\pm$ 1.4	63.7 $\pm$ 1.5	48.3 $\pm$ 1.0	28.9 $\pm$ 1.1	50.6 $\pm$ 1.3	59.2 $\pm$ 1.2	55.6 $\pm$ 1.0	48.1 $\pm$ 1.4	52.5 $\pm$ 1.0	49.5 $\pm$ 1.2
SGDA	52.5 $\pm$ 1.6	59.6 $\pm$ 1.3	48.2 $\pm$ 1.4	48.8 $\pm$ 1.5	41.1 $\pm$ 1.0	27.8 $\pm$ 1.0	47.3 $\pm$ 1.2	49.0 $\pm$ 1.2	53.6 $\pm$ 1.3	51.1 $\pm$ 1.5	49.4 $\pm$ 1.1	44.0 $\pm$ 1.2
A2GNN	55.4 $\pm$ 1.5	49.8 $\pm$ 1.2	46.3 $\pm$ 1.1	58.7 $\pm$ 1.3	48.2 $\pm$ 1.0	24.7 $\pm$ 1.0	43.5 $\pm$ 1.0	53.0 $\pm$ 1.2	51.5 $\pm$ 1.0	47.1 $\pm$ 1.3	51.2 $\pm$ 1.1	50.2 $\pm$ 1.2
StruRW	48.6 $\pm$ 1.4	58.8 $\pm$ 1.3	48.5 $\pm$ 1.2	52.4 $\pm$ 1.0	46.0 $\pm$ 1.1	25.3 $\pm$ 1.0	46.1 $\pm$ 1.3	55.5 $\pm$ 1.2	45.9 $\pm$ 1.0	44.9 $\pm$ 1.2	53.2 $\pm$ 1.1	46.2 $\pm$ 1.0
PA-BOTH	58.4 $\pm$ 1.5	48.8 $\pm$ 1.2	52.8 $\pm$ 1.3	59.6 $\pm$ 1.2	50.2 $\pm$ 1.1	28.3 $\pm$ 1.0	51.9 $\pm$ 1.1	53.6 $\pm$ 1.4	60.2 $\pm$ 1.0	54.1 $\pm$ 1.3	51.1 $\pm$ 1.0	51.5 $\pm$ 1.2
ROAD	55.2 $\pm$ 2.3	57.8 $\pm$ 3.4	53.7 $\pm$ 2.4	53.0 $\pm$ 2.3	57.4 $\pm$ 2.2	50.1 $\pm$ 2.8	54.5 $\pm$ 2.5	56.2 $\pm$ 2.4	58.1 $\pm$ 2.2	51.9 $\pm$ 2.4	59.4 $\pm$ 3.0	56.5 $\pm$ 2.9
ALEX	57.7 $\pm$ 2.3	59.0 $\pm$ 2.8	57.1 $\pm$ 2.1	59.4 $\pm$ 2.3	<b>61.1<math>\pm</math>2.1</b>	<b>57.4<math>\pm</math>1.5</b>	57.2 $\pm$ 2.7	55.8 $\pm$ 1.8	58.6 $\pm$ 2.3	56.0 $\pm$ 2.2	60.4 $\pm$ 1.6	58.1 $\pm$ 2.1
NeGPR	<b>60.7<math>\pm</math>2.7</b>	<b>61.9<math>\pm</math>1.8</b>	<b>61.4<math>\pm</math>2.2</b>	<b>66.8<math>\pm</math>1.5</b>	60.5 $\pm$ 1.2	52.3 $\pm$ 1.9	<b>60.6<math>\pm</math>2.8</b>	<b>62.8<math>\pm</math>2.2</b>	<b>61.5<math>\pm</math>2.5</b>	<b>60.6<math>\pm</math>2.7</b>	<b>63.4<math>\pm</math>1.3</b>	<b>59.6<math>\pm</math>2.5</b>

Table 11: The classification results (in %) on the NCI1 dataset under edge density domain shift (source  $\rightarrow$  target). N0, N1, N2 and N3 denote the sub-datasets partitioned with edge density. **Bold** results indicate the best performance.

Methods	N0 $\rightarrow$ N1	N1 $\rightarrow$ N0	N0 $\rightarrow$ N2	N2 $\rightarrow$ N0	N0 $\rightarrow$ N3	N3 $\rightarrow$ N0	N1 $\rightarrow$ N2	N2 $\rightarrow$ N1	N1 $\rightarrow$ N3	N3 $\rightarrow$ N1	N2 $\rightarrow$ N3	N3 $\rightarrow$ N2
WL	46.7 $\pm$ 0.7	56.1 $\pm$ 1.8	45.2 $\pm$ 1.6	34.4 $\pm$ 1.4	33.3 $\pm$ 2.6	29.2 $\pm$ 1.5	48.4 $\pm$ 3.7	52.7 $\pm$ 1.4	61.7 $\pm$ 1.9	50.8 $\pm$ 0.7	46.8 $\pm$ 2.3	47.8 $\pm$ 2.5
PathNN	52.9 $\pm$ 2.2	41.4 $\pm$ 3.7	53.5 $\pm$ 3.0	63.7 $\pm$ 1.8	43.5 $\pm$ 1.5	30.1 $\pm$ 1.9	51.4 $\pm$ 2.6	55.0 $\pm$ 2.3	59.5 $\pm$ 1.8	47.6 $\pm$ 1.2	59.5 $\pm$ 1.4	52.1 $\pm$ 1.7
GCN	46.1 $\pm$ 2.8	64.9 $\pm$ 1.4	45.0 $\pm$ 1.7	27.9 $\pm$ 1.8	33.9 $\pm$ 1.3	29.7 $\pm$ 1.9	49.9 $\pm$ 0.8	47.1 $\pm$ 1.6	41.6 $\pm$ 1.9	44.8 $\pm$ 3.5	56.4 $\pm$ 3.2	44.5 $\pm$ 3.7
GIN	46.8 $\pm$ 2.1	64.4 $\pm$ 2.5	46.8 $\pm$ 2.2	33.6 $\pm$ 2.7	56.4 $\pm$ 1.3	29.7 $\pm$ 1.3	45.6 $\pm$ 1.7	47.3 $\pm$ 1.2	60.6 $\pm$ 0.8	49.9 $\pm$ 1.7	60.1 $\pm$ 1.3	50.6 $\pm$ 1.5
GAT	46.3 $\pm$ 1.9	30.6 $\pm$ 2.4	45.1 $\pm$ 2.3	63.4 $\pm$ 2.8	33.6 $\pm$ 2.5	29.8 $\pm$ 2.7	46.3 $\pm$ 1.9	47.5 $\pm$ 1.0	56.9 $\pm$ 1.4	49.5 $\pm$ 1.3	55.5 $\pm$ 1.7	46.8 $\pm$ 1.9
GMT	50.1 $\pm$ 1.2	49.2 $\pm$ 0.8	49.4 $\pm$ 1.3	50.2 $\pm$ 0.8	47.1 $\pm$ 1.4	50.3 $\pm$ 0.6	48.9 $\pm$ 1.3	49.8 $\pm$ 1.6	53.8 $\pm$ 1.7	51.5 $\pm$ 1.5	53.0 $\pm$ 1.6	49.9 $\pm$ 1.0
Co-teaching	49.4 $\pm$ 2.2	52.0 $\pm$ 1.8	48.1 $\pm$ 0.9	61.8 $\pm$ 1.5	32.1 $\pm$ 1.7	28.7 $\pm$ 2.5	46.0 $\pm$ 2.4	48.7 $\pm$ 1.3	45.3 $\pm$ 1.7	41.4 $\pm$ 1.9	57.5 $\pm$ 2.4	45.9 $\pm$ 1.6
Taylor-CE	55.6 $\pm$ 0.8	57.2 $\pm$ 0.7	44.8 $\pm$ 0.5	51.5 $\pm$ 0.9	49.3 $\pm$ 1.2	29.0 $\pm$ 1.4	45.8 $\pm$ 1.9	54.7 $\pm$ 1.8	60.1 $\pm$ 1.3	46.3 $\pm$ 1.7	55.4 $\pm$ 1.2	52.8 $\pm$ 2.8
RTGNN	41.3 $\pm$ 1.3	61.4 $\pm$ 1.7	48.2 $\pm$ 1.2	31.4 $\pm$ 1.9	38.9 $\pm$ 1.8	27.3 $\pm$ 1.4	52.2 $\pm$ 1.7	53.0 $\pm$ 1.5	43.8 $\pm$ 1.9	50.8 $\pm$ 1.3	58.5 $\pm$ 2.7	42.1 $\pm$ 1.8
OMG	51.1 $\pm$ 0.9	34.4 $\pm$ 4.1	48.5 $\pm$ 3.7	66.0 $\pm$ 3.2	36.1 $\pm$ 3.6	27.1 $\pm$ 2.7	50.1 $\pm$ 2.4	52.0 $\pm$ 1.8	53.5 $\pm$ 1.5	47.9 $\pm$ 1.7	58.3 $\pm$ 1.2	41.1 $\pm$ 1.9
SPORT	52.7 $\pm$ 2.2	45.6 $\pm$ 1.3	50.1 $\pm$ 2.7	57.1 $\pm$ 2.0	51.7 $\pm$ 2.5	28.7 $\pm$ 1.4	51.2 $\pm$ 1.9	51.6 $\pm$ 1.4	49.5 $\pm$ 1.7	53.4 $\pm$ 1.2	52.8 $\pm$ 1.4	46.6 $\pm$ 1.8
CoCo	51.8 $\pm$ 1.0	56.2 $\pm$ 1.3	47.1 $\pm$ 1.5	41.6 $\pm$ 1.9	36.2 $\pm$ 2.6	31.0 $\pm$ 2.3	48.6 $\pm$ 2.7	55.6 $\pm$ 1.8	52.6 $\pm$ 1.5	52.9 $\pm$ 1.2	56.4 $\pm$ 1.7	50.1 $\pm$ 2.1
DEAL	57.6 $\pm$ 0.9	53.2 $\pm$ 0.7	56.2 $\pm$ 1.8	63.2 $\pm$ 1.2	48.1 $\pm$ 1.5	28.3 $\pm$ 1.6	51.0 $\pm$ 1.4	58.9 $\pm$ 1.6	55.3 $\pm$ 1.9	49.5 $\pm$ 2.3	52.0 $\pm$ 2.7	49.7 $\pm$ 3.5
SGDA	52.2 $\pm$ 3.6	59.3 $\pm$ 3.3	48.6 $\pm$ 1.8	48.5 $\pm$ 2.7	41.5 $\pm$ 1.4	28.2 $\pm$ 1.9	46.8 $\pm$ 1.2	48.8 $\pm$ 1.9	54.0 $\pm$ 1.3	50.6 $\pm$ 1.5	49.2 $\pm$ 1.5	43.7 $\pm$ 2.0
A2GNN	55.2 $\pm$ 0.7	50.0 $\pm$ 1.8	46.7 $\pm$ 1.4	58.3 $\pm$ 1.2	48.6 $\pm$ 1.1	24.9 $\pm$ 0.9	43.0 $\pm$ 1.5	52.8 $\pm$ 1.0	51.3 $\pm$ 3.3	47.3 $\pm$ 1.8	50.9 $\pm$ 1.4	50.4 $\pm$ 1.5
StruRW	49.1 $\pm$ 1.2	58.6 $\pm$ 1.8	48.1 $\pm$ 1.4	52.9 $\pm$ 1.1	45.8 $\pm$ 2.7	25.8 $\pm$ 1.8	45.6 $\pm$ 1.3	55.2 $\pm$ 1.0	46.3 $\pm$ 1.9	44.7 $\pm$ 2.2	53.0 $\pm$ 1.3	45.6 $\pm$ 1.5
PA-BOTH	57.9 $\pm$ 0.8	49.2 $\pm$ 1.5	52.2 $\pm$ 1.4	59.3 $\pm$ 2.3	49.9 $\pm$ 2.2	28.0 $\pm$ 3.4	51.6 $\pm$ 2.1	53.3 $\pm$ 2.7	59.9 $\pm$ 1.5	53.8 $\pm$ 1.2	50.7 $\pm$ 0.9	51.9 $\pm$ 1.8
ROAD	54.4 $\pm$ 2.1	61.0 $\pm$ 2.7	53.2 $\pm$ 1.9	60.1 $\pm$ 2.4	57.5 $\pm$ 3.0	53.2 $\pm$ 2.4	53.5 $\pm$ 2.2	54.7 $\pm$ 2.5	62.7 $\pm$ 2.0	55.6 $\pm$ 1.7	58.3 $\pm$ 2.0	53.2 $\pm$ 2.4
ALEX	50.8 $\pm$ 2.0	62.7 $\pm$ 3.0	50.4 $\pm$ 2.2	61.3 $\pm$ 2.0	<b>67.9<math>\pm</math>2.4</b>	53.7 $\pm$ 1.8	53.3 $\pm$ 1.9	55.8 $\pm$ 1.8	64.9 $\pm$ 2.5	59.1 $\pm$ 2.0	60.3 $\pm$ 2.4	53.3 $\pm$ 1.6
NeGPR	<b>60.7<math>\pm</math>1.7</b>	<b>63.9<math>\pm</math>2.8</b>	<b>58.4<math>\pm</math>2.2</b>	<b>65.8<math>\pm</math>1.5</b>	64.5 $\pm$ 2.2	<b>59.3<math>\pm</math>1.9</b>	<b>62.6<math>\pm</math>1.8</b>	<b>60.8<math>\pm</math>1.2</b>	<b>66.5<math>\pm</math>2.5</b>	<b>61.6<math>\pm</math>1.7</b>	<b>62.4<math>\pm</math>2.3</b>	<b>58.6<math>\pm</math>1.5</b>

Table 12: The classification results (in %) on the NCI1 under node density domain shift (source  $\rightarrow$  target). N0, N1, N2 and N3 denote the sub-datasets partitioned with node density. **Bold** results indicate the best performance.

Methods	N0 $\rightarrow$ N1	N1 $\rightarrow$ N0	N0 $\rightarrow$ N2	N2 $\rightarrow$ N0	N0 $\rightarrow$ N3	N3 $\rightarrow$ N0	N1 $\rightarrow$ N2	N2 $\rightarrow$ N1	N1 $\rightarrow$ N3	N3 $\rightarrow$ N1	N2 $\rightarrow$ N3	N3 $\rightarrow$ N2
WL	47.9 $\pm$ 1.5	53.8 $\pm$ 0.7	45.7 $\pm$ 1.9	33.7 $\pm$ 2.3	34.8 $\pm$ 1.1	28.3 $\pm$ 0.6	51.4 $\pm$ 2.0	51.6 $\pm$ 1.8	62.0 $\pm$ 2.5	50.3 $\pm$ 1.2	47.8 $\pm$ 0.9	45.8 $\pm$ 1.0
PathNN	52.2 $\pm$ 2.1	41.1 $\pm$ 1.8	52.9 $\pm$ 2.6	64.2 $\pm$ 1.4	42.3 $\pm$ 2.0	29.4 $\pm$ 1.5	51.1 $\pm$ 2.3	55.7 $\pm$ 1.0	58.7 $\pm$ 2.0	47.9 $\pm$ 2.2	58.1 $\pm$ 3.0	51.5 $\pm$ 1.4
GCN	46.6 $\pm$ 2.1	63.7 $\pm$ 1.7	46.8 $\pm$ 3.1	26.5 $\pm$ 0.9	32.2 $\pm$ 2.4	31.1 $\pm$ 2.0	51.2 $\pm$ 1.6	48.2 $\pm$ 1.5	41.0 $\pm$ 2.2	45.0 $\pm$ 2.0	55.8 $\pm$ 1.5	45.7 $\pm$ 3.3
GIN	45.5 $\pm$ 2.3	63.1 $\pm$ 1.8	47.4 $\pm$ 3.2	34.4 $\pm$ 2.1	54.9 $\pm$ 2.0	30.4 $\pm$ 1.5	47.2 $\pm$ 2.7	48.1 $\pm$ 0.9	61.3 $\pm$ 1.7	48.5 $\pm$ 1.4	59.2 $\pm$ 3.0	49.2 $\pm$ 2.5
GAT	47.0 $\pm$ 2.1	31.4 $\pm$ 1.2	44.2 $\pm$ 2.8	62.0 $\pm$ 1.5	34.2 $\pm$ 2.0	30.1 $\pm$ 1.7	45.9 $\pm$ 2.5	46.8 $\pm$ 1.3	58.2 $\pm$ 1.9	50.1 $\pm$ 2.0	56.1 $\pm$ 3.2	47.4 $\pm$ 0.9
GMT	53.3 $\pm$ 1.1	49.5 $\pm$ 1.0	50.2 $\pm$ 2.1	49.8 $\pm$ 1.7	47.8 $\pm$ 1.7	49.8 $\pm$ 1.8	50.4 $\pm$ 2.6	49.8 $\pm$ 0.2	47.4 $\pm$ 0.8	49.5 $\pm$ 1.8	50.2 $\pm$ 0.4	48.5 $\pm$ 0.2
Co-teaching	48.6 $\pm$ 1.9	52.9 $\pm$ 2.3	47.3 $\pm$ 1.8	61.4 $\pm$ 1.5	31.6 $\pm$ 1.7	28.2 $\pm$ 2.0	46.8 $\pm$ 2.5	49.3 $\pm$ 1.1	44.8 $\pm$ 2.2	42.2 $\pm$ 1.5	56.9 $\pm$ 3.0	46.2 $\pm$ 2.3
Taylor-CE	56.0 $\pm$ 2.1	58.0 $\pm$ 1.5	45.3 $\pm$ 2.4	50.9 $\pm$ 1.7	49.7 $\pm$ 2.1	28.4 $\pm$ 1.9	46.2 $\pm$ 1.6	54.9 $\pm$ 0.9	59.6 $\pm$ 1.8	45.9 $\pm$ 1.3	55.7 $\pm$ 2.2	53.1 $\pm$ 1.5
RTGNN	41.8 $\pm$ 1.9	61.1 $\pm$ 2.1	48.6 $\pm$ 2.0	31.1 $\pm$ 1.4	39.2 $\pm$ 1.8	27.6 $\pm$ 2.0	52.5 $\pm$ 2.3	52.5 $\pm$ 1.2	44.0 $\pm$ 1.7	51.0 $\pm$ 2.0	59.0 $\pm$ 2.4	42.6 $\pm$ 1.3
OMG	51.3 $\pm$ 2.2	34.7 $\pm$ 1.5	47.8 $\pm$ 1.9	65.5 $\pm$ 2.0	35.7 $\pm$ 1.8	27.4 $\pm$ 1.7	50.4 $\pm$ 2.1	51.8 $\pm$ 1.3	54.1 $\pm$ 1.8	48.3 $\pm$ 2.1	59.1 $\pm$ 2.2	40.8 $\pm$ 1.6
SPORT	53.0 $\pm$ 2.0	45.2 $\pm$ 1.7	50.3 $\pm$ 2.1	56.7 $\pm$ 1.5	51.2 $\pm$ 1.6	28.9 $\pm$ 1.8	51.8 $\pm$ 1.9	52.1 $\pm$ 2.0	49.2 $\pm$ 1.8	53.0 $\pm$ 2.1	52.4 $\pm$ 1.4	46.9 $\pm$ 2.3
CoCo	51.4 $\pm$ 2.1	56.8 $\pm$ 1.7	47.4 $\pm$ 1.8	41.2 $\pm$ 1.4	36.5 $\pm$ 1.9	30.7 $\pm$ 1.5	48.2 $\pm$ 2.0	55.9 $\pm$ 2.1	52.3 $\pm$ 1.5	53.3 $\pm$ 1.6	56.0 $\pm$ 2.2	50.4 $\pm$ 1.8
DEAL	57.2 $\pm$ 1.8	53.6 $\pm$ 2.1	56.6 $\pm$ 1.7	63.5 $\pm$ 1.9	48.4 $\pm$ 1.5	28.0 $\pm$ 1.7	51.2 $\pm$ 2.0	59.1 $\pm$ 2.2	55.0 $\pm$ 1.9	49.8 $\pm$ 1.6	52.2 $\pm$ 1.8	50.1 $\pm$ 1.5
SGDA	52.0 $\pm$ 1.9	59.7 $\pm$ 1.8	48.3 $\pm$ 2.0	48.9 $\pm$ 1.6	41.8 $\pm$ 1.4	28.0 $\pm$ 1.7	46.2 $\pm$ 2.1	48.6 $\pm$ 1.5	54.4 $\pm$ 2.0	50.3 $\pm$ 1.7	48.9 $\pm$ 2.2	44.2 $\pm$ 1.6
A2GNN	55.5 $\pm$ 1.8	50.4 $\pm$ 1.7	46.3 $\pm$ 1.9	58.7 $\pm$ 1.6	48.3 $\pm$ 1.5	25.1 $\pm$ 2.0	42.8 $\pm$ 1.8	53.1 $\pm$ 2.2	51.7 $\pm$ 1.5	47.0 $\pm$ 1.7	50.7 $\pm$ 1.9	50.2 $\pm$ 1.6
StruRW	49.3 $\pm$ 1.6	58.9 $\pm$ 1.7	47.8 $\pm$ 2.0	53.1 $\pm$ 1.9	45.3 $\pm$ 1.6	26.0 $\pm$ 2.0	45.9 $\pm$ 1.7	55.4 $\pm$ 2.1	46.5 $\pm$ 1.5	44.9 $\pm$ 1.6	53.2 $\pm$ 1.8	45.8 $\pm$ 1.7
PA-BOTH	57.7 $\pm$ 1.9	49.5 $\pm$ 1.6	52.4 $\pm$ 1.8	59.6 $\pm$ 1.7	49.5 $\pm$ 1.9	28.2 $\pm$ 1.7	51.2 $\pm$ 2.0	53.5 $\pm$ 1.8	59.7 $\pm$ 1.6	54.1 $\pm$ 2.1	50.9 $\pm$ 1.7	52.0 $\pm$ 1.5
ROAD	54.2 $\pm$ 2.0	63.8 $\pm$ 2.7	56.0 $\pm$ 2.2	63.2 $\pm$ 2.1	59.4 $\pm$ 2.2	50.3 $\pm$ 1.5	52.5 $\pm$ 2.2	53.3 $\pm$ 1.8	56.6 $\pm$ 2.0	52.2 $\pm$ 1.6	61.7 $\pm$ 2.1	52.3 $\pm$ 1.7
ALEX	50.9 $\pm$ 2.0	67.2 $\pm$ 2.1	56.6 $\pm$ 3.1	<b>68.9<math>\pm</math>2.4</b>	61.6 $\pm$ 1.9	53.1 $\pm$ 2.5	57.4 $\pm$ 1.8	54.5 $\pm$ 2.2	60.2 $\pm$ 2.3	57.8 $\pm$ 2.6	63.6 $\pm$ 2.0	55.6 $\pm$ 2.3
NeGPR	<b>61.8<math>\pm</math>1.5</b>	<b>65.2<math>\pm</math>2.9</b>	<b>59.8<math>\pm</math>2.8</b>	64.2 $\pm$ 2.4	<b>63.1<math>\pm</math>2.6</b>	<b>58.3<math>\pm</math>1.5</b>	<b>61.8<math>\pm</math>2.6</b>	<b>60.5<math>\pm</math>1.4</b>	<b>62.5<math>\pm</math>2.4</b>	<b>59.2<math>\pm</math>1.6</b>	<b>66.1<math>\pm</math>2.1</b>	<b>57.3<math>\pm</math>2.0</b>

Table 13: The classification results (in %) on the FRANKENSTEIN dataset under graph flux density domain shift (source  $\rightarrow$  target). F0, F1, F2 and F3 denote the sub-datasets partitioned with graph flux density. **Bold** results indicate the best performance.

Methods	F0 $\rightarrow$ F1	F1 $\rightarrow$ F0	F0 $\rightarrow$ F2	F2 $\rightarrow$ F0	F0 $\rightarrow$ F3	F3 $\rightarrow$ F0	F1 $\rightarrow$ F2	F2 $\rightarrow$ F1	F1 $\rightarrow$ F3	F3 $\rightarrow$ F1	F2 $\rightarrow$ F3	F3 $\rightarrow$ F2
WL	50.4 $\pm$ 3.6	48.9 $\pm$ 0.8	49.6 $\pm$ 2.0	50.3 $\pm$ 2.6	49.7 $\pm$ 3.4	50.7 $\pm$ 4.2	48.9 $\pm$ 6.3	50.4 $\pm$ 2.0	49.4 $\pm$ 2.2	49.1 $\pm$ 3.3	50.5 $\pm$ 1.1	49.2 $\pm$ 1.2
PathNN	51.9 $\pm$ 3.1	49.3 $\pm$ 3.3	49.1 $\pm$ 2.4	49.2 $\pm$ 2.1	53.0 $\pm$ 1.3	50.0 $\pm$ 0.8	49.7 $\pm$ 2.5	49.5 $\pm$ 1.4	48.9 $\pm$ 2.3	50.2 $\pm$ 1.1	49.5 $\pm$ 3.1	50.3 $\pm$ 1.7
GCN	50.3 $\pm$ 1.5	49.9 $\pm$ 3.2	49.6 $\pm$ 1.0	50.0 $\pm$ 2.6	48.4 $\pm$ 1.1	49.4 $\pm$ 3.3	48.4 $\pm$ 2.5	49.8 $\pm$ 3.9	48.3 $\pm$ 7.0	49.2 $\pm$ 2.1	49.6 $\pm$ 3.7	50.6 $\pm$ 5.8
GIN	50.5 $\pm$ 1.7	51.1 $\pm$ 0.2	48.4 $\pm$ 2.5	50.3 $\pm$ 2.3	48.9 $\pm$ 1.8	49.8 $\pm$ 2.1	50.9 $\pm$ 2.7	49.4 $\pm$ 3.4	55.9 $\pm$ 1.1	49.6 $\pm$ 3.4	52.1 $\pm$ 1.7	49.5 $\pm$ 1.5
GAT	49.4 $\pm$ 1.9	49.9 $\pm$ 0.6	47.7 $\pm$ 1.7	50.0 $\pm$ 0.6	52.3 $\pm$ 2.9	49.5 $\pm$ 0.9	49.7 $\pm$ 4.4	51.4 $\pm$ 2.4	50.6 $\pm$ 2.5	49.5 $\pm$ 1.4	52.5 $\pm$ 2.5	48.9 $\pm$ 1.3
GMT	50.6 $\pm$ 1.1	50.6 $\pm$ 2.0	47.6 $\pm$ 1.2	50.4 $\pm$ 2.9	52.1 $\pm$ 1.9	48.8 $\pm$ 3.6	48.9 $\pm$ 5.3	48.8 $\pm$ 4.7	56.0 $\pm$ 1.5	49.9 $\pm$ 3.3	52.8 $\pm$ 2.1	49.0 $\pm$ 2.6
Co-teaching	52.4 $\pm$ 1.4	49.4 $\pm$ 1.2	48.8 $\pm$ 1.2	50.0 $\pm$ 0.9	57.4 $\pm$ 1.8	50.9 $\pm$ 1.5	51.0 $\pm$ 1.6	49.7 $\pm$ 2.4	45.0 $\pm$ 1.3	51.1 $\pm$ 0.6	49.2 $\pm$ 2.0	50.4 $\pm$ 0.7
Taylor-CE	50.7 $\pm$ 1.5	50.4 $\pm$ 2.1	47.8 $\pm$ 1.9	49.6 $\pm$ 2.0	42.9 $\pm$ 1.8	49.6 $\pm$ 2.1	52.7 $\pm$ 1.2	49.4 $\pm$ 3.4	56.9 $\pm$ 1.7	49.0 $\pm$ 2.6	57.1 $\pm$ 1.8	49.8 $\pm$ 1.9
RTGNN	49.6 $\pm$ 1.7	49.6 $\pm$ 2.1	49.2 $\pm$ 1.4	49.6 $\pm$ 1.6	45.1 $\pm$ 1.5	50.0 $\pm$ 1.4	51.3 $\pm$ 1.9	49.8 $\pm$ 2.4	51.0 $\pm$ 1.9	50.4 $\pm$ 2.5	46.9 $\pm$ 1.8	49.5 $\pm$ 1.6
OMG	51.6 $\pm$ 1.4	50.2 $\pm$ 1.4	48.9 $\pm$ 1.6	50.3 $\pm$ 0.5	55.5 $\pm$ 1.1	51.0 $\pm$ 1.8	49.8 $\pm$ 1.2	50.0 $\pm$ 0.2	51.6 $\pm$ 1.4	49.7 $\pm$ 1.7	45.1 $\pm$ 1.4	50.0 $\pm$ 2.8
SPORT	62.5 $\pm$ 0.9	58.6 $\pm$ 2.2	53.1 $\pm$ 1.4	53.2 $\pm$ 1.2	44.7 $\pm$ 2.0	51.4 $\pm$ 0.9	53.9 $\pm$ 1.5	62.1 $\pm$ 1.9	42.6 $\pm$ 1.1	49.8 $\pm$ 1.6	43.2 $\pm$ 2.0	48.6 $\pm$ 1.8
CoCo	53.4 $\pm$ 1.4	51.2 $\pm$ 1.5	53.4 $\pm$ 8.6	51.1 $\pm$ 1.6	57.7 $\pm$ 1.7	52.1 $\pm$ 0.8	52.9 $\pm$ 0.5	52.6 $\pm$ 1.1	58.7 $\pm$ 1.7	51.9 $\pm$ 0.9	58.1 $\pm$ 1.5	52.5 $\pm$ 1.3
DEAL	57.1 $\pm$ 1.6	54.9 $\pm$ 2.5	54.3 $\pm$ 0.0	52.7 $\pm$ 1.0	65.9 $\pm$ 1.4	52.4 $\pm$ 0.2	56.8 $\pm$ 1.9	51.3 $\pm$ 0.6	70.2 $\pm$ 1.3	51.8 $\pm$ 1.0	71.1 $\pm$ 2.0	51.3 $\pm$ 0.6
SGDA	52.7 $\pm$ 0.8	51.0 $\pm$ 1.7	53.3 $\pm$ 0.4	55.1 $\pm$ 1.3	52.8 $\pm$ 1.6	53.2 $\pm$ 0.6	54.4 $\pm$ 1.2	52.3 $\pm$ 1.3	51.7 $\pm$ 1.0	57.3 $\pm$ 1.1	52.1 $\pm$ 1.2	55.1 $\pm$ 1.9
A2GNN	54.7 $\pm$ 1.3	53.0 $\pm$ 0.7	53.5 $\pm$ 3.9	52.5 $\pm$ 3.1	51.9 $\pm$ 1.1	52.7 $\pm$ 0.8	54.1 $\pm$ 2.8	53.0 $\pm$ 0.6	57.7 $\pm$ 1.4	52.6 $\pm$ 1.7	55.1 $\pm$ 1.8	53.4 $\pm$ 1.2
StruRW	52.7 $\pm$ 1.9	50.1 $\pm$ 1.5	50.3 $\pm$ 4.1	49.0 $\pm$ 2.1	50.8 $\pm$ 0.5	49.7 $\pm$ 3.6	50.5 $\pm$ 1.5	49.1 $\pm$ 1.6	50.6 $\pm$ 3.3	49.9 $\pm$ 1.2	50.7 $\pm$ 2.5	50.2 $\pm$ 2.9
PA-BOTH	51.5 $\pm$ 1.6	49.0 $\pm$ 1.4	50.7 $\pm$ 2.2	49.0 $\pm$ 2.2	48.8 $\pm$ 2.5	48.6 $\pm$ 0.8	50.7 $\pm$ 0.7	50.4 $\pm$ 1.2	51.1 $\pm$ 1.1	49.5 $\pm$ 1.4	51.1 $\pm$ 1.2	49.7 $\pm$ 2.8
ROAD	54.3 $\pm$ 2.0	58.4 $\pm$ 1.8	55.4 $\pm$ 2.2	48.0 $\pm$ 1.7	66.1 $\pm$ 2.0	52.0 $\pm$ 2.3	55.3 $\pm$ 2.1	51.2 $\pm$ 1.8	65.6 $\pm$ 2.1	46.3 $\pm$ 2.6	70.8 $\pm$ 1.8	56.6 $\pm$ 2.2
ALEX	56.2 $\pm$ 2.0	59.8 $\pm$ 2.0	59.3 $\pm$ 1.9	59.0 $\pm$ 3.5	<b>68.9<math>\pm</math>2.0</b>	54.1 $\pm$ 2.5	58.6 $\pm$ 1.7	56.2 $\pm$ 1.9	70.9 $\pm$ 2.2	58.0 $\pm$ 1.9	72.9 $\pm$ 2.0	58.9 $\pm$ 2.3
NeGPR	<b>63.9<math>\pm</math>3.1</b>	<b>60.4<math>\pm</math>2.6</b>	<b>60.9<math>\pm</math>2.7</b>	<b>63.4<math>\pm</math>1.5</b>	68.2 $\pm$ 2.1	<b>59.9<math>\pm</math>2.6</b>	<b>60.6<math>\pm</math>1.7</b>	<b>59.7<math>\pm</math>1.9</b>	<b>72.1<math>\pm</math>1.7</b>	<b>59.6<math>\pm</math>2.5</b>	<b>74.7<math>\pm</math>1.9</b>	<b>59.4<math>\pm</math>2.2</b>

Table 14: The classification results (in %) on the FRANKENSTEIN dataset under edge density domain shift (source  $\rightarrow$  target). F0, F1, F2 and F3 denote the sub-datasets partitioned with edge density. **Bold** results indicate the best performance.

Methods	F0 $\rightarrow$ F1	F1 $\rightarrow$ F0	F0 $\rightarrow$ F2	F2 $\rightarrow$ F0	F0 $\rightarrow$ F3	F3 $\rightarrow$ F0	F1 $\rightarrow$ F2	F2 $\rightarrow$ F1	F1 $\rightarrow$ F3	F3 $\rightarrow$ F1	F2 $\rightarrow$ F3	F3 $\rightarrow$ F2
WL	49.5 $\pm$ 1.0	50.7 $\pm$ 5.2	49.3 $\pm$ 1.7	50.2 $\pm$ 0.3	50.0 $\pm$ 2.4	50.1 $\pm$ 1.2	50.0 $\pm$ 2.4	49.1 $\pm$ 2.1	49.8 $\pm$ 3.0	50.5 $\pm$ 1.3	50.6 $\pm$ 2.3	49.4 $\pm$ 4.6
PathNN	49.4 $\pm$ 3.0	50.1 $\pm$ 3.0	52.1 $\pm$ 2.3	50.4 $\pm$ 2.8	50.5 $\pm$ 11.5	51.5 $\pm$ 2.5	50.1 $\pm$ 2.0	50.0 $\pm$ 1.7	50.6 $\pm$ 2.2	49.8 $\pm$ 2.4	50.7 $\pm$ 3.7	50.0 $\pm$ 0.7
GCN	49.4 $\pm$ 5.4	49.5 $\pm$ 3.0	49.1 $\pm$ 1.2	50.5 $\pm$ 1.4	50.8 $\pm$ 5.5	50.8 $\pm$ 1.6	48.2 $\pm$ 5.7	51.4 $\pm$ 0.5	51.4 $\pm$ 1.7	51.0 $\pm$ 2.3	53.1 $\pm$ 1.2	50.1 $\pm$ 3.1
GIN	49.5 $\pm$ 2.5	50.7 $\pm$ 2.0	50.8 $\pm$ 9.1	50.0 $\pm$ 2.3	53.1 $\pm$ 1.2	50.8 $\pm$ 2.3	49.3 $\pm$ 1.9	51.5 $\pm$ 0.5	52.6 $\pm$ 2.6	51.6 $\pm$ 0.5	52.2 $\pm$ 2.7	49.3 $\pm$ 2.8
GAT	51.2 $\pm$ 5.4	48.3 $\pm$ 4.2	50.6 $\pm$ 5.1	51.0 $\pm$ 1.8	50.4 $\pm$ 1.8	49.9 $\pm$ 1.4	50.6 $\pm$ 4.2	51.0 $\pm$ 1.2	48.7 $\pm$ 1.9	50.4 $\pm$ 6.2	51.0 $\pm$ 1.9	49.6 $\pm$ 1.9
GMT	53.7 $\pm$ 2.3	50.7 $\pm$ 0.9	52.1 $\pm$ 3.8	50.4 $\pm$ 3.5	52.3 $\pm$ 2.1	50.2 $\pm$ 2.0	50.0 $\pm$ 2.5	48.8 $\pm$ 0.7	52.9 $\pm$ 2.6	50.6 $\pm$ 2.4	50.0 $\pm$ 5.1	49.9 $\pm$ 1.4
Co-teaching	47.4 $\pm$ 1.6	49.6 $\pm$ 1.8	51.2 $\pm$ 1.9	50.0 $\pm$ 2.0	47.3 $\pm$ 1.5	50.2 $\pm$ 0.8	51.3 $\pm$ 1.8	49.1 $\pm$ 0.7	49.1 $\pm$ 2.2	50.1 $\pm$ 1.8	50.6 $\pm$ 1.8	50.6 $\pm$ 1.8
Taylor-CE	53.4 $\pm$ 2.7	50.9 $\pm$ 1.3	51.0 $\pm$ 2.7	49.4 $\pm$ 1.7	53.1 $\pm$ 1.2	50.8 $\pm$ 1.5	49.7 $\pm$ 1.9	50.6 $\pm$ 1.6	48.8 $\pm$ 0.8	51.5 $\pm$ 0.5	46.9 $\pm$ 1.2	49.7 $\pm$ 2.0
RTGNN	50.8 $\pm$ 1.0	48.7 $\pm$ 0.8	49.6 $\pm$ 2.5	51.0 $\pm$ 1.9	52.3 $\pm$ 1.6	50.8 $\pm$ 1.4	50.6 $\pm$ 2.1	49.4 $\pm$ 1.5	50.1 $\pm$ 1.8	50.4 $\pm$ 2.6	51.3 $\pm$ 1.9	50.0 $\pm$ 1.7
OMG	51.9 $\pm$ 1.4	50.0 $\pm$ 2.5	48.9 $\pm$ 2.1	49.3 $\pm$ 0.3	51.7 $\pm$ 1.5	49.9 $\pm$ 1.4	51.1 $\pm$ 1.6	49.7 $\pm$ 1.9	48.7 $\pm$ 2.1	50.1 $\pm$ 2.7	51.5 $\pm$ 1.4	50.4 $\pm$ 2.6
SPORT	66.5 $\pm$ 1.0	60.0 $\pm$ 0.9	55.4 $\pm$ 1.6	60.0 $\pm$ 1.9	39.6 $\pm$ 1.6	44.2 $\pm$ 1.2	55.4 $\pm$ 0.6	59.9 $\pm$ 1.1	39.6 $\pm$ 2.0	46.7 $\pm$ 2.2	39.6 $\pm$ 1.7	46.8 $\pm$ 1.9
CoCo	54.8 $\pm$ 0.6	52.2 $\pm$ 1.0	53.5 $\pm$ 6.6	51.8 $\pm$ 0.6	53.8 $\pm$ 1.3	52.1 $\pm$ 0.6	53.3 $\pm$ 8.2	52.0 $\pm$ 0.2	53.5 $\pm$ 1.9	51.5 $\pm$ 0.8	53.5 $\pm$ 3.9	52.2 $\pm$ 1.0
DEAL	55.2 $\pm$ 3.8	51.7 $\pm$ 0.4	53.7 $\pm$ 4.7	52.5 $\pm$ 0.4	53.7 $\pm$ 1.8	52.4 $\pm$ 1.2	52.5 $\pm$ 3.9	52.6 $\pm$ 0.6	54.0 $\pm$ 1.2	53.1 $\pm$ 3.5	54.8 $\pm$ 9.5	53.0 $\pm$ 0.7
SGDA	53.3 $\pm$ 1.2	52.6 $\pm$ 0.1	51.5 $\pm$ 1.3	53.2 $\pm$ 1.3	54.3 $\pm$ 0.9	51.1 $\pm$ 1.0	52.4 $\pm$ 1.3	54.5 $\pm$ 0.8	52.6 $\pm$ 0.7	53.2 $\pm$ 1.2	51.3 $\pm$ 1.8	52.1 $\pm$ 1.6
A2GNN	56.4 $\pm$ 1.0	52.0 $\pm$ 1.1	53.6 $\pm$ 1.6	52.8 $\pm$ 1.3	55.1 $\pm$ 1.8	53.2 $\pm$ 1.0	53.4 $\pm$ 2.0	52.2 $\pm$ 0.8	55.0 $\pm$ 1.1	53.0 $\pm$ 0.8	54.6 $\pm$ 1.1	53.3 $\pm$ 1.2
StruRW	52.7 $\pm$ 1.9	50.1 $\pm$ 1.5	50.3 $\pm$ 1.1	49.0 $\pm$ 2.1	50.8 $\pm$ 0.5	50.3 $\pm$ 0.9	50.5 $\pm$ 1.5	49.1 $\pm$ 1.6	50.6 $\pm$ 3.3	49.9 $\pm$ 1.2	50.7 $\pm$ 1.5	50.2 $\pm$ 2.9
PA-BOTH	52.3 $\pm$ 1.5	49.3 $\pm$ 1.5	50.6 $\pm$ 2.8	51.1 $\pm$ 2.0	50.5 $\pm$ 1.5	50.8 $\pm$ 1.2	50.4 $\pm$ 1.2	49.9 $\pm$ 1.0	50.4 $\pm$ 2.3	51.2 $\pm$ 0.9	49.5 $\pm$ 1.4	50.2 $\pm$ 1.3
ROAD	67.7 $\pm$ 2.4	60.1 $\pm$ 2.2	57.3 $\pm$ 1.9	60.0 $\pm$ 2.0	60.6 $\pm$ 2.1	60.0 $\pm$ 1.8	55.5 $\pm$ 3.1	<b>67.7<math>\pm</math>2.8</b>	47.9 $\pm$ 2.7	62.4 $\pm$ 2.3	49.9 $\pm$ 1.8	53.2 $\pm$ 2.0
ALEX	69.5 $\pm$ 2.6	61.5 $\pm$ 2.0	57.9 $\pm$ 2.2	62.6 $\pm$ 1.9	64.2 $\pm$ 1.6	61.0 $\pm$ 2.0	58.7 $\pm$ 2.7	65.8 $\pm$ 2.4	56.2 $\pm$ 1.9	64.2 $\pm$ 2.0	<b>60.3<math>\pm</math>2.1</b>	57.5 $\pm$ 1.8
NeGPR	<b>70.2<math>\pm</math>2.0</b>	<b>67.6<math>\pm</math>2.3</b>	<b>62.6<math>\pm</math>1.4</b>	<b>64.6<math>\pm</math>1.7</b>	<b>66.0<math>\pm</math>2.4</b>	<b>61.9<math>\pm</math>2.1</b>	<b>63.6<math>\pm</math>2.0</b>	63.2 $\pm$ 2.8	<b>63.3<math>\pm</math>1.5</b>	<b>65.3<math>\pm</math>2.8</b>	59.8 $\pm$ 2.1	<b>60.2<math>\pm</math>1.9</b>

Table 15: The classification results (in %) on the FRANKENSTEIN dataset under node density domain shift (source  $\rightarrow$  target). F0, F1, F2 and F3 denote the sub-datasets partitioned with node density. **Bold** results indicate the best performance.

Methods	F0 $\rightarrow$ F1	F1 $\rightarrow$ F0	F0 $\rightarrow$ F2	F2 $\rightarrow$ F0	F0 $\rightarrow$ F3	F3 $\rightarrow$ F0	F1 $\rightarrow$ F2	F2 $\rightarrow$ F1	F1 $\rightarrow$ F3	F3 $\rightarrow$ F1	F2 $\rightarrow$ F3	F3 $\rightarrow$ F2
WL	49.6 $\pm$ 0.9	49.6 $\pm$ 2.7	49.7 $\pm$ 0.8	48.9 $\pm$ 1.4	50.2 $\pm$ 1.5	51.1 $\pm$ 1.1	51.0 $\pm$ 3.1	49.3 $\pm$ 3.0	49.2 $\pm$ 3.9	50.1 $\pm$ 1.0	51.3 $\pm$ 4.2	50.7 $\pm$ 4.9
PathNN	53.1 $\pm$ 1.9	49.1 $\pm$ 2.0	50.4 $\pm$ 1.3	49.8 $\pm$ 1.2	48.8 $\pm$ 1.0	50.6 $\pm$ 0.9	50.4 $\pm$ 1.5	50.4 $\pm$ 1.1	51.2 $\pm$ 1.6	48.2 $\pm$ 0.4	49.7 $\pm$ 2.2	48.5 $\pm$ 2.4
GCN	49.4 $\pm$ 1.9	49.9 $\pm$ 0.6	47.7 $\pm$ 1.7	50.0 $\pm$ 0.6	52.3 $\pm$ 2.9	49.5 $\pm$ 0.9	49.7 $\pm$ 4.4	51.4 $\pm$ 2.4	50.6 $\pm$ 2.5	49.5 $\pm$ 1.4	52.5 $\pm$ 2.5	48.9 $\pm$ 1.3
GIN	46.3 $\pm$ 1.7	50.3 $\pm$ 0.5	51.4 $\pm$ 1.6	49.7 $\pm$ 0.3	51.7 $\pm$ 2.0	49.7 $\pm$ 0.7	51.8 $\pm$ 1.0	50.2 $\pm$ 1.5	48.5 $\pm$ 2.1	50.3 $\pm$ 1.2	51.9 $\pm$ 2.7	48.7 $\pm$ 2.2
GAT	50.0 $\pm$ 1.7	49.7 $\pm$ 2.5	49.3 $\pm$ 1.6	50.4 $\pm$ 1.9	49.7 $\pm$ 4.7	49.9 $\pm$ 0.8	49.8 $\pm$ 3.2	50.4 $\pm$ 3.3	51.3 $\pm$ 2.3	49.4 $\pm$ 1.9	51.1 $\pm$ 1.9	48.2 $\pm$ 1.3
GMT	53.4 $\pm$ 1.9	49.8 $\pm$ 0.4	51.5 $\pm$ 1.6	49.3 $\pm$ 1.3	47.3 $\pm$ 2.0	49.2 $\pm$ 2.7	50.5 $\pm$ 3.8	49.7 $\pm$ 1.3	47.3 $\pm$ 2.0	49.7 $\pm$ 1.9	49.1 $\pm$ 1.0	49.2 $\pm$ 0.4
Co-teaching	54.0 $\pm$ 1.6	50.4 $\pm$ 2.6	49.8 $\pm$ 1.3	50.3 $\pm$ 1.3	50.0 $\pm$ 2.3	49.6 $\pm$ 0.9	48.0 $\pm$ 2.5	48.8 $\pm$ 1.2	49.6 $\pm$ 1.3	48.8 $\pm$ 0.7	48.8 $\pm$ 2.3	49.0 $\pm$ 2.0
Taylor-CE	53.9 $\pm$ 2.0	50.3 $\pm$ 0.5	52.3 $\pm$ 1.7	49.9 $\pm$ 0.6	47.8 $\pm$ 1.8	49.8 $\pm$ 0.5	52.2 $\pm$ 1.9	50.6 $\pm$ 1.2	48.2 $\pm$ 1.8	50.2 $\pm$ 1.5	48.0 $\pm$ 2.8	49.3 $\pm$ 2.2
RTGNN	53.7 $\pm$ 1.7	50.2 $\pm$ 2.4	48.7 $\pm$ 2.6	49.5 $\pm$ 1.5	47.8 $\pm$ 1.1	50.0 $\pm$ 1.4	51.6 $\pm$ 1.4	49.4 $\pm$ 1.6	51.5 $\pm$ 2.0	48.9 $\pm$ 1.6	48.1 $\pm$ 1.4	49.7 $\pm$ 1.7
OMG	50.1 $\pm$ 1.2	49.8 $\pm$ 2.3	51.4 $\pm$ 2.2	50.5 $\pm$ 1.6	49.3 $\pm$ 2.3	50.0 $\pm$ 2.0	51.2 $\pm$ 1.2	50.7 $\pm$ 1.0	51.4 $\pm$ 1.1	50.7 $\pm$ 0.9	49.7 $\pm$ 0.5	50.4 $\pm$ 1.5
SPORT	67.3 $\pm$ 1.2	56.8 $\pm$ 2.3	57.8 $\pm$ 1.7	56.8 $\pm$ 0.9	39.5 $\pm$ 1.4	48.8 $\pm$ 1.7	57.8 $\pm$ 1.2	67.3 $\pm$ 0.6	39.5 $\pm$ 2.3	46.5 $\pm$ 2.1	39.7 $\pm$ 1.1	42.2 $\pm$ 1.6
CoCo	54.6 $\pm$ 1.4	52.6 $\pm$ 0.4	54.0 $\pm$ 1.6	52.7 $\pm$ 0.7	54.1 $\pm$ 8.9	52.5 $\pm$ 0.8	52.0 $\pm$ 0.4	52.3 $\pm$ 0.4	54.5 $\pm$ 1.0	53.3 $\pm$ 0.3	53.5 $\pm$ 2.2	52.7 $\pm$ 0.1
DEAL	56.0 $\pm$ 2.0	53.3 $\pm$ 1.9	53.2 $\pm$ 2.8	53.4 $\pm$ 0.6	53.1 $\pm$ 2.5	53.1 $\pm$ 0.6	53.3 $\pm$ 5.6	52.0 $\pm$ 0.6	53.5 $\pm$ 1.0	53.2 $\pm$ 0.6	54.5 $\pm$ 1.4	53.2 $\pm$ 0.5
SGDA	52.2 $\pm$ 1.3	53.4 $\pm$ 0.9	52.4 $\pm$ 1.2	54.1 $\pm$ 1.1	55.2 $\pm$ 1.6	51.3 $\pm$ 0.7	52.2 $\pm$ 0.9	54.5 $\pm$ 1.3	53.6 $\pm$ 1.8	52.5 $\pm$ 2.2	53.9 $\pm$ 1.8	51.7 $\pm$ 2.2
A2GNN	56.0 $\pm$ 1.4	52.2 $\pm$ 1.6	53.3 $\pm$ 1.3	52.5 $\pm$ 1.1	54.7 $\pm$ 1.5	52.9 $\pm$ 1.7	54.0 $\pm$ 1.3	52.5 $\pm$ 0.3	52.7 $\pm$ 2.0	51.8 $\pm$ 1.0	54.3 $\pm$ 1.9	52.3 $\pm$ 0.5
StruRW	51.0 $\pm$ 1.3	49.8 $\pm$ 2.1	50.3 $\pm$ 1.0	50.3 $\pm$ 1.4	50.3 $\pm$ 1.9	50.5 $\pm$ 1.0	51.1 $\pm$ 1.2	50.2 $\pm$ 0.6	50.9 $\pm$ 1.7	49.4 $\pm$ 0.8	49.9 $\pm$ 1.2	49.3 $\pm$ 2.2
PA-BOTH	51.3 $\pm$ 1.4	50.0 $\pm$ 1.0	51.2 $\pm$ 2.0	50.1 $\pm$ 1.3	49.4 $\pm$ 3.3	49.7 $\pm$ 1.3	50.8 $\pm$ 1.8	51.1 $\pm$ 1.2	52.1 $\pm$ 3.3	49.2 $\pm$ 1.5	49.2 $\pm$ 2.7	49.4 $\pm$ 2.0
ROAD	67.8 $\pm$ 2.3	56.8 $\pm$ 2.8	56.7 $\pm$ 2.4	57.1 $\pm$ 2.3	58.5 $\pm$ 1.6	57.0 $\pm$ 1.9	57.9 $\pm$ 2.0	67.4 $\pm$ 2.1	47.9 $\pm$ 3.0	61.0 $\pm$ 2.1	46.0 $\pm$ 2.4	54.3 $\pm$ 2.0
ALEX	69.2 $\pm$ 2.2	60.2 $\pm$ 1.8	<b>60.1<math>\pm</math>1.7</b>	61.4 $\pm$ 2.5	58.3 $\pm$ 1.9	<b>61.1<math>\pm</math>2.4</b>	61.8 $\pm$ 1.7	68.8 $\pm$ 1.5	53.2 $\pm$ 2.1	61.5 $\pm$ 2.8	60.0 $\pm$ 2.0	<b>59.7<math>\pm</math>1.7</b>
NeGPR	<b>71.7<math>\pm</math>2.0</b>	<b>60.6<math>\pm</math>1.6</b>	59.6 $\pm$ 2.1	<b>61.5<math>\pm</math>1.7</b>	<b>62.7<math>\pm</math>1.9</b>	60.0 $\pm$ 2.0	<b>62.6<math>\pm</math>1.3</b>	<b>70.3<math>\pm</math>2.6</b>	<b>58.9<math>\pm</math>1.6</b>	<b>62.5<math>\pm</math>2.0</b>	<b>60.6<math>\pm</math>2.4</b>	58.4 $\pm$ 2.2

Table 16: The classification results (in %) on the MUTAGENICITY dataset under graph flux density domain shift (source  $\rightarrow$  target). M0, M1, M2, and M3 denote the sub-datasets partitioned with node density. **Bold** results indicate the best performance.

Methods	M0 $\rightarrow$ M1	M1 $\rightarrow$ M0	M0 $\rightarrow$ M2	M2 $\rightarrow$ M0	M0 $\rightarrow$ M3	M3 $\rightarrow$ M0	M1 $\rightarrow$ M2	M2 $\rightarrow$ M1	M1 $\rightarrow$ M3	M3 $\rightarrow$ M1	M2 $\rightarrow$ M3	M3 $\rightarrow$ M2
WL	58.1 $\pm$ 2.1	47.6 $\pm$ 1.4	53.3 $\pm$ 2.2	54.8 $\pm$ 3.0	45.7 $\pm$ 1.3	47.0 $\pm$ 1.8	53.3 $\pm$ 2.6	64.2 $\pm$ 2.1	45.3 $\pm$ 0.9	40.7 $\pm$ 2.3	46.0 $\pm$ 1.0	45.5 $\pm$ 2.5
PathNN	45.0 $\pm$ 2.1	61.7 $\pm$ 1.9	58.4 $\pm$ 3.2	53.5 $\pm$ 1.1	49.0 $\pm$ 0.7	46.3 $\pm$ 2.0	58.2 $\pm$ 2.5	67.1 $\pm$ 1.8	50.2 $\pm$ 2.4	57.3 $\pm$ 1.5	52.4 $\pm$ 0.9	60.2 $\pm$ 1.8
GCN	61.1 $\pm$ 1.8	52.0 $\pm$ 2.3	42.9 $\pm$ 1.1	47.1 $\pm$ 0.8	46.7 $\pm$ 1.2	56.4 $\pm$ 1.7	51.4 $\pm$ 3.0	33.4 $\pm$ 1.3	54.9 $\pm$ 0.6	37.1 $\pm$ 2.4	50.6 $\pm$ 1.5	58.2 $\pm$ 2.2
GIN	54.0 $\pm$ 1.7	48.2 $\pm$ 2.1	51.3 $\pm$ 2.3	58.4 $\pm$ 0.9	46.2 $\pm$ 1.3	47.2 $\pm$ 1.5	51.8 $\pm$ 2.0	55.0 $\pm$ 2.4	47.6 $\pm$ 2.1	55.8 $\pm$ 1.2	54.0 $\pm$ 1.5	56.0 $\pm$ 3.1
GAT	59.0 $\pm$ 2.2	56.3 $\pm$ 2.7	63.7 $\pm$ 1.9	56.4 $\pm$ 2.4	48.6 $\pm$ 3.2	53.0 $\pm$ 1.6	51.5 $\pm$ 1.4	67.3 $\pm$ 2.5	44.8 $\pm$ 1.8	48.5 $\pm$ 0.7	46.3 $\pm$ 2.0	56.3 $\pm$ 1.0
GMT	52.1 $\pm$ 1.6	50.7 $\pm$ 3.1	51.0 $\pm$ 5.8	49.4 $\pm$ 1.2	55.8 $\pm$ 1.7	50.6 $\pm$ 0.7	51.5 $\pm$ 2.1	50.3 $\pm$ 4.5	45.5 $\pm$ 2.7	49.6 $\pm$ 4.6	57.1 $\pm$ 1.1	51.4 $\pm$ 1.2
Co-teaching	56.4 $\pm$ 2.1	62.2 $\pm$ 1.7	61.2 $\pm$ 2.5	50.5 $\pm$ 1.3	42.9 $\pm$ 2.0	53.7 $\pm$ 1.9	55.1 $\pm$ 2.3	61.3 $\pm$ 1.4	45.9 $\pm$ 2.2	39.9 $\pm$ 1.1	48.1 $\pm$ 2.4	53.8 $\pm$ 0.7
Taylor-CE	56.7 $\pm$ 1.2	53.6 $\pm$ 2.3	51.2 $\pm$ 1.8	61.8 $\pm$ 0.9	55.1 $\pm$ 3.0	47.6 $\pm$ 2.2	48.3 $\pm$ 1.4	57.9 $\pm$ 1.6	50.2 $\pm$ 2.5	55.3 $\pm$ 1.1	50.7 $\pm$ 1.7	53.9 $\pm$ 3.2
RTGNN	66.9 $\pm$ 2.0	49.7 $\pm$ 1.3	40.7 $\pm$ 1.9	53.4 $\pm$ 3.0	48.6 $\pm$ 1.7	60.2 $\pm$ 2.3	55.4 $\pm$ 0.8	30.5 $\pm$ 2.0	59.1 $\pm$ 3.1	43.9 $\pm$ 1.5	55.1 $\pm$ 1.0	62.9 $\pm$ 2.4
OMG	63.2 $\pm$ 1.5	61.3 $\pm$ 0.8	59.1 $\pm$ 2.2	54.0 $\pm$ 1.9	47.9 $\pm$ 1.3	56.1 $\pm$ 2.5	59.0 $\pm$ 1.7	68.5 $\pm$ 2.8	46.5 $\pm$ 1.1	43.3 $\pm$ 0.7	50.0 $\pm$ 1.0	59.7 $\pm$ 2.1
SPORT	60.7 $\pm$ 2.0	53.2 $\pm$ 1.5	58.3 $\pm$ 3.3	58.0 $\pm$ 1.2	49.2 $\pm$ 2.3	57.1 $\pm$ 3.1	54.6 $\pm$ 0.8	67.3 $\pm$ 2.6	45.5 $\pm$ 0.7	59.4 $\pm$ 1.0	49.9 $\pm$ 2.1	59.9 $\pm$ 2.5
CoCo	54.4 $\pm$ 2.2	51.7 $\pm$ 1.6	49.7 $\pm$ 0.9	56.0 $\pm$ 3.2	45.1 $\pm$ 2.7	47.1 $\pm$ 1.0	55.9 $\pm$ 3.3	57.9 $\pm$ 2.0	50.7 $\pm$ 1.8	36.5 $\pm$ 1.3	49.7 $\pm$ 2.5	52.1 $\pm$ 0.6
DEAL	59.1 $\pm$ 3.0	59.6 $\pm$ 2.2	56.7 $\pm$ 1.7	56.0 $\pm$ 0.8	52.1 $\pm$ 1.3	56.5 $\pm$ 0.9	57.6 $\pm$ 2.5	70.9 $\pm$ 1.6	44.3 $\pm$ 1.4	54.1 $\pm$ 3.1	50.6 $\pm$ 2.0	57.0 $\pm$ 1.2
SGDA	61.4 $\pm$ 1.5	45.1 $\pm$ 0.9	58.0 $\pm$ 1.7	52.0 $\pm$ 2.0	51.2 $\pm$ 1.2	41.1 $\pm$ 0.7	59.4 $\pm$ 2.3	69.1 $\pm$ 3.4	45.1 $\pm$ 1.1	48.5 $\pm$ 2.2	46.3 $\pm$ 0.6	54.0 $\pm$ 2.0
A2GNN	57.0 $\pm$ 1.8	50.4 $\pm$ 2.1	57.6 $\pm$ 1.5	59.5 $\pm$ 2.0	54.0 $\pm$ 1.4	45.8 $\pm$ 0.9	49.9 $\pm$ 3.3	63.7 $\pm$ 2.5	41.5 $\pm$ 1.0	56.0 $\pm$ 0.7	46.5 $\pm$ 1.8	62.3 $\pm$ 1.2
StruRW	61.7 $\pm$ 2.3	54.5 $\pm$ 1.4	48.2 $\pm$ 1.8	56.0 $\pm$ 0.9	46.3 $\pm$ 1.6	61.1 $\pm$ 3.0	55.7 $\pm$ 2.1	42.9 $\pm$ 0.5	53.3 $\pm$ 1.2	51.4 $\pm$ 0.9	52.8 $\pm$ 3.1	61.7 $\pm$ 2.4
PA-BOTH	60.5 $\pm$ 2.0	54.8 $\pm$ 1.1	57.6 $\pm$ 1.9	59.4 $\pm$ 2.3	53.0 $\pm$ 1.4	54.1 $\pm$ 2.2	60.7 $\pm$ 3.0	67.1 $\pm$ 0.8	52.1 $\pm$ 2.3	59.1 $\pm$ 1.7	44.7 $\pm$ 2.5	55.3 $\pm$ 1.3
ROAD	56.6 $\pm$ 2.2	61.3 $\pm$ 1.3	52.2 $\pm$ 2.1	59.4 $\pm$ 2.0	55.0 $\pm$ 2.5	51.1 $\pm$ 2.3	59.1 $\pm$ 2.2	63.8 $\pm$ 1.9	56.6 $\pm$ 2.2	59.4 $\pm$ 3.0	58.7 $\pm$ 2.0	60.1 $\pm$ 1.8
ALEX	60.8 $\pm$ 2.4	63.3 $\pm$ 3.3	64.1 $\pm$ 2.6	<b>64.1<math>\pm</math>2.4</b>	60.5 $\pm$ 1.9	56.9 $\pm$ 2.9	59.6 $\pm$ 2.0	62.5 $\pm$ 2.3	63.7 $\pm$ 2.6	51.9 $\pm$ 1.8	<b>61.2<math>\pm</math>1.9</b>	63.6 $\pm$ 3.0
NeGPR	<b>70.1<math>\pm</math>2.1</b>	<b>65.6<math>\pm</math>1.8</b>	<b>66.7<math>\pm</math>2.4</b>	63.9 $\pm$ 1.7	<b>59.7<math>\pm</math>2.0</b>	<b>65.9<math>\pm</math>1.6</b>	<b>65.8<math>\pm</math>2.3</b>	<b>72.3<math>\pm</math>2.1</b>	<b>64.2<math>\pm</math>1.2</b>	<b>63.6<math>\pm</math>1.8</b>	59.1 $\pm$ 2.3	<b>65.6<math>\pm</math>2.0</b>

Table 17: The classification results (in %) on the MUTAGENICITY dataset under edge density domain shift (source  $\rightarrow$  target). M0, M1, M2, and M3 denote the sub-datasets partitioned with edge density. **Bold** results indicate the best performance.

Methods	M0 $\rightarrow$ M1	M1 $\rightarrow$ M0	M0 $\rightarrow$ M2	M2 $\rightarrow$ M0	M0 $\rightarrow$ M3	M3 $\rightarrow$ M0	M1 $\rightarrow$ M2	M2 $\rightarrow$ M1	M1 $\rightarrow$ M3	M3 $\rightarrow$ M1	M2 $\rightarrow$ M3	M3 $\rightarrow$ M2
WL	57.5 $\pm$ 1.2	48.8 $\pm$ 1.2	52.9 $\pm$ 1.2	54.2 $\pm$ 2.4	46.2 $\pm$ 1.8	47.4 $\pm$ 3.4	53.9 $\pm$ 2.7	63.9 $\pm$ 2.1	44.8 $\pm$ 1.7	41.3 $\pm$ 1.1	46.7 $\pm$ 3.2	45.7 $\pm$ 3.9
PathNN	45.6 $\pm$ 2.3	60.3 $\pm$ 2.7	59.5 $\pm$ 2.8	52.8 $\pm$ 1.5	48.7 $\pm$ 1.9	47.9 $\pm$ 4.1	57.4 $\pm$ 0.9	68.2 $\pm$ 1.5	50.6 $\pm$ 1.6	58.0 $\pm$ 2.7	51.2 $\pm$ 1.4	59.6 $\pm$ 0.6
GCN	61.1 $\pm$ 2.1	52.0 $\pm$ 0.9	43.6 $\pm$ 1.8	47.8 $\pm$ 1.4	47.1 $\pm$ 3.3	56.2 $\pm$ 2.6	51.8 $\pm$ 1.9	34.2 $\pm$ 2.0	54.2 $\pm$ 1.5	36.6 $\pm$ 0.7	50.8 $\pm$ 2.2	57.9 $\pm$ 1.5
GIN	51.4 $\pm$ 0.6	47.7 $\pm$ 1.4	49.9 $\pm$ 3.6	57.0 $\pm$ 2.9	45.5 $\pm$ 1.4	46.5 $\pm$ 4.3	52.0 $\pm$ 3.5	53.9 $\pm$ 3.1	46.7 $\pm$ 1.9	54.7 $\pm$ 1.7	55.4 $\pm$ 2.1	55.7 $\pm$ 2.8
GAT	59.4 $\pm$ 0.9	56.0 $\pm$ 1.7	63.4 $\pm$ 1.4	57.1 $\pm$ 0.8	49.3 $\pm$ 2.6	52.3 $\pm$ 3.1	52.8 $\pm$ 3.3	68.4 $\pm$ 2.5	45.0 $\pm$ 1.4	48.8 $\pm$ 3.3	45.7 $\pm$ 2.9	55.8 $\pm$ 1.8
GMT	51.0 $\pm$ 1.7	49.9 $\pm$ 3.0	51.6 $\pm$ 1.3	51.5 $\pm$ 1.6	50.6 $\pm$ 1.6	49.3 $\pm$ 1.5	53.3 $\pm$ 2.7	50.4 $\pm$ 2.9	49.4 $\pm$ 2.0	52.1 $\pm$ 1.0	50.8 $\pm$ 1.1	50.5 $\pm$ 1.4
Co-teaching	53.9 $\pm$ 3.3	61.0 $\pm$ 3.6	60.8 $\pm$ 2.1	49.9 $\pm$ 1.8	43.6 $\pm$ 0.7	53.3 $\pm$ 1.7	55.6 $\pm$ 2.6	62.0 $\pm$ 2.1	46.4 $\pm$ 1.5	39.1 $\pm$ 1.3	48.4 $\pm$ 1.9	54.0 $\pm$ 2.6
Taylor-CE	56.3 $\pm$ 0.5	52.4 $\pm$ 1.7	50.3 $\pm$ 2.3	60.9 $\pm$ 1.8	53.9 $\pm$ 3.3	46.9 $\pm$ 0.6	49.4 $\pm$ 1.8	56.1 $\pm$ 1.4	49.9 $\pm$ 1.7	55.6 $\pm$ 2.2	49.9 $\pm$ 2.6	51.7 $\pm$ 1.5
RTGNN	66.4 $\pm$ 3.0	48.1 $\pm$ 2.6	40.3 $\pm$ 2.4	52.2 $\pm$ 1.2	49.2 $\pm$ 0.7	60.9 $\pm$ 1.6	56.0 $\pm$ 2.3	31.2 $\pm$ 2.7	59.4 $\pm$ 1.6	43.3 $\pm$ 0.9	54.4 $\pm$ 4.2	62.4 $\pm$ 0.5
OMG	62.6 $\pm$ 1.8	60.9 $\pm$ 1.6	58.6 $\pm$ 2.1	53.4 $\pm$ 1.7	47.2 $\pm$ 1.6	55.9 $\pm$ 0.9	58.0 $\pm$ 4.7	68.3 $\pm$ 3.3	47.1 $\pm$ 1.9	44.1 $\pm$ 1.8	49.6 $\pm$ 1.5	59.5 $\pm$ 1.7
SPORT	60.6 $\pm$ 2.6	54.1 $\pm$ 2.7	56.7 $\pm$ 2.4	57.1 $\pm$ 1.8	48.0 $\pm$ 1.9	57.9 $\pm$ 3.3	53.1 $\pm$ 3.6	66.8 $\pm$ 1.5	45.8 $\pm$ 1.9	60.7 $\pm$ 0.7	48.7 $\pm$ 3.6	59.6 $\pm$ 1.6
CoCo	53.3 $\pm$ 2.8	52.2 $\pm$ 0.5	47.4 $\pm$ 1.7	57.8 $\pm$ 1.6	45.8 $\pm$ 2.3	46.5 $\pm$ 1.5	55.1 $\pm$ 0.9	61.4 $\pm$ 1.8	50.3 $\pm$ 0.4	37.7 $\pm$ 3.3	50.6 $\pm$ 3.7	50.8 $\pm$ 2.6
DEAL	56.9 $\pm$ 0.8	60.9 $\pm$ 1.3	56.2 $\pm$ 1.6	56.9 $\pm$ 1.9	50.3 $\pm$ 0.7	56.2 $\pm$ 2.5	59.3 $\pm$ 2.0	67.8 $\pm$ 3.1	46.6 $\pm$ 1.4	54.6 $\pm$ 1.4	51.7 $\pm$ 1.1	56.2 $\pm$ 1.5
SGDA	59.3 $\pm$ 1.9	46.4 $\pm$ 2.3	57.2 $\pm$ 2.1	54.5 $\pm$ 2.7	49.3 $\pm$ 0.8	41.6 $\pm$ 1.7	56.1 $\pm$ 0.9	68.0 $\pm$ 2.3	46.0 $\pm$ 0.8	48.1 $\pm$ 1.5	46.5 $\pm$ 1.7	51.0 $\pm$ 1.3
A2GNN	55.8 $\pm$ 0.9	52.4 $\pm$ 1.8	58.1 $\pm$ 2.7	56.5 $\pm$ 1.5	52.5 $\pm$ 1.7	46.6 $\pm$ 0.4	48.9 $\pm$ 0.9	65.2 $\pm$ 1.1	40.6 $\pm$ 2.6	53.5 $\pm$ 2.9	49.8 $\pm$ 2.3	60.1 $\pm$ 1.8
StruRW	60.6 $\pm$ 1.4	55.4 $\pm$ 0.8	45.9 $\pm$ 1.9	58.0 $\pm$ 1.7	44.7 $\pm$ 2.2	61.9 $\pm$ 1.5	55.2 $\pm$ 1.8	39.6 $\pm$ 0.6	52.6 $\pm$ 1.4	51.8 $\pm$ 2.4	53.1 $\pm$ 1.8	59.7 $\pm$ 1.6
PA-BOTH	59.3 $\pm$ 2.2	56.6 $\pm$ 2.8	58.3 $\pm$ 2.1	60.1 $\pm$ 1.9	51.6 $\pm$ 0.9	53.5 $\pm$ 1.4	60.3 $\pm$ 1.8	67.9 $\pm$ 2.2	50.6 $\pm$ 1.5	60.5 $\pm$ 1.8	46.0 $\pm$ 4.1	57.2 $\pm$ 1.7
ROAD	60.1 $\pm$ 2.2	62.6 $\pm$ 2.8	61.5 $\pm$ 2.0	57.0 $\pm$ 1.6	55.5 $\pm$ 1.9	52.0 $\pm$ 2.2	60.3 $\pm$ 2.7	71.1 $\pm$ 2.2	53.5 $\pm$ 1.9	61.5 $\pm$ 2.7	54.0 $\pm$ 2.3	57.4 $\pm$ 1.9
ALEX	63.8 $\pm$ 2.1	62.9 $\pm$ 1.8	<b>64.7<math>\pm</math>2.0</b>	<b>63.4<math>\pm</math>2.3</b>	56.5 $\pm$ 2.4	54.8 $\pm$ 1.6	61.4 $\pm$ 2.5	70.3 $\pm$ 2.3	55.0 $\pm$ 1.5	61.2 $\pm$ 1.8	59.5 $\pm$ 2.9	57.5 $\pm$ 2.3
NeGPR	<b>67.8<math>\pm</math>2.1</b>	<b>61.7<math>\pm</math>2.5</b>	64.5 $\pm$ 1.8	62.9 $\pm$ 2.3	<b>59.7<math>\pm</math>1.4</b>	<b>64.3<math>\pm</math>1.5</b>	<b>62.4<math>\pm</math>2.4</b>	<b>70.9<math>\pm</math>2.5</b>	<b>60.8<math>\pm</math>2.4</b>	<b>65.1<math>\pm</math>1.5</b>	<b>60.2<math>\pm</math>2.0</b>	<b>65.4<math>\pm</math>1.5</b>

Table 18: The classification results (in %) on the MUTAGENICITY dataset under node density domain shift (source  $\rightarrow$  target). M0, M1, M2, and M3 denote the sub-datasets partitioned with node density. **Bold** results indicate the best performance.

Methods	M0 $\rightarrow$ M1	M1 $\rightarrow$ M0	M0 $\rightarrow$ M2	M2 $\rightarrow$ M0	M0 $\rightarrow$ M3	M3 $\rightarrow$ M0	M1 $\rightarrow$ M2	M2 $\rightarrow$ M1	M1 $\rightarrow$ M3	M3 $\rightarrow$ M1	M2 $\rightarrow$ M3	M3 $\rightarrow$ M2
WL	56.7 $\pm$ 3.8	50.9 $\pm$ 4.5	54.4 $\pm$ 4.8	51.9 $\pm$ 2.1	46.4 $\pm$ 1.5	45.9 $\pm$ 1.3	55.1 $\pm$ 2.2	64.5 $\pm$ 1.8	42.2 $\pm$ 1.2	43.0 $\pm$ 3.9	46.6 $\pm$ 3.1	48.6 $\pm$ 0.8
PathNN	43.7 $\pm$ 2.2	59.8 $\pm$ 4.1	56.9 $\pm$ 3.3	51.7 $\pm$ 4.2	50.1 $\pm$ 4.3	45.2 $\pm$ 2.6	58.0 $\pm$ 2.5	69.2 $\pm$ 3.0	51.1 $\pm$ 2.1	55.8 $\pm$ 2.2	50.3 $\pm$ 3.4	59.2 $\pm$ 1.6
GCN	61.8 $\pm$ 2.0	51.0 $\pm$ 2.7	41.5 $\pm$ 3.0	48.2 $\pm$ 4.2	46.7 $\pm$ 3.9	57.1 $\pm$ 1.4	53.5 $\pm$ 4.0	35.5 $\pm$ 4.3	56.4 $\pm$ 1.5	34.3 $\pm$ 2.5	50.1 $\pm$ 1.4	59.7 $\pm$ 3.9
GIN	48.9 $\pm$ 1.8	48.0 $\pm$ 2.3	48.2 $\pm$ 2.2	55.7 $\pm$ 3.5	47.5 $\pm$ 3.1	44.5 $\pm$ 2.3	53.4 $\pm$ 3.0	55.8 $\pm$ 2.9	47.2 $\pm$ 3.7	52.8 $\pm$ 2.8	56.6 $\pm$ 1.7	55.1 $\pm$ 3.2
GAT	59.8 $\pm$ 1.7	53.2 $\pm$ 1.6	63.2 $\pm$ 2.4	58.2 $\pm$ 2.0	52.1 $\pm$ 4.4	53.1 $\pm$ 3.6	50.6 $\pm$ 4.1	66.8 $\pm$ 0.7	45.7 $\pm$ 4.0	47.6 $\pm$ 1.4	47.3 $\pm$ 1.1	56.1 $\pm$ 4.9
GMT	54.7 $\pm$ 1.2	51.0 $\pm$ 0.9	53.2 $\pm$ 1.9	50.5 $\pm$ 0.3	50.5 $\pm$ 2.8	50.5 $\pm$ 0.6	53.2 $\pm$ 1.6	48.4 $\pm$ 1.1	50.8 $\pm$ 1.8	51.1 $\pm$ 1.8	50.1 $\pm$ 2.1	49.8 $\pm$ 1.1
Co-teaching	55.4 $\pm$ 1.5	60.8 $\pm$ 1.0	63.2 $\pm$ 3.2	51.2 $\pm$ 2.7	42.0 $\pm$ 4.7	55.4 $\pm$ 4.0	55.7 $\pm$ 1.9	61.3 $\pm$ 3.3	48.4 $\pm$ 4.6	38.2 $\pm$ 4.5	49.5 $\pm$ 3.2	53.7 $\pm$ 2.8
Taylor-CE	56.5 $\pm$ 3.3	51.3 $\pm$ 3.8	48.9 $\pm$ 3.1	62.5 $\pm$ 2.3	54.6 $\pm$ 2.1	46.8 $\pm$ 4.4	48.6 $\pm$ 3.7	58.3 $\pm$ 1.7	51.4 $\pm$ 4.6	53.3 $\pm$ 4.3	51.8 $\pm$ 2.4	52.7 $\pm$ 1.9
RTGNN	68.7 $\pm$ 1.3	46.6 $\pm$ 4.8	42.9 $\pm$ 3.0	53.4 $\pm$ 3.4	47.2 $\pm$ 1.5	60.5 $\pm$ 4.7	55.7 $\pm$ 3.5	28.5 $\pm$ 2.7	60.4 $\pm$ 2.0	41.5 $\pm$ 4.0	52.9 $\pm$ 2.8	62.2 $\pm$ 2.3
OMG	63.0 $\pm$ 4.2	61.9 $\pm$ 3.6	57.7 $\pm$ 3.5	55.0 $\pm$ 2.3	45.4 $\pm$ 1.8	58.4 $\pm$ 1.9	59.7 $\pm$ 2.2	68.9 $\pm$ 3.7	46.0 $\pm$ 2.9	41.7 $\pm$ 3.6	49.4 $\pm$ 3.7	61.7 $\pm$ 1.4
SPORT	61.7 $\pm$ 2.7	54.3 $\pm$ 4.8	56.0 $\pm$ 4.2	55.9 $\pm$ 2.9	47.9 $\pm$ 2.6	60.7 $\pm$ 4.5	53.5 $\pm$ 1.6	64.5 $\pm$ 2.5	45.5 $\pm$ 2.9	62.7 $\pm$ 3.2	47.6 $\pm$ 3.8	57.0 $\pm$ 4.9
Coco	54.1 $\pm$ 3.7	51.3 $\pm$ 3.4	45.2 $\pm$ 3.3	59.9 $\pm$ 3.2	46.4 $\pm$ 4.1	45.0 $\pm$ 4.4	56.5 $\pm$ 1.3	58.8 $\pm$ 2.8	51.8 $\pm$ 1.1	37.5 $\pm$ 1.2	52.9 $\pm$ 4.6	50.9 $\pm$ 1.9
DEAL	59.8 $\pm$ 3.8	60.8 $\pm$ 2.1	54.2 $\pm$ 2.1	57.6 $\pm$ 4.9	50.0 $\pm$ 2.6	56.0 $\pm$ 4.5	59.6 $\pm$ 1.9	68.7 $\pm$ 2.1	48.7 $\pm$ 4.0	52.1 $\pm$ 3.2	51.1 $\pm$ 3.5	57.2 $\pm$ 2.6
SGDA	58.1 $\pm$ 3.1	46.5 $\pm$ 2.4	55.9 $\pm$ 3.0	57.0 $\pm$ 4.3	48.6 $\pm$ 3.1	43.5 $\pm$ 1.5	53.9 $\pm$ 2.7	70.3 $\pm$ 2.4	45.0 $\pm$ 3.4	46.2 $\pm$ 2.8	47.1 $\pm$ 1.0	52.2 $\pm$ 4.9
A2GNN	57.1 $\pm$ 4.0	51.4 $\pm$ 1.6	57.3 $\pm$ 4.4	57.6 $\pm$ 2.6	51.9 $\pm$ 3.4	44.6 $\pm$ 4.9	48.0 $\pm$ 2.0	65.6 $\pm$ 1.2	42.3 $\pm$ 4.5	56.3 $\pm$ 1.4	52.0 $\pm$ 2.0	57.4 $\pm$ 3.9
StruRW	60.3 $\pm$ 3.6	56.1 $\pm$ 2.0	43.0 $\pm$ 4.7	56.6 $\pm$ 1.2	44.9 $\pm$ 2.2	59.7 $\pm$ 3.3	55.7 $\pm$ 2.9	38.6 $\pm$ 3.6	53.8 $\pm$ 3.8	52.2 $\pm$ 2.7	52.4 $\pm$ 2.3	58.0 $\pm$ 1.8
PA-BOTH	60.9 $\pm$ 2.8	55.8 $\pm$ 4.7	60.7 $\pm$ 2.3	60.4 $\pm$ 4.8	51.1 $\pm$ 1.6	51.4 $\pm$ 1.7	62.3 $\pm$ 2.5	66.8 $\pm$ 3.0	49.7 $\pm$ 4.6	60.6 $\pm$ 3.6	48.2 $\pm$ 3.9	57.8 $\pm$ 4.3
ROAD	64.3 $\pm$ 1.8	60.6 $\pm$ 1.7	61.0 $\pm$ 2.9	57.7 $\pm$ 2.0	56.9 $\pm$ 2.7	56.4 $\pm$ 1.8	63.2 $\pm$ 2.1	68.3 $\pm$ 2.0	47.7 $\pm$ 1.7	59.2 $\pm$ 2.6	51.2 $\pm$ 1.9	63.1 $\pm$ 2.2
ALEX	65.3 $\pm$ 2.7	63.5 $\pm$ 2.3	<b>64.2<math>\pm</math>3.1</b>	<b>65.8<math>\pm</math>2.1</b>	56.4 $\pm$ 2.2	54.1 $\pm$ 2.6	64.2 $\pm$ 1.9	70.0 $\pm$ 2.0	56.5 $\pm$ 1.9	62.1 $\pm$ 2.1	58.5 $\pm$ 2.2	62.0 $\pm$ 2.5
NeGPR	<b>70.1<math>\pm</math>2.1</b>	<b>65.6<math>\pm</math>1.8</b>	63.7 $\pm$ 2.4	63.9 $\pm$ 1.7	<b>58.7<math>\pm</math>2.0</b>	<b>61.9<math>\pm</math>1.6</b>	<b>65.8<math>\pm</math>2.1</b>	<b>71.3<math>\pm</math>1.7</b>	<b>62.2<math>\pm</math>1.9</b>	<b>63.6<math>\pm</math>1.8</b>	<b>60.1<math>\pm</math>2.3</b>	<b>64.6<math>\pm</math>2.0</b>